이학박사 학위논문

A Study on Modeling HIV Infection Dynamics

항레트로바이러스 감염 역학에 관한 모델링연구

2018 년 2 월

서울대학교 대학원

협동과정 계산과학전공

김 효 은

이학박사 학위논문

A Study on Modeling HIV Infection Dynamics

항레트로바이러스 감염 역학에 관한 모델링연구

2018 년 2 월

서울대학교 대학원

협동과정 계산과학전공

김 효 은

Abstract

A Study on Modeling HIV Infection Dynamics

Hyoeun Kim
The Interdisciplinary Program
in Computational Science and Technology
The Graduate School
Seoul National University

A focus of this thesis is to develop a mathematical modeling approach to analyze the clinical data of Human immunodeficiency virus(HIV) acute infection. From the several studies, a remarkable stability of the HIV latent reservoir is detected despite the long-term treatment and advances in anti–retroviral therapy, and it has been recognized as a major barrier to HIV cure. We analyze several nonlinear mathematical models including the one that contains latent reservoir effect which provides consecutive viral replication and derive reproductive number (R_0) which is a key index on HIV dynamics. For a quantitative analysis, we estimated parameters best describe time-series viral load measurements, obtained from published clinical study. We implement an efficient estimation method for the relevant parameters and numerical algorithm to solve the HIV infection dynamics. By using a nonlinear least square method for parameter estimation, analysis on the sensitivity parameters are performed for each model. In addition, we can obtain the total contribution of the reservoir processes to the productively infected T lymphocyte cells is also examined.

We also propose a new model for HIV infection dynamics. There has been some researches that some influencing fractions on the dynamics of blood flow

have been associated with the severity of HIV infection. In order to explain the rheological behavior of HIV infection in T lymphocyte populations we attempt to modify Latent cell model with fractional order differentiation of order $\alpha \in (0, 1]$. The hemorheological parameters and fractional-order derivative in HIV system embody essential features of influencing fractions on the dynamics of blood flow associated with the severity of HIV infection. We show that the modified model has non-negative, bounded solutions. Optimal fractional order and kinetic parameters are estimated by using the nonlinear weighted least-square method, the Levenberg-Marquardt algorithm, and Adams-type predictor-corrector method is employed for the numerical solution. The numerical results confirm that a value of fractional order (α) representing the rheological behavior in plasma is significantly related with a density of lymphocyte population.

Keywords : HIV infection dynamics, latent reservoir, reproductive number, parameter estimation, fractional derivative

Student Number : 2010-20405

Contents

List of Figures

List of Tables

Chapter 1

Introduction

The human immunodeficiency virus(HIV), an etiological agent for acquired immunodeficiency syndrome (AIDS), has been a significant transmitted disease throughout the world. AIDS is one of the most serious public health concerns affecting people all over the world, and in some areas, affecting population imbalances. Despite many successful public health and clinical interventions since the first identification of HIV-positive patients in 1981, there remains no cure and the HIV/AIDS epidemic continues to grow. Highly active antiretroviral therapy (HAART) denotes a use of multiple antiretroviral drugs that act on different stage of the life-cycle of virus, and treatment of HIV infection with HAART is the most common administration method that can significantly decrease HIV-RNA levels and permit immune reconstitution. Antiretroviral drugs are widely available in the United States and Western Europe, but difficult to use due to cost and side effects. In developing countries, The Joint United Nations Programme on HIV/AIDS(UNAIDS) estimates that

only 7% of its infected population has accessing to HAART. In both developed and underdeveloped countries, effective and appropriate use of pharmacotherapy are requires improved strategies.

The rest of this chapter is organized as follows. In Section 1.1, a brief introduction to virology and current ART for HIV are introduced. In Section 1.2, the latent reservoir and mutation of virus, which is one of major issues for HIV treatment, are implemented. Section 1.3 devotes for a review for previous modeling HIV infection dynamics. In Section 1.4, the organization of the thesis is stated.

1.1 Infection mechanism of HIV and Antiretroviral treatment

HIV is a pathogen of AIDS(Acquired Immune Deficiency Syndrome). When infected with HIV, CD4 + T lymphocytes related to cellular immunity among the immune functions of the human body are mainly destroyed. AIDS is a collective term referring to the occurrence of various complications such as infectious diseases or malignant tumors caused by viruses, bacteria, fungi, protozoa or parasites which are not visible to healthy people, due to the loss of immunity to human defense after infection of HIV. Although HIV infection often tends to be confused with AIDS, not all HIV-infected people are HIV-positive. The term "HIV infected person" is a generic term referring to people with HIV in the body. It is a concept that includes all pathogen holders, HIV-positive, and AIDS patients. In contrast, "AIDS patients" refers to patients who have developed HIV infection and become ill with immune deficiency, resulting in opportunistic infections or complications such as tumors. However, people with AIDS and those without symptoms can spread HIV to others.

HIV belongs to the lentivirus of the human retroviridae. HIV is a single-

stranded, positive sense, enveloped RNA virus. The viral particles have outer protrusions composed of a coat protein on the surface. The inside of the viral envelope is covered with a protein grain, and the inside further forms a nucleocapsid. At the core of the virus particle surrounded by the nucleocapsid is reverse transcriptase (reverse transcriptase, integrase, protease and viral enzymes are associated with the viral genome. There are two types of HIV, HIV-1 and HIV-2, which are categorized by their nucleotide sequence and the genes they carry. HIV-2 can cause the same symptoms and illnesses as HIV-1, but spreads slowly and progressively slower than HIV-1. Throughout this thesis, we refer to HIV as HIV-1.

The most widely used classification of HIV infection and the definition of AIDS in adolescents and adults follows the US CDC classification system, which is classified according to the number of $CD4^+$ T lymphocytes and clinical features. A healthy human body has about $1000 cells/mm^3$ of $CD4^+$ T cell. In general, HIV-infected persons are classified as AIDS patients when the number of $CD4^+$ T lymphocytes is less than $200 cells/mm^3$ or is in a condition suitable for 'AIDS- Surveillance Case Definition' regardless of the symptom. This reduction in the number of $CD4^+$ T lymphocytes may result in a variety of life-threatening complications (opportunistic infections, etc.) as the immune function is significantly reduced.

As the infection progresses, the risk of complications increases and most of the complications lead to death. Recently, however, the incidence of complications such as opportunistic infections has been significantly reduced due to the combination of strong ART for HIV and chemotherapy to prevent opportunistic infections. Therefore, the life span of HIV-infected persons is being prolonged, and even if the antiviral treatment is well received, the normal life span can be prolonged.

There are two classes of anti–retroviral agents that have been developed and are currently used to cure HIV infection; reverse transcriptase inhibitors (RTIs) and protease inhibitors (PIs). RTIs inhibit the activity of viral DNA polymerases necessary for a reverse transcriptase and replication of HIV and other retroviruses. PIs prevent viral replication from selectively binding to HIV-1 protease and block proteolytic cleavage of the protein precursor required for the reproduction of infectious viral particles. A process of HIV proliferation along with anti-retroviral treatment(ART) is as follows:

1. HIV binds to the target cell, and the membrane of the virus and the membrane of the target cell are fused to each other.

2. HIV enters the cell and the RNA of the virus is released into the cytoplasm.

3. The reverse transcriptase of the virus makes the DNA with the viral RNA as a template. The reverse transcriptase inhibitors block this step.

4. Viral DNA (proviral DNA) enters the nucleus of the target cell and enters the chromosome DNA of the integrase.

5. Viral DNA that is caught in the chromosome of the target cell is activated by RNA polymerase and transcribed into mRNA and translated into the protein of the virus.

6. The produced virus protein is cleaved by protease and becomes a protein constituting the virus. Protease inhibitors block this step.

7. The newly created virus RNA and viral proteins come together to destroy the host cell while escaping the target cell membrane.

During during an initial phase of the illness, lasting for about 30 days, the concentration of infected cells and free virus in the body is very small.

After this period, a fast growth of the concentration of virus and infected cells is noticed, together with a major decrease of healthy $CD4^+$ T cells. After 6 months the infection stabilizes, and its kept in an approximated steady state for a period lasting between 2 and 10 years. After this period, the number of healthy $CD4^+$ T cells is drastically reduced and the patient develops AIDS.

To reduce this risk of the development of drug-resistant mutated viruses, it is common to use these two types of inhibitors together that are each aimed at different targets. The use of multiple antiretroviral drugs that act on different stage of the life-cycle of virus is known as HAART. Antiretroviral treatment (ART) is a long-term commitment. The HIV treatment guidelines recommend continuous ART for most infected individuals [58]. However, variability in treatment access, difficulties with consistent drug adherence, unknown side effect of lifelong ART, and unsustainable cost of lifelong treatment have provided impetus to the search for new strategies for cure.

In recent years, various treatment strategies aiming to improve the quality of life of HIV patients during their treatment period, have been developed to alleviate above problems [23, 89, 122]. Several safe and well-tolerated agents have been approved, and once daily dosing now allows for simpler prescriptions and a fixed dose of antiretroviral agents. In addition, deferred initiation of ART which delay the initiation of therapy in asymptomatic patients with a $CD4^+$ count above a certain threshold level, has been widely recommended. [63, 73, 150]. Above all, there have been a lot of interest in the study of treatment interruptions, also known as "structured treatment interruptions(STI)". Several STIs strategies are under evaluation as an alternative approach with the potential to reduce drug exposure, promote drug adherence, and reduce treatment-related fatigue. Treatment interruption has been explored in a variety of clinical trials with different goals. [101, 139]. Treatment interruptions

have also been studied as a way to boost the immune system and to help people who have tried and failed numerous antiretroviral drugs in the past respond better to "salvage" drug regimens. In patients who started treatment in acute seroconversion, STI was explored as a means of improving the HIV-specific immune response, resulting in better control of viral replication in the absence of continued treatment. [86, 137].

1.2 Latent reservoir and drug-resistant mutant in HIV infection

Despite the dramatic therapeutic effect of HAART on HIV infection, currently available therapies are suppressive and can not eradicate HIV infection [112, 167, 48]. A greatest obstacle to treating HIV-1 infection is a latent reservoir which contains unexpressed, replication-competent copies of the HIV-1 genome integrated into the host DNA. This latent reservoir is characterized by remarkable stability that explains why it is a lifelong barrier to treatment. Numerous studies have explored the correlation between HIV-1 persistence and the latent viral reservoir[24, 26, 48, 59, 145, 166]. Longitudinal analysis demonstrated that the latent viral reservoir is extremely stable and provides a mechanism for lifelong persistence of HIV-1 infection [48, 152].

The stability of latent HIV-1 is not affected by HAART because antiretroviral inhibitors does not eliminate proviruses integrated into the cellular genome. To date, latently infected resting memory $CD4^+$ T cells are the most studied and best characterized reservoir for HIV-1. Phylogenetic analysis showed that in patients under long term efficient ART, rebounding plasma viruses after structured therapeutic interruptions (STI) were from long-lived, latent infected resting $CD4^+$ T cells [71, 166]. Since no viral protein is produced, latently infected resting $CD4^+$ T cells in which latent infection had been reversed

are essentially indistinguishable from uninfected ones and therefore cannot be selectively targeted for elimination by either viral cytopathic effects(CPE) or cytolytic T-lymphocyte responses. Among several therapeutic strategies now being pursued in the clinic, inducing an expression of latent proviruses by a latency reversal agents(LRAs) while patients are staying at HAART is currently one of the best strategies for the depletion of latent reservoir. However, none of the studies demonstrated a significant reduction in the frequency of infected cells as measured by HIV DNA or quantitative viral outgrowth assay. A number of clinical trials have now begun with a broadening range of LRA classes, dosing intervals and combination strategies [33].

HIV-1 are vulnerable to the emergence of drug-resistant viruses in many ways. Due to the long half-life of virus-infected host T cells and the rapid rate of viral replication, viral infection continues to be maintained. HIV is an RNA virus, and it has a characteristic of reverse transcription. As it is known, due to the nature of the reverse transcription stage that does not have an ability to correct a mutation, a mutation that occurs once is accumulated as it is. It is a naturally occurring environment in patients with chronic infection regardless of the treatment. If selective pressures such as antiviral therapy or host immune response are applied, mutants favoring survival will survive. Drug resistance is a phenomenon in which mutations that are relatively favorable for viral replication during the treatment period are selectively survived due to less susceptibility to the drug[169].

A selective survival of a particular mutated virus is governed by the ability of the antiretroviral agent to inhibit virus multiplication. If the drug's ability to inhibit the growth of viruses is insignificant, it does not affect virus survival. If the ability to inhibit virus growth is perfect, however, mutation is replication-dependent and there is no chance for mutation to occur. Thus,

the moderate antiviral agent having the ability to inhibit the proliferation of viruses provides the best environment for resistance development[88]. Most patients with chronic HIV-1 infection require lifelong disease management, and more and more of them are taking antiretroviral drugs. However, the advent of drug-resistant viruses due to the long duration of antiviral drug administration is a major obstacle to the patient's long-term infection journey. In addition, from the viewpoint of public health, if the occurrence of drug-resistant viruses increases within the community, immense expense will be required. In order to prevent and treat the emergence of resistant viruses, the choice of the correct anti-retroviral therapy and the careful decision on the duration of consecutive dosing are important. Understanding the mechanism of resistance virus, risk factors are essential.

Ultimately, there is an opinion that 'combinatory therapy', which combines at least two drugs from the first treatment stage, is ideal for more effective inhibition of virus growth and prevention of long-term drug resistance. Although simple mutations are always present, the likelihood of multiple mutations occurring in a single virus is very low, and the sequential use of two types of drugs is a selective option for the survival of viruses with partial cross resistance. Therefore, theoretically, it is recommended to use a combinatory therapy from the first treatment, and the ideal combinations of drugs have different mechanisms of action, no cross-resistance among the drugs, and drugs with aggressive antiviral effects. These combined therapies may work with different selective pressures on several simple mutations that may be present in an individual, thereby reducing the selective survival of certain resistant mutations. However, combination therapies still leave significant challenges to be addressed through clinical trials, such as unexpected drug side effects and toxicity, excessive costs, and the emergence of multidrug-resistant viruses over

long-term use and the potential for fatal flares.

1.3 Modeling HIV infection dynamics in lymphocyte

Mathematical models for *in vivo* HIV dynamics have been used to understand the mechanisms involved in the evolution of the infection at the microscopic level and to ascertain the effects of various anti-retroviral treatments, such as reverse transcriptase inhibitors and protease inhibitors [78, 156, 113]. The studies on modelling have been also used to estimate several biologically informative values including life-span of infected population and virions, daily production number of viral load, reproductive number, infection susceptivity and sensitivity on drug for each patient. Such predictions provide not only a kinetic picture of HIV-1 pathogenesis, but theoretical principle to guide the development of treatment strategies by examining closely the interactions between the quantities being analyzed [116].

As we implemented in the Section 2.3 and Section 2.4, existence of long-lived latent reservoir in resting memory $CD4^+$T cell population and drug-resistance due to the mutation of virus has been recognized as major barriers to HIV-1 cure by causing the virus to grow out to detectable levels upon removal of drug therapy. To date, deterministic models of HIV dynamics have concerned at least these three components: the productively infected $CD4^+$ T cells, along with uninfected healthy $CD4^+$ T cells and free floating HIV. Various models from the simplest 3 component models to the comprehensive models which consider several components as populations within the the blood or lymphatic tissue, including latently-infected $CD4^+$ T-cells, cytotoxic T-lymphocytes, macrophages, have been proposed since 1995[106, 116]. The early linear models developed in Bryson[20], Perelson[116], Ho[61] are approximations to more realistic nonlinear models for viral and infected cell decay, and

thus are applicable only over short periods of time, most likely on the order of days. While these linear models have been extremely useful in characterizing short-term dynamics of HIV infection after therapy, several researchers have attempted to use these models to estimate time to eradication of virus from individuals.

To model data over longer periods of time and make predictions about long-term outcomes, nonlinear mathematical models are necessary. In addition to the unrealistic simplifying assumptions that make it difficult for linear models to accurately describe long-term HIV infection dynamics, factors that could play an important role in dynamic disease outcomes may be omitted in linear models. For example, several authors have raised the question as to whether or not these linear mathematical models have adequately described the decay of compartments relevant to HIV infection dynamics. Bonhoeffer[110] argues that more complex nonlinear models are needed to accurately describe long-term viral decay.

According to Perelson and Alan et al. [112], there are different phases of plasma viral dynamics following antiviral drug treatment. When three or more inhibitors are given to HIV-infected patients, plasma virus undergoes transition phase reflecting decay of free virus and productively infected T(PIT) cells and rapid decay phase reflecting decay of PIT, long-lived and latently infected T cells(LIT), and virus decays with an initial rapid exponential decline of nearly 2logs(first phase). Then it is followed by a slower exponential decline(second phase) after several week, which reflect decay of long-lived and LIT cells and other residual infected cells, and this phase leads to the virus falling below levels of detection($< 50 copies/m\ell$). They present that the slope of the decline depends on the efficacy of the therapy, with faster declines corresponding with more potent therapy. To interpret these two phase decline,

a new model was suggested by [112], which postulated that the second phase was due to sources of HIV-1 not included in the basic three-component model. They also report that the decline in plasma HIV RNA after the initiation of therapy has two phases and the second one was attributed to long-lived, release of virus from tissue reservoirs, of the activation of latently infected cells. Several mathematics models have been proposed to describe *in vivo* dynamics of T cell and HIV interaction with these three processes [112, 136, 135, 91].

Meanwhile, the basic model and a variant containing latently infected cells have been used to model the abrupt rise, peak, subsequent fall, and the establishment of the set-point viral load that characterizes acute HIV infection. In chronic infeciton, it is predicted that the immune response is constant, but during primary infection an HIV–specific cytotoxic T lymphocyte(CTL) response is generated and correlates temporally with the decline in viraemia[79]. In the basic model, the decrease in virus concentration after reaching the peak is due to target-cell limitation, i.e., running out of cells to infect[119]. This property of the basic model reveals a shortage in data fitting in previous work by Stafford et al.[149]. They fit viral-load data from ten primary infection patients and they found that the decline in virus after peak was more profound than the basic target-cell-limited model could explain. They suggested that by the immune response might have a role in decreasing viral loads. Moreover, the researchers of the clinical data used for parameter estimation in a following section, strived to assess whether repeated interruptions in treatment could restore or expand HIV specific immune responses, helping to control viral replication. So far, however, a few HIV investigators have proposed mathematical models to describe the dynamics of long-term latent reservoirs [91], [135], [136].

1.4 Thesis overview

The aim of this thesis is compare an analyze some HIV models which can explain persistence of low-level virus and emergence of viral blips in the long-term virus dynamics with treatment. We also purpose to propose the new model based on those works. In Chapter 2 begins with a survey of several existence models of in-host HIV infection dynamics that illustrate the various disease features and pathways. While complex models may be needed to provide accurate descriptions of the underlying dynamics, the models are most useful when they can be compared to clinical data we have. The complexity of nonlinear HIV models and data sets may necessitate the extraction of only essential states to balance between complexity and utility.

We then describe the several kinds of systems of differential equations which used to model HIV infection in our work and discuss its analysis. Among them, we consider a model with latent reservoir known to be related with a successive viral rebound mention in 1.3 and compare it with other model. With careful qualitative analysis of mathematical models that describe HIV infection dynamics, we estimated parameters best describe viral measurement during STI, which shows successive viral rebound. We examine the ability to estimate parameters in a typical nonlinear model of HIV infection dynamics. In doing so, we describe a relevant inverse problem methodology, including sensitivity analysis and the nonlinear least squares method in the estimation process.

In Chapter 3, we propose a system of fractional-order differential equations for the dynamics of HIV infection. In this chapter, we introduce a fractional-order derivative of order $0 < \alpha \leq 1$ into Latent cell activation model. We present a derivation and analysis of this fractional-order system in HIV model. We describe the numerical method and semi-sensitivity analysis. The optimal

fractional order and parameters are estimated for 9 infection patients. From these results, we verify that the density of healthy $CD4^+$ T lymphocyte population when the fractional order α is less than 1, which corresponds to the previous clinical findings.

Chapter 2

Mathematical models for HIV infection dynamics

2.1 Models and their analysis

In modelling HIV infection dynamics, only a major subset of biological compartments and their interactions must be typically chosen. We focus on compartmental models where each of compartments corresponds to a type of lymphocyte population throughout the body. We do not attempt to offer comprehensive investigations into a extensive range of mathematical models used for HIV infection dynamics. Rather, we refer the reader one of the outstanding survey articles [115, 22] that have already been published. We provide overview of some pioneering developments here. Using the measurement from patients undergoing HAART, mathematical models investigate the kinetics of viruses

and $CD4^+$ lymphocyte cell populations and it support the theory that virus and infected cell populations show a very rapid and consistent turnover in all patients. Ho, et al. [61], Wei, et al. [155], and Perelson, et al. [116].

This is in contrast to the previous assumption of researchers, that a stable virus and $CD4^+$T cell concentrations observed during the clinical latency of chronic HIV infection were due to the absence of any significant virus replication. According to Ho, Wei and Perelson's studies, both viruses and infected cell populations are turning over rapidly and continuously.

A further work by Perelson, et al. [112] discovered a second subpopulation of lymphocytes, longer-lived and productively infected cells, contributing the population of viral load. Since these reports, numerous researcher groups used mathematical models to calculate the decay rates of the infected cell populations [92, 97, 163, 108]. In Section2.1, we present basic three-component model and two representative models that can predict the observed persistent low–level replication of virus by including subpopulation of infected lymphocyte cells.

We consider (1) A general three-component model; (2) A four-component HIV infection dynamical model with chronically infected T lymphocyte subpopulation; (3) A four-component HIV dynamical model which includes activation of latently infected $CD4^+$ T lymphocyte cell population. An aspect of the HIV model's derivation involves incorporating the interactions between these populations and deriving their corresponding mathematical representation.

For each system we find equilibrium points and analyse their local stability properties in order to obtain a global phase portrait. The models that will be discussed in this Section 2.1 have multiple equilibria; different equilibria describe the success or failure of the immune system to control infection and the

initial conditions and parameters of the system determine which equilibrium is realized. A qualitative analysis is performed for each model to contribute to understanding of fundamental qualitative features of viral replication dynamics.

2.1.1 Three-component model

There have been several efforts to mathematically model the battle between the immune system and HIV within an infected host. Perelson and Nelson [116] provide an overview of some common models which have been used. Many biological operators are involved in the interaction between HIV and cells within the human body.

Among them, the first group is a subset of lymphocytes population, which in turn are a type of white blood cell. This subset is known as $CD4^+$ T cells or helper T cells. These T cells detect and direct the immune system response to invading viruses. Without them, the human body are seriously affected by opportunistic infections, which have a greater severity and duration than those without it. HIV, which refers in this case to the plasma virus, is a pathogen of AIDS and belongs to a class of retrovirus that infects population of helper T cells. They use an enzyme called reverse transcriptase to make a DNA copy of their RNA genome to be integrated into the targeted host cell's genes by breaching the cell wall and transporting their RNA into the T-cell nucleus. Then the infected T cell population ceases its function as part of the immune system and instead reproduce copies of HIV. These infected T-cells, along with the healthy $CD4^+$ T-cells and free floating HIV, are the populations with which we are concerned, and will appear within the mathematical model.

Here, we describe the three-component model that has been widely used and is the most basic and ubiquitous model in the study of HIV. It is suggested

by De Boer and Perelson et al.,[32] and concerned with three quantities: $T(t)$, the density of uninfected CD4$^+$ cells, $T^*(t)$, the density of infected CD4$^+$ cells and $V(t)$, the density of free virions. The corresponding dynamical system is:

$$\begin{aligned}
\frac{dT}{dt} &= \lambda - \rho T - (1-\theta_{RT}u(t))kTV_I, \quad T(0) = T_0 \\
\frac{dT^*}{dt} &= (1-\theta_{RT}u(t))kTV_I - \delta T^*, \quad T^*(0) = T_0^* \\
\frac{dV_I}{dt} &= (1-\theta_{PI}u(t))N\delta T^* - cV_I, \quad V_I(0) = V_{I,0} \\
\frac{dV_{NI}}{dt} &= \theta_{PI}u(t)N\delta T^* - cV_{NI}, \quad V_{NI}(0) = V_{NI,0}
\end{aligned} \tag{2.1}$$

This model includes T representing uninfected target CD4$^+$ T cells that are susceptible to infection, T^* productively infected T cells, V_I infectious virus, and V_{NI} non-infectious virus produced by the action of protease inhibitors (PIs), respectively. A total amount of virus is then $V_I + V_{NI}$. Target cells are replenished from stem cells in the bone marrow at rate λ, and mature in the thymus. It is assumed that the overall number of T-cells lost in a group over a certain period of time is proportional to the number of T-cells within the group at rate ρT. They are infected by virus, with infectivity k; note that healthy T cells become infected at a rate proportional to the product of the density of T cells and the density of free virion. This is essentially an application of the mass-action principle. Productively infected T cells are produced by infection of target cells and they die(lysis) at rate δT^* either from viral cytopathic effects(CPE) or by host immune response. Virus particles are generated from productively infected cells (T^*), where N is the number of virion produced during the average lifespan of T^*, and it is also called a burst size.

The model considers two conventional drug categories; reverse transcriptase inhibitors(RTIs) and protease inhibitors(PIs), which are implemented in 2.2. Here, a time-dependent treatment function $u(t) \in [0, 1]$ represents HAART

drug protocol, where $u(t) = 0$ is off-treatment and $u(t) = 1$, fully on. Following the [2], to describe control input (time-varying treatment protocol) $u(t)$ representing structured treatment interruption, which need not be periodic, we assume the piecewise constant ramp-shaped function assuming that it takes for 1 day for the absorption and dissipation of the drug.

The RTIs prevent HIV RNA from being converted into DNA and thereby block the viral infection, reducing the infectivity, k, by quantity $1-\theta_{RT}$, where θ_{RT} represents the efficacy of RTIs and $0 \leq \theta_{RT} \leq 1$. The PIs, on the other hand, do not directly inhibit the infectiousness of virus. Rather, they alter part of the viral assembly process in the final stage of the viral life cycle, and as a result cause the production of defective, noninfectious virus. Here, due to the action of PIs with an efficacy θ_{PI}, only a fraction $(1 - \theta_{PI})$ of the virion are infectious.

Thus, in the presence of a PIs, one can consider two types of virus particles: infectious virions at concentration V_I and noninfectious virions at concentration V_{NI}. This notation is somewhat imprecise, since even in the absence of a protease inhibitor, not every virus particle is infectious. Thus, according to [116], to be more precise, V_I denotes the population of virus particles that have not been influenced by a PIs and hence had their polyproteins cleaved, whereas V_{NI} denotes the population of virus particles with uncleaved polyproteins. The sum of these two types of virus particles $V_I + V_{NI}$ corresponds to the total plasma viral load, a quantity typically monitored in a clinical setting. Thus, it is assumed that all virus belong to the V_I in the absence of a protease inhibitor[116]. Both type of virus particles are cleared from the plasma with a rate c. Then the half-life of virions in plasma is given by $ln(\frac{2}{c})$ and the half-life of productively infected cells is obtained by $ln(\frac{2}{\delta})$. A detail of viral life cycle is implemented in 2.2. Let $T_0, T_0^*, V_{I,0}, V_{NI,0} \in \mathbb{R}$ be a given initial conditions

for the states when $t = 0$.

Model reduction

Denoting by $V(t)$ the total virus at time t, $V(t) = V_I(t) + V_{NI}(t)$, the summation of the third and fourth equaitons in (2.2) leads to the equation $\frac{dV(t)}{dt} = N\delta T^*(t) - cV(t)$. Note that this equation can also be obtained by substituting $V_I(t) = (1 - \theta_{RT}u(t))V(t)$ and $V_{NI}(t) = (\theta_{PI}u(t))V(t)$ into (2.2). Following the assumption of [116] that all virus belongs to the infectious virus population in the absence of a protease inhibitor, we have $V(t) = V_I(t)$ and $V_{NI}(t) = 0$ when $u(t) = 0$, and thus conditions $V_I(t) = (1 - \theta_{RT}u(t))V(t)$ and $V_{NI}(t) = (\theta_{PI}u(t))V(t)$, are satisfied. Finally, one can define a composite parameter θ as $1 - \theta u(t) = (1 - \theta_{RT}u(t))(1 - \theta_{PI}u(t))$, and then θ is usually represented by the total combined drug efficacy [134, 22, 156]. Then a resulting simplified system of equations is obtained as below.

$$\begin{aligned}
\frac{dT(t)}{dt} &= \lambda - \rho T(t) - (1 - \theta u(t))kT(t)V(t), \qquad T(t_0) = T_0 \\
\frac{dT^*(t)}{dt} &= (1 - \theta u(t))kT(t)V(t) - \delta T^*(t), \qquad T^*(t_0) = T_0^* \\
\frac{dV(t)}{dt} &= N\delta T^*(t) - cV(t), \qquad V(t_0) = V_0.
\end{aligned} \tag{2.2}$$

A description for the parameters are listed in Table 2.1.

Remark 2.1.1. *In* (2.2)*, $u(t)$ is an input variable which is considered to be a bounded and piecewise C^1 function. The states $T(t), T^*(t)$ and $V(t)$ are output variables and they affect each other in a nonlinear fashion physiologically with underlying biological logic among them.*

For the notational convenience, let $\mathbf{x}(t) = (x_1(t), x_2(t), x_3(t))^T = (T(t), T^*(t), V(t))^T$ denotes a continuously differentiable functions mapping $\mathbb{R}_+$ into $\mathbb{R}^3$

Variable	Units	Description
T	$cells/ml$	Uninfected healthy $CD4^+$ T cell density.
T^*	$cells/ml$	Productively infected $CD4^+$ T cell density.
V_I	$copies/ml$	Infectious HIV load.
V_{NI}	$copies/ml$	Non-infectious HIV load.
V	$copies/ml$	Total amount of HIV load.
Parameter	**Units**	**Description**
λ	$\frac{cells}{ml \cdot day}$	Rate of supply of uninfected T cell from precursors.
ρ	day^{-1}	Death rate of uninfected T cells(natural death).
k	$\frac{ml}{copies \cdot day}$	Rate constant for T cells becoming infected by free virus.
δ	day^{-1}	Death rate of productively infected T cell(lysis).
N	$\frac{copies}{cell}$	Number of free virus produced by a T cell.
c	day^{-1}	Death rate of free virus.
$\theta_{RT} \in [0,1]$	-	Primary efficacy of Reverse transcriptase inhibitor.
$\theta_{PI} \in [0,1]$	-	Primary efficacy of Protease inhibitor.
$\theta \in [0,1]$	-	Overall efficacy of combinatory ART.

Table 2.1: A description of variables and parameters of the three-component model

and the right hand side in (2.2) be prescribed by

$$\mathbf{f}(t, \mathbf{x}; \mathbf{p}) = \begin{pmatrix} \lambda - \rho x_1 - (1 - \theta u(t)) k x_1 x_3 \\ (1 - \theta u(t)) k x_1 x_3 - \delta x_2, \\ N\delta x_2 - c x_3 \end{pmatrix}, \tag{2.3}$$

where $\mathbf{p}$ denotes the vector of model parameters listed in Table 2.1. Then system (2.2) can be rewritten as

$$\begin{aligned} \dot{\mathbf{x}}(t) &= \mathbf{f}(t, \mathbf{x}(t)), \quad t \geq 0 \\ \mathbf{x}(0) &= \mathbf{x}_0 = (T_0, T_0^*, V_0)^T. \end{aligned} \tag{2.4}$$

For being biologically reasonable, we assume the the initial conditions for states variable, $\mathbf{x}_0$, are non–negative.

We first prove that a solution to the initial-value problem (2.4) does exist, and that this solution is unique.

Proposition 2.1.2. *Let $T_0, T_0^*, V_0 \in \mathbb{R}$ be given. There exist $t_1 > 0$ and*

continuously differentiable functions $\mathbf{x}(t)$ *satisfies* (2.4) *and initial condition* $\mathbf{x}_0$.

Proof. To prove the result, we note that the classical existence and uniqueness theorem due to Picard-Lindelöf [13] works just as well for the non–autonomous system. Then, it suffices to show that the function $\mathbf{f}$ in (2.4) is locally Lipschitz in its second argument, $\mathbf{x}$ and continuous in t. Note that the value of piecewise-continuous function $u(t)$ is bounded in $[0, 1]$, it is enough to notice that the Jacobian matrix, and denote by J,

$$J(\mathbf{x}) = \begin{bmatrix} -\rho - (1-\theta u(t))kx_3 & 0 & -(1-\theta u(t))kx_1 \\ (1-\theta u(t))kx_3 & -\delta & (1-\theta u(t))kx_1 \\ 0 & N\delta & -c \end{bmatrix} \tag{2.5}$$

is linear in $\mathbf{x}$ and therefore locally bounded for every $\mathbf{x} \in \mathbb{R}^3$. Hence, $\mathbf{f}$ has a continuous, bounded derivative on any compact subsets of $\mathbb{R}^3$ and so $\mathbf{f}$ is locally Lipschitz in $\mathbf{x}$. By the Picard-Lindelöf Theorem, there exists a unique solution, $\mathbf{x}(t)$, to the system (2.4) on $[0, t_1]$ for some time $t_1 > 0$. □

Definition 2.1.3. *[130] The basic reproductive number The basic reproductive number disease to reproduce, and is denoted by* R_0*. This is defined as the expected number of secondary cases reproduced by one infected individual in his/her entire infectious period. When* $R_0 < 1$*, each infected individual can produce an average of less than one new infected individual during his entire period of infectiousness. In this case the disease will not persist in the population and may be eradicated. But in a situation where* $R_0 > 1$ *implies that each infected individuals during the entire period of infectiousness can produce more than one new infected individual. This is a strong indication that the disease can persist and invade the population.*

Using the model equations, we investigate the basic reproductive number, denoted by R_0, which measures the average number of secondary infected cells which will result from the introduction of a single infected cell into a population of completely uninfected $CD4^+$ cells (Anderson and May, 1991 when there is no target cell limitation. We derive R_0 of the above model equations following the formal derivation presented in [130]. During uninfected period with no virus, the number of uninfected T cell can be assumed to be approximately constant, so that $T(t) = \frac{\lambda}{\rho}$ from the model equations (2.2). By denoting productively infected T cell population in a unit volume at $t = 0$ as T_1^*, its density at time t can be given by $T^*(t) = T_1^* e^{-\delta t}$ and

$$V(t) = \frac{N\delta T_1^*}{(c-\delta)}(e^{-\delta t} - e^{-ct}). \tag{2.6}$$

The rate at which virions infect target cells is kTV, and a total number of target cells infected by these virions is given by

$$\int_0^\infty kT(t)V(t)dt \quad = \quad \frac{kNT_0T_1^*}{c}. \tag{2.7}$$

By the definition of R_0, we have $T_1^* = 1$ and obtain $R_0 = \frac{\lambda kN}{\rho c}$ as a basic reproductive ratio prior to drug therapy for this system. When $0 < R_0 < 1$, the population is able to reproduce, but the death rate exceeds the growth rate and the population size will asymptotically approach zero. If R_0 greater than 1, it refers that one infected T cell infects more than 1 susceptible T cell on average, and generally the viral infection typically persists. A magnitude of R_0 determines the speed, scale, and spread of the viral infectivity.

In order to fully understand the dynamics of the three component model(2.2), it is necessary to first determine values of equilibria. An equilibrium point is a constant solution of (2.2) so that if the system begins at such a value, it

will remain there for all time. In other words, the populations are unchanging; so, the rate of change for each population is zero. The system (2.2) possesses two off treatment equilibria, the first one written in ordered-form (T, T^*, V) is given by

$$E_0 = \left(\frac{\lambda}{\rho}, 0, 0\right), \tag{2.8}$$

and we can categorize these points to be when the HIV virus is either extinct from the body. We call this viral extinction equilibrium point, since there are no virus particles or infected cells. We can also consider that E_0 is the case in which an infection exists for a short period of time, then is removed from the body by natural means. when the virus persists within the body as time t grows large, we refer to this equilibrium point as viral persistence, given by $\bar{E} = (\bar{T}, \bar{T^*}, \bar{V})$ where

$$\bar{T} = \frac{\lambda}{\rho}\frac{1}{R_0}, \qquad \bar{T^*} = \frac{\lambda}{\delta}\left(1 - \frac{1}{R_0}\right), \qquad \bar{V} = \frac{\rho}{k}(R_0 - 1) \tag{2.9}$$

in term of the reproductive number R_0. We remark that in the rare event that $R_0 = 1$, the equilibria E_0 and $\bar{E}$ are identical. We note that the equilibrium $\bar{E}$ is nonnegative if $R_0 \geq 1$, and the system of equations tends to $\bar{E}$, denotes that situation where the body is unable to clear the infection by itself. In order to understand the stability properties of the system (2.2) which explicitly depends on a time-varying input signal, we introduce a concept of input–to–state stability by recalling Definition 2.1.4 to Theorem 2.1.7(See the pages $135 - 136$ and $217 - 222$ in [74]). Let us denote the ℓ_2 norm by $||\cdot||$.

Consider the system of ODEs

$$\dot{\mathbf{x}} = \mathbf{f}(t, \mathbf{x}, \mathbf{u}), \tag{2.10}$$

where $\mathbf{f} : [0, \infty) \times D \times D_u \to \mathbb{R}^n$ is piecewise continuous in time t and locally Lipschitz in $\mathbf{x}$ and $\mathbf{u}$, $D \subset \mathbb{R}^n$ is a domain that contains $\mathbf{x} = \mathbf{0}$, and $D_u \subset \mathbb{R}^m$ is a domain that contains $\mathbf{u} = \mathbf{0}$. The input $\mathbf{u}$ is a piecewise continuous and bounded function of t for all $t \in [0, \infty)$.

Definition 2.1.4. *A continuous function $\alpha : [0, a) \to [0, \infty)$ is said to belong to class $\mathcal{K}$ if it is strictly increasing and $\alpha(0) = 0$. It is said to belong to class $\mathcal{K}_\infty$ if $a = \infty$ and $\alpha(r) \to \infty$ as $r \to \infty$.*

Definition 2.1.5. *A continuous function $\beta : [0, \infty) \times [0, a) \to [0, \infty)$ is said to belong to class $\mathcal{KL}$ if for each fixed s, the mapping $\beta(s, r)$ belongs to class $\mathcal{K}$ with respect to r and, for each fixed r, the mapping $\beta(s, r)$ is decreasing with respect to s and $\beta(s, r) \to 0$ as $s \to \infty$.*

Definition 2.1.6. *The system* (2.10) *is said to be locally input–to–state stable if there exist a class $\mathcal{KL}$ function β, a calss $\mathcal{K}$ function γ, and positive constants k_1 and k_2 such that for any initial state $\mathbf{x}(t_0)$ with $||\mathbf{x}(t_0)|| < k_1$ and any input $\mathbf{u}(t)$ with $\sup_{t \geq t_0} ||\mathbf{u}(t)|| < k_2$, the solution $\mathbf{x}$ exists and satisfies*

$$||\mathbf{x}(t)|| \leq \beta(t - t_0, ||\mathbf{x}(t_0)||) + \gamma(\sup_{t_0 \leq \tau \leq t} ||\mathbf{u}(\tau)||) \tag{2.11}$$

for all $t \geq t_0 \geq 0$. It is said to be input–to–state stable if $D = \mathbb{R}^n$, $D_u = \mathbb{R}^m$, and inequality (2.11) *is satisfied for any initial state $\mathbf{x}(t_0)$ and any bounded input $\mathbf{u}(t)$.*

Then the inequality equation (2.11) implies that for a bounded input $\mathbf{u}(t)$, the state $\mathbf{x}(t)$ will be bounded. The following theorem gives a sufficient condition for input–to–state stability.

Theorem 2.1.7. *Let $D_r = \{\mathbf{x} \in \mathbb{R}^n | ||\mathbf{x}|| < r\}$, $D_{r_u} = \{\mathbf{u} \in \mathbb{R}^m | ||\mathbf{u}|| < r_u\}$, and $\mathbf{f} : [0, \infty) \times D_r \times D_{r_u} \to \mathbb{R}^n$ is piecewise continuous in t and locally*

Lipschitz in $\mathbf{x}$ *and* $\mathbf{u}$. *Let* $U : [0, \infty) \times D_r \to \mathbb{R}$ *be a continuously differentiable function such that*

$$\alpha_1(||\mathbf{x}||) \leq U(t, \mathbf{x}) \leq \alpha_2(||\mathbf{x}||), \tag{2.12}$$

$$U_t + \nabla_{\mathbf{x}} U \dot{f}(t, \mathbf{x}, \mathbf{u}) \leq \alpha_3(||\mathbf{x}||), \quad \forall ||\mathbf{x}(t)|| \geq \omega(||\mathbf{u}(t)||) > 0, \tag{2.13}$$

$\forall (t, \mathbf{x}, \mathbf{u}) \in [0, \infty) \times D_r \times D_{r_u}$ *where* $\alpha_1, \alpha_2, \alpha_3$ *and* ω *are calss* $\mathcal{K}$ *functions. Then the system* (2.10) *is locally input–to–state stable with* $\gamma = \alpha_1^{-1} \circ \alpha_2 \circ \omega$, $k_1 = \alpha_2^{-1}(\alpha_1(r))$, *and* $k_2 = \omega^{-1}(\min\{k_1, \omega(r_u)\})$. *Moreover, if* $D_r = \mathbb{R}^n, D_{r_u} = \mathbb{R}^m$, *and* α_1 *is a calss* $\mathcal{K}_\infty$ *function, then the system* (2.10) *is input–to–state stable with* $\gamma = \alpha_1^{-1} \circ \alpha_2 \circ \omega$. *Here* γ, k_1 *and* k_2 *are referred in Definition2.1.6.*

It is well known that a Lyapunov function is a convenient tool to analyze stability, evaluate the system's robustness to perturbations. We need following preliminaries for using Lyapunov function in stability analysis.

Consider a linear time–invariant system

$$\dot{\mathbf{x}} = \mathbf{A}\mathbf{x}, \tag{2.14}$$

where $\mathbf{x} \in \mathbb{R}^n$ and $\mathbf{A}$ is an $n \times n$ matrix with real components. Then the system (2.14) has an equilibrium point at the origin. Recall that all eigenvalues of a *Hurwitz matrix* are negative, we note that the origin of the system (2.14) is asymptotically stable if and only if $\mathbf{A}$ is a *Hurwitz matrix*.

Consider a quadratic Lyapunov function candidate

$$U(\mathbf{x}) = \mathbf{x}^T \mathbf{P} \mathbf{x} \tag{2.15}$$

where $\mathbf{P}$ is a real symmetric positive definite matrix. Then a derivative of U

along the trajectories of the linear system (2.14) is given by

$$\dot{U}(\mathbf{x}) = \mathbf{x}^T\mathbf{P}\dot{\mathbf{x}} + \dot{\mathbf{x}}^T\mathbf{P}\mathbf{x} = \mathbf{x}^T(\mathbf{P}\mathbf{A} + \mathbf{A}^T\mathbf{P})\mathbf{x} = -\mathbf{x}^T\mathbf{Q}\mathbf{x} \tag{2.16}$$

where $\mathbf{Q}$ is a symmetric matrix defined by

$$\mathbf{P}\mathbf{A} + \mathbf{A}^T\mathbf{P} = -\mathbf{Q}. \tag{2.17}$$

Equation (2.17) is called a Lyapunov equation. The following theorem interprets the asymptotic stability of the origin in terms of the solution of the Lyapunov equation (2.17).

Theorem 2.1.8. *An $n \times n$ matrix $\mathbf{A}$ is a Hurwitz matrix if and only if, for given $n \times n$ symmetric positive definite matrix $\mathbf{Q}$, there exists a $n \times n$ symmetric positive definite matrix $\mathbf{P}$ that satisfies the equation* (2.17)*. Moreover, if $\mathbf{A}$ is a Hurwitz matrix and $\mathbf{Q}$ is a symmetric positive definite matrix, then there exists a unique symmetric positive definite matrix $\mathbf{P}$ satisfying* (2.17)*.*

The Routh–Hurwitz criteria [64, 138] for differential equations are used to determine local asymptotic stability of an equilibrium for nonlinear systems of differential equations. The Routh–Hurwitz criteria are stated in the next theorem.

Theorem 2.1.9. *(***Routh–Hurwitz criteria***, [64, 138]) Given the polynomial,*

$$P(\xi) = \xi^n + a_1\xi^{n-1} + \cdots + a_{n-1}\xi + a_n,$$

where the coefficients a_i are real constants for $i = 1, \ldots, n$, define tha n Hur-

witz matrices using the coefficients a_i of the characteristic polynomial:

$$H_1 = (a_1), \quad H_2 = \begin{pmatrix} a_1 & 1 \\ a_3 & a_2 \end{pmatrix}, \quad H_3 = \begin{pmatrix} a_1 & 1 & 0 \\ a_3 & a_2 & a_1 \\ a_5 & a_4 & a_3 \end{pmatrix},$$

and

$$H_n = \begin{pmatrix} a_1 & 1 & 0 & 0 & \cdots & 0 \\ a_3 & a_2 & a_1 & 1 & \cdots & 0 \\ a_5 & a_4 & a_3 & a_2 & \cdots & 0 \\ \vdots & \vdots & \vdots & \vdots & \cdots & \vdots \\ 0 & 0 & 0 & 0 & \cdots & a_n \end{pmatrix}.$$

where$a_j = 0$ if $j > n$. All of the roots of the polynomial $P(\xi)$ are negative or have negative real part if and only if the determinants of all Hurwitz matrices are positive:

$$\det H_j > 0, \quad j = 1, 2, \ldots, n.$$

When $n = 2$, the Routh-Hurwitz criteria simplify to $\det H_1 = a_1 > 0$ *and*

$$\det H_2 = \det \begin{pmatrix} a_1 & 1 \\ 0 & a_2 \end{pmatrix} = a_1 a_2 > 0$$

or $a_1 > 0$ and $a_2 > 0$. For polynomials of degree $n = 2, 3$ and 4, the Routh-Hurwitz criteria are summarized as follows.

$$n = 2: \ a_1 > 0 \quad \textit{and} \quad a_2 > 0, \tag{2.18a}$$

$$n = 3: \ a_1 > 0, a_3 > 0, \quad \textit{and} \quad a_1 a_2 > a_3, \tag{2.18b}$$

$$n = 4: \ a_1 > 0, a_3 > 0, a_4 > 0 \quad \textit{and} \quad a_1 a_2 a_3 > {a_3}^2 + a_4 {a_1}^2, \tag{2.18c}$$

The following proposition shows that the equilibrium point E_0 of system (2.2) is stable under certain condition on model parameters.

Proposition 2.1.10. *The system* (2.2) *is locally input–to–state stable in some neighborhood of* $(T(t), T^*(t), V(t),\, u(t))^T = (\frac{\lambda}{\rho}, 0, 0, 0)^T$. *Moreover, a viral extinction equilibrium point* $(\frac{\lambda}{\rho}, 0, 0)^T$ *of the system* (2.2) *is stable if* $1 > R_0$.

Proof. In order to apply Theorem 2.1.7, we need to find a proper lyapunov function U satisfying (2.12). For this purpose, we consider a system in the absence of the forcing input, i.e., $u(t) = 0$, which is called an unforced system of (2.2). Then it has equilibrium point $E_0 = (\frac{\lambda}{\rho}, 0, 0)^T$ which is called as viral extinction equilibrium. A change of variable $\widetilde{T}(t) = T(t) - \frac{\lambda}{\rho}$ transforms the homogeneous system into

$$\begin{aligned}
\frac{d\widetilde{T}(t)}{dt} &= -\left(\rho + kV(t)\right)\widetilde{T}(t) - \left(\frac{k\lambda}{\rho}\right)V(t),\\
\frac{dT^*(t)}{dt} &= k\widetilde{T}(t)V(t) + \left(\frac{k\lambda}{\rho}\right)V(t) - \delta T^*(t),\\
\frac{dV(t)}{dt} &= N\delta T^*(t) - cV(t).
\end{aligned} \tag{2.19}$$

To clarify notation, we introduce $\widetilde{\mathbf{x}} = (\widetilde{T}(t), T^*(t), V(t))^T$, then the linearized system of(2.34) at the zero equilibrium point is

$$\dot{\widetilde{\mathbf{x}}} = \mathbf{A}\widetilde{\mathbf{x}} + \mathbf{h}(\widetilde{\mathbf{x}}), \tag{2.20}$$

where the Jacobian matrix $\mathbf{A}$ and the nonlinear part $\mathbf{h}(\widetilde{\mathbf{x}})$ are given by

$$\mathbf{A} = \begin{pmatrix} -\rho & 0 & -\left(\frac{k\lambda}{\rho}\right) \\ 0 & -\delta & \left(\frac{k\lambda}{\rho}\right) \\ 0 & N\delta & -c \end{pmatrix}, \quad \mathbf{h}(\widetilde{\mathbf{x}}) = k\widetilde{T}(t)V(t)\begin{pmatrix} -1 \\ 1 \\ 0 \end{pmatrix}. \tag{2.21}$$

Then the eigenvalues of $\mathbf{A}$ are

$$-\rho \quad \text{and} \quad \frac{-(c+\delta) \pm \sqrt{(c+\delta)^2 - 4c\delta(1-R_0)}}{2}. \tag{2.22}$$

where $R_0 = \frac{k\lambda N}{c\rho}$ is reproductive number of the system (2.2). Since all model parameters are positive, we see that all eigenvalues of $\mathbf{A}$ have negative real part if and only if $1 - R_0 > 0$. Therefore, the linear system $\dot{\widetilde{\mathbf{x}}} = \mathbf{A}\widetilde{\mathbf{x}}$ has an asymptotically stable equilibrium point at the origin only when $1 > R_0$. $\square$

From Theorem 2.1.8, a symmetric positive definite matrix $\mathbf{P}$, the solution of the following equation

$$\mathbf{PA} + \mathbf{A}^T\mathbf{P} = -\mathbf{I} \quad (3 \times 3 \text{ identity matrix}) \tag{2.23}$$

is given by

$$\mathbf{P} = -\frac{c\rho(1-R_0)}{2} \begin{pmatrix} \frac{1}{c\rho^2(1-R_0)} & -cR_0 & -\frac{c}{N}R_0 \\ 0 & \frac{c\rho}{\delta} & \frac{k\lambda}{\delta} \\ 0 & N\rho & \rho \end{pmatrix}. \tag{2.24}$$

.

For the linear system $\dot{\widetilde{\mathbf{x}}} = \mathbf{A}\widetilde{\mathbf{x}}$, we consider the lyapunov function $U(\widetilde{\mathbf{x}}) = \widetilde{\mathbf{x}}^T\mathbf{P}\widetilde{\mathbf{x}}$. Then we have the inequalities as follows:

$$\begin{aligned} \xi_{\min}(\mathbf{P})||\widetilde{\mathbf{x}}||^2 &\leq U(\widetilde{\mathbf{x}}) \leq \xi_{\max}(\mathbf{P})||\widetilde{\mathbf{x}}||^2, && \text{(2.25a)} \\ \nabla_{\widetilde{\mathbf{x}}}U \cdot \mathbf{A}\widetilde{\mathbf{x}} = -\widetilde{\mathbf{x}}^T\mathbf{I}\widetilde{\mathbf{x}} &\leq -\xi_{\min}(\mathbf{I})||\widetilde{\mathbf{x}}||^2 = -||\widetilde{\mathbf{x}}||^2, && \text{(2.25b)} \\ ||\nabla_{\widetilde{\mathbf{x}}}U|| = ||2\widetilde{\mathbf{x}}^T\mathbf{P}|| &\leq 2||\mathbf{P}||\ ||\widetilde{\mathbf{x}}|| = 2\xi_{\max}(\mathbf{P})||\widetilde{\mathbf{x}}||, && \text{(2.25c)} \end{aligned}$$

where $\xi_{\min}(\mathbf{P})$ and $\xi_{\max}(\mathbf{P})$ denote the positive minimum and maximum eigen-

values of matrix $\mathbf{P}$, respectively. Let us split the system (2.2) by

$$\dot{\widetilde{\mathbf{x}}} = \mathbf{A}\widetilde{\mathbf{x}} + \mathbf{h}(\widetilde{\mathbf{x}}) + \mathbf{g}(u(t)), \tag{2.26}$$

where $\mathbf{g}(u(t))$ with the input function $u(t)$ is given by

$$\mathbf{g}(u(t)) = k\theta V(t)\left(\widetilde{T}(t) + \frac{\lambda}{\rho}\right)\begin{pmatrix} u(t) \\ -u(t) \\ 0 \end{pmatrix}. \tag{2.27}$$

Now, we are going to show that the Lyapunov function $U(\widetilde{\mathbf{x}})$ for the linear system $\dot{\widetilde{\mathbf{x}}} = \mathbf{A}\widetilde{\mathbf{x}}$ is indeed the proper function the system (2.78) satisfying (2.12).

By using (2.25b), we obtain

$$\dot{U}(\widetilde{\mathbf{x}}) = \nabla_{\widetilde{\mathbf{x}}} U \cdot \dot{\widetilde{\mathbf{x}}} \leq -||\widetilde{\mathbf{x}}||^2 + ||\nabla_{\widetilde{\mathbf{x}}} U||\ ||\mathbf{h}(\widetilde{\mathbf{x}})|| + ||\nabla_{\widetilde{\mathbf{x}}} U||\ ||\mathbf{g}(u(t))||. \tag{2.28}$$

Since the nonlinear part $\mathbf{h}(\widetilde{\mathbf{x}})$ satisfies $\lim_{||\widetilde{\mathbf{x}}||\to 0} ||\mathbf{h}(\widetilde{\mathbf{x}})|| = 0$, for any $\epsilon > 0$, there exists a constant $r > 0$ such that

$$||\mathbf{h}(\widetilde{\mathbf{x}})|| < \epsilon \quad \text{as} \quad ||\widetilde{\mathbf{x}}|| < r. \tag{2.29}$$

In addition, $\mathbf{g}(u(t))$ with the input function $u(t)$ satisfies the following inequality:

$$||\mathbf{g}(u(t))|| < \theta\left(\epsilon + \frac{\lambda k}{\rho}||\widetilde{\mathbf{x}}||\right)||u(t)|| \tag{2.30}$$

Substituting (2.29) and (2.30) into (2.28), and using the inequality (2.25c),

we have

$$\dot{U}(\widetilde{\mathbf{x}}) < -||\widetilde{\mathbf{x}}||^2 + 2\xi_{\max}(\mathbf{P})\epsilon||\widetilde{\mathbf{x}}|| + 2\xi_{\max}(\mathbf{P})\theta\left(\epsilon||\widetilde{\mathbf{x}}|| + \frac{\lambda k}{\rho}||\widetilde{\mathbf{x}}||^2\right)||u(t)||. \quad (2.31)$$

Let $D_{r_u} = \{u(t) \in \mathbb{R} \mid ||u(t)|| < r_u\}$ and $D_r = \{\widetilde{\mathbf{x}} \in \mathbb{R}^3 \mid ||\widetilde{\mathbf{x}}|| < r\}$. We choose a sufficiently small constant $r_u > 0$ and consider a constant r satisfying

$$\left(2\xi_{\max}(\mathbf{P})r\left(\epsilon + \theta\left(\epsilon + \frac{\lambda k}{\rho}r\right)r_u\right)z^{-1}\right)^{1/2} < r\left(\frac{\xi_{\min}(\mathbf{p})}{\xi_{\max}(\mathbf{p})}\right)^{1/2}. \quad (2.32a)$$

in order to estimate the bounds on the initial state and input (the constants k_1 and k_2 in Definition 2.1.6 and Theorem 2.1.7). By recalling (2.31), we get

$$\begin{aligned}\dot{U}(\widetilde{\mathbf{x}}) &< -(1-z)||\widetilde{\mathbf{x}}||^2 - z||\widetilde{\mathbf{x}}||^2 \\ &\quad 2\xi_{\max}(\mathbf{P})\left(\epsilon r + \theta\left(\epsilon r + \frac{\lambda k}{\rho}r^2\right)||u(t)||\right),\ (0<z<1) \quad (2.33)\\ &\leq -(1-z)||\widetilde{\mathbf{x}}||^2,\end{aligned}$$

where $\left(\frac{2\xi_{\max}(\mathbf{P})r\left(\epsilon+\theta\left(\epsilon+\frac{\lambda k}{\rho}r\right)||u(t)||\right)}{z}\right)^{1/2} < ||\widetilde{\mathbf{x}}|| < r$. From (2.25c) and (2.33), we finally find the explicit forms of class $\mathcal{K}$ functions on $D_r \times D_{r_u}$,

$$\begin{aligned}\alpha_1(||\widetilde{\mathbf{x}}||) &= \xi_{\min}(\mathbf{P})||\widetilde{\mathbf{x}}||^2,\\ \alpha_2(||\widetilde{\mathbf{x}}||) &= \xi_{\max}(\mathbf{P})||\widetilde{\mathbf{x}}||^2,\\ \alpha_3(||\widetilde{\mathbf{x}}||) &= (1-z)||\widetilde{\mathbf{x}}||^2\\ \omega(||u||) &= \left(\frac{2\xi_{\max}(\mathbf{P})r\left(\epsilon + \theta\left(\epsilon + \frac{\lambda k}{\rho}r\right)||u(t)||\right)}{z}\right)^{1/2}\end{aligned}$$

Therefore, the system (2.78) is locally input–to–state stable by Theorem 2.1.7

with

$$
\begin{aligned}
k_1 &= \alpha_2^{-1}(\alpha_1(r)) = r\left(\frac{\xi_{\min}(\mathbf{P})}{\xi_{\max}(\mathbf{P})}\right)^{1/2}, \\
k_2 &= \omega^{-1}(\min\{k_1, \omega(r_u)\}) = r_u, \\
\gamma(a) &= \alpha_1^{-1} \circ \alpha_2 \circ \omega(a) = \left(\frac{2\xi_{\max}^2(\mathbf{p}) r \left(\epsilon + \theta\left(\epsilon + \frac{\lambda k}{\rho} r\right) a\right)}{z\xi_{\min}(\mathbf{p})}\right)^{1/2}
\end{aligned}
$$

Note that the condition (2.32a) of choosing r is equivalent to $\frac{k_1}{\omega(r_u)} > 1$.
In addition, following proposition shows the stability property for the second equilibrium point $\bar{E}$ of system (2.2).

Proposition 2.1.11. *The system* (2.2) *is locally input–to–state stable in some neighborhood of* $(T(t), T^*(t), V(t),\, u(t))^T = (\frac{\lambda}{\rho}\frac{1}{R_0}, \frac{\lambda}{\delta}\left(1 - \frac{1}{R_0}\right), \frac{\rho}{k}(R_0 - 1), 0)^T$. *Moreover, a viral persistence equilibrium point* $\bar{E}$ *of the system* (2.2) *is stable if* $R_0 > 1$.

Proof. In order to apply Theorem 2.1.7, a proper lyapunov function U satisfying (2.12) is needed. For this purpose, we consider the unforced system of (2.2) which is the system when the forcing input function $u(t) = 0$. Then it has the second equilibrium point $\bar{E} = \left(\frac{\lambda}{\rho}\frac{1}{R_0}, \frac{\lambda}{\delta}\left(1 - \frac{1}{R_0}\right), \frac{\rho}{k}(R_0 - 1)\right)^T$ which is called as viral persistence equilibrium. By using the change of variable

$$
\widetilde{T}(t) = T(t) - \frac{\lambda}{\rho}\frac{1}{R_0}.\ \widetilde{T^*}(t) = T^*(t) - \frac{\lambda}{\delta}\left(1 - \frac{1}{R_0}\right),\ \widetilde{V}(t) = V(t) - \frac{\rho}{k}(R_0 - 1),
$$

the unforced system becomes

$$
\begin{aligned}
\frac{d\widetilde{T}(t)}{dt} &= -(\rho R_0)\widetilde{T}(t) - \frac{c\widetilde{V}(t)}{N} - k\widetilde{T}(t)\widetilde{V}(t), \\
\frac{d\widetilde{T^*}(t)}{dt} &= k\widetilde{T}(t)\widetilde{V}(t) + \rho(R_0 - 1)\widetilde{T}(t) + \frac{c\widetilde{V}(t)}{N} - \delta\widetilde{T^*}(t), \\
\frac{d\widetilde{V}(t)}{dt} &= N\delta\widetilde{T^*}(t) - c\widetilde{V}(t).
\end{aligned} \tag{2.34}
$$

By introducing $\widetilde{\mathbf{x}} = (\widetilde{T}(t), \widetilde{T^*}(t), \widetilde{V}(t))^T$, the linearized system of(2.34) at the viral persistence equilibrium point can be expressed as

$$\dot{\widetilde{\mathbf{x}}} = \mathbf{A}\widetilde{\mathbf{x}} + \mathbf{h}(\widetilde{\mathbf{x}}),$$

where the Jacobian matrix $\mathbf{A}$ and the nonlinear part $\mathbf{h}(\widetilde{\mathbf{x}})$ are given by

$$\mathbf{A} = \begin{pmatrix} -\rho R_0 & 0 & -\frac{c}{N} \\ \rho(R_0 - 1) & -\delta & \frac{c}{N} \\ 0 & N\delta & -c \end{pmatrix}, \quad \mathbf{h}(\widetilde{\mathbf{x}}) = k\widetilde{T}(t)\widetilde{V}(t) \begin{pmatrix} -1 \\ 1 \\ 0 \end{pmatrix}.$$

From the Routh-Hurwitz criteria in Theorem 2.1.9, all eigenvalues of $\mathbf{A}$ have negative real parts if and only if $R_0 - 1 > 0$. Hence the persistence equilibrium point of the linear system $\dot{\widetilde{\mathbf{x}}} = \mathbf{A}\widetilde{\mathbf{x}}$ is uniformly asymptotically stable only when $R_0 > 1$.

Theorem 2.1.8 gives a symmetric positive definite matrix $\mathbf{P}$, given by

$$\mathbf{p} = \frac{1}{2(R_0 - 1)} \begin{pmatrix} 0 & -\frac{1}{\rho} & -\frac{1}{N\rho} \\ \frac{(R_0-1)}{\delta} & \frac{R_0}{\delta} & \frac{1}{N\delta} \\ \frac{N(R_0-1)}{c} & \frac{(NR_0)}{c} & \frac{R_0}{c} \end{pmatrix}.$$

For the linear system $\dot{\widetilde{\mathbf{x}}} = \mathbf{A}\widetilde{\mathbf{x}}$, we consider the Lyapunov function $U(\widetilde{\mathbf{x}}) = \widetilde{\mathbf{x}}^T\mathbf{P}\widetilde{\mathbf{x}}$ and we have the inequalities (2.25).

Let us split the system (2.2) by

$$\dot{\widetilde{\mathbf{x}}} = \mathbf{A}\widetilde{\mathbf{x}} + \mathbf{h}(\widetilde{\mathbf{x}}) + \mathbf{g}(u(t)), \tag{2.35}$$

where $\mathbf{g}(u(t))$ with the input function $u(t)$ is given by

$$\mathbf{g}(u(t)) = \theta \left(\rho(R_0 - 1)\widetilde{T}(t) + \frac{c\widetilde{V}(t)}{N} + \lambda(1 - \frac{1}{R_0}) + k\widetilde{T}(t)\widetilde{V}(t) \right) \begin{pmatrix} u(t) \\ -u(t) \\ 0 \end{pmatrix}.$$

Now, we are going to show that the Lyapunov function $U(\widetilde{\mathbf{x}})$ for the linear system $\dot{\widetilde{\mathbf{x}}} = \mathbf{A}\widetilde{\mathbf{x}}$ is indeed the proper function the system (2.78) satisfying (2.12).

By using (2.25b), we obtain

$$\dot{U}(\widetilde{\mathbf{x}}) = \nabla_{\widetilde{\mathbf{x}}} U \cdot \dot{\widetilde{\mathbf{x}}} \leq -||\widetilde{\mathbf{x}}||^2 + ||\nabla_{\widetilde{\mathbf{x}}} U||\ ||\mathbf{h}(\widetilde{\mathbf{x}})|| + ||\nabla_{\widetilde{\mathbf{x}}} U||\ ||\mathbf{g}(u(t))||. \quad (2.36)$$

Since the nonlinear part $\mathbf{h}(\widetilde{\mathbf{x}})$ satisfy $\lim_{||\widetilde{\mathbf{x}}|| \to 0} ||\mathbf{h}(\widetilde{\mathbf{x}})|| = 0$, for any $\epsilon > 0$, there exists a constant $r > 0$ such that

$$||\mathbf{h}(\widetilde{\mathbf{x}})|| < \epsilon \quad \text{as} \quad ||\widetilde{\mathbf{x}}|| < r. \quad (2.37)$$

Moreover, $\mathbf{g}(u(t))$ with the input function $u(t)$ satisfies the following inequality:

$$||\mathbf{g}(u(t))|| < \theta \left(\rho R_0 \widetilde{T}(t) + \frac{c\widetilde{V}(t)}{N} + \lambda + \epsilon \right) ||u(t)||. \quad (2.38)$$

Substituting (2.37) and (2.38) into (2.36), and using the inequality (2.25c), we have

$$\begin{aligned} \dot{U}(\widetilde{\mathbf{x}}) < & - ||\widetilde{\mathbf{x}}||^2 + 2\xi_{\max}(\mathbf{P})\theta \left(\rho R_0 + \frac{c}{N} \right) ||u(t)||||\widetilde{\mathbf{x}}||^2 \\ & + 2\xi_{\max}(\mathbf{P})||\widetilde{\mathbf{x}}|| \left(\epsilon + (\lambda + \epsilon)||u(t)|| \right). \end{aligned} \quad (2.39)$$

Let $D_{r_u} = \{u(t) \in \mathbb{R} \mid ||u(t)|| < r_u\}$ and $D_r = \{\widetilde{\mathbf{x}} \in \mathbb{R}^3 \mid ||\widetilde{\mathbf{x}}|| < r\}$. We choose constant r_u and r satisfying

$$\left(\frac{2\xi_{\max}(\mathbf{p})r\left(\theta\left(\rho R_0 + \frac{c}{N}\right)r_u r + (\epsilon + (\lambda+\epsilon)r_u)\right)}{z}\right)^{1/2} < r\left(\frac{\xi_{\min}(\mathbf{P})}{\xi_{\max}(\mathbf{P})}\right)^{1/2}, \tag{2.40a}$$

for $0 < z < 1$, in order to estimate the bounds on the initial state and input (the constants k_1 and k_2 in Definition 2.1.6 and Theorem 2.1.7).
By recalling (2.39), we get

$$\begin{aligned}\dot{U}(\widetilde{\mathbf{x}}) &< -(1-z)||\widetilde{\mathbf{x}}||^2 - z||\widetilde{\mathbf{x}}||^2 \\ &\quad + 2\xi_{\max}(\mathbf{p})r\left(\theta\left(\rho R_0 + \frac{c}{N}\right)||u(t)||r + (\epsilon + (\lambda+\epsilon)||u(t)||)\right), (0 < z < 1) \\ &\leq -(1-z)||\widetilde{\mathbf{x}}||^2,\end{aligned} \tag{2.41}$$

where $\left(\frac{2\xi_{\max}(\mathbf{p})r\left(\theta\left(\rho R_0+\frac{c}{N}\right)||u(t)||r+(\epsilon+(\lambda+\epsilon)||u(t)||)\right)}{z}\right)^{1/2} \leq ||\widetilde{\mathbf{x}}|| < r$. From (2.25c) and (2.41), we finally find the explicit forms of class $\mathcal{K}$ functions on $D_r \times D_{r_u}$,

$$\begin{aligned}&\alpha_1(||\widetilde{\mathbf{x}}||) = \xi_{\min}(\mathbf{P})||\widetilde{\mathbf{x}}||^2, \quad \alpha_2(||\widetilde{\mathbf{x}}||) = \xi_{\max}(\mathbf{P})||\widetilde{\mathbf{x}}||^2, \\ &\alpha_3(||\widetilde{\mathbf{x}}||) = (1-z)||\widetilde{\mathbf{x}}||^2 \\ &\omega(||u||) = \left(\frac{2\xi_{\max}(\mathbf{p})r\left(\theta\left(\rho R_0 + \frac{c}{N}\right)||u(t)||r + (\epsilon + (\lambda+\epsilon)||u(t)||)\right)}{z}\right)^{1/2}.\end{aligned}$$

Therefore, the split system is locally input–to–state stable by Theorem 2.1.7

with

$$\begin{aligned} k_1 &= \alpha_2^{-1}(\alpha_1(r)) = r\left(\frac{\xi_{\min}(\mathbf{P})}{\xi_{\max}(\mathbf{P})}\right)^{1/2}, \\ k_2 &= \omega^{-1}(\min\{k_1, \omega(r_u)\}) = r_u, \\ \gamma(a) &= \alpha_1^{-1} \circ \alpha_2 \circ \omega(a) = \left(\frac{2\xi_{\max}^2(\mathbf{p}) r \left(\theta\left(\rho R_0 + \frac{c}{N}\right) ar + (\epsilon + (\lambda + \epsilon)a)\right)}{z\xi_{\min}(\mathbf{p})}\right)^{1/2} \end{aligned}$$

□

From the above analysis, it is revealed that, for starting values sufficiently close to equilibrium, the long-term behavior depends solely on the value of R_0. It is a biologically reasonable explanation, given the definition of reproductive number.

We then discuss the positivity and boundedness of solutions to system (2.2).

Proposition 2.1.12. *Suppose* $\mathbf{x}$ *satisfy* (2.2) *and* $T_0 > 0, T_0^* > 0$ *and* $V_0 > 0$. *Then for any* $t_1 > 0$, $T(t), T^*(t)$, *and* $V(t)$ *will be bounded and remain in positive for all* $t \in [0, t_1]$.

Proof. Recall that all parameters $\mathbf{p}$ in the system (2.2) are positive. We first establish the property for some time interval $[0, t_1]$, then extend the proof to an arbitrary interval. Since we assumed positivity of initial conditions, there must be some $t_1 > 0$ such that $T(t), T^*(t)$, and $V(t)$ are positive. On this interval,

$$\frac{dT(t)}{dt} = \lambda - \rho T(t) - (1 - \theta u(t)) k T(t) V(t) \leq \lambda. \tag{2.42}$$

Solving for T gives

$$T(t) \leq T_0 + \lambda t \leq C_1(1+t), \tag{2.43}$$

where the constant C_1 satisfying $C_1 \leq \max\{\lambda, T_0\}$. In particular, there is constant bound for T which is uniform in time. Next, we can place lower bounds on $\frac{dT^*}{dt}$ and $\frac{dV}{dt}$. On the interval $(0, t_1]$, we have

$$\frac{dT^*(t)}{dt} = (1-\theta u(t))kT(t)V(t) - \delta T^*(t) \geq -\delta T^*(t)$$

and

$$\frac{dV(t)}{dt} = N\delta T^*(t) - cV(t) \geq -cV(t).$$

Using separation of variables, we re–write these differential inequalities to find

$$T^*(t) \geq T_0^* e^{-\delta t} > 0 \quad \text{and} \quad V(t) \geq V_0 e^{-ct} > 0. \tag{2.44}$$

Meanwhile, a summation of $\frac{dT^*(t)}{dt}$ with $\frac{dV(t)}{dt}$ has bounds,

$$\begin{aligned}\frac{d}{dt}(T^*+V)(t) &= (1-\theta u(t))kT(t)V(t) + (N-1)\delta T^*(t) - cV(t) \\ &\leq kT(t)V(t) + N\delta T^*(t), \quad t \in [0, t_1].\end{aligned}$$

Recall that the bound on $T(t)$, a substitution gives

$$\frac{d}{dt}(T^*+V)(t) \leq kC_1(1+t)V(t) + N\delta T^*(t) \leq C_2(1+t)(T^*+V)(t), \tag{2.45}$$

where $C_2 \geq \max\{kC_1, N\delta\}$. Solving the differential equation (2.45) yields

$$(T^*(t) + V(t)) \leq C_3 e^{t^2}$$

for $t \in [0, t_1]$ where C_3 depends upon C_2, T_0^* and V_0 only. Since $T^*(t)$ is positive from (2.44), we can place an upper bound on $V(t)$ by $V(t) \leq C_3 e^{t^2}$.

Additionally, since $V(t)$ is also positive, it follows that $T^*(t)$ must be as well, hence, $T^*(t) \leq C_3 e^{t^2}$. With these bounds in place, we can now examine $T(t)$ and bound it from below using

$$\begin{aligned} \frac{dT(t)}{dt} &= \lambda - \rho T(t) - kT(t)V(t) \geq -\rho T(t) - (1 - \theta u(t))kT(t)V(t) \\ &\geq -\rho T(t) - kC_3 e^{t^2} T(t) \geq -C_4(1 + e^{t^2})T(t), \quad t \in [0, t_1], \end{aligned} \tag{2.46}$$

where $C_4 \geq \max\{\rho, kC_3\}$. Shifting the last term to the other side of the in equation (2.46) gives

$$\frac{dT(t)}{dt} + C_4(1 + e^{t^2})T(t) \geq 0,$$

and we find that for $t \in [0, t_1]$,

$$T(t) \geq T_0 \exp(-C_4 \int_0^t (1 + e^{\tau^2}) d\tau) > 0.$$

We have proven boundedness and positivity of solution on the interval $(0, t_1]$ for some $t_1 > 0$. We attempt to establish the property for any positive time. We note that at this t_1, T, T^*, V are positive and continuous so there is some c_1 such that T, T^*, V remain positive for $t \in (t_1, t_1 + c_1]$. Repeating this argument indefinitely, we arrive a maximal interval of existence for the solutions. It we assume this interval is finite, then we may say the interval is $(0, S]$, where

$$S = \sup\{t \in \mathbb{R} : T(\tau), T^*(\tau), V(\tau) > 0 \text{ for all } \tau \in [0, t]\} < \infty.$$

On the interval $(0, S]$, the solution will remain positive and bounded. However,

by the definition of S, one of $\mathbf{x}(S)$ must be equal to zero or else, by continuity, S would not be the supremum of the set. This we see that our solutions are positive on the closed interval $(0, S]$ and yet one of the solution must equal to zero at S. This provides a contradiction so we see that this interval must be infinite. □

Therefore, we conclude that the solutions remain positive and bounded for all positive time. That is, for any $t_1 > 0$, $T(t), T^*(t), V(t)$ are bounded and remain positive for all $t \in [0, t_1]$.

Decline phase analysis with perfect inhibition

If one assume that initially a person is uninfected and then introduces a small amount of virus, the solution of equation (2.2) mimics the kinetics of primary HIV infection. To analyze the effects of giving an ART drug, if a 100% effective RTIs and PIs are given to an individual at steady state with viral load, $\bar{V}$, one can investigate the decline dynamics of free virus, and this approach is proposed by Perelson et al.,[116, 112] to measure the rate of loss of viral infectivity. Applying this, the model equations (2.2) become:

$$\begin{aligned} \frac{dT}{dt} &= \lambda - \rho T, \qquad T(t_0) = \bar{T} \\ \frac{dT^*}{dt} &= -\delta T^*, \qquad T^*(t_0) = \bar{T^*} \\ \frac{dV}{dt} &= N\delta T^* - cV, \qquad V(t_0) = \bar{V} \end{aligned} \tag{2.47}$$

and this gives rise to the following state solution for virion population

$$V(t) = \bar{V}e^{-ct} + \frac{N\delta \bar{T^*}}{c-\delta}(e^{-\delta t} - e^{-ct}). \tag{2.48}$$

From the above equation, we can find that in a perfect inhibition, the infectious virus should decay exponentially with slope c. Assuming that the viral load

decay will obey above equation, one can confirm the estimate of parameters c, the rate of clearance of free virions, and δ, lifespan of productively infected $CD4^+$ lymphocytes, using patient data. Perelson et al.[116, 112] proposed this method to independently estimate model parameters so that prevent multiple local solutions which confound nonlinear least squares or maximum-likelihood fitting.

Parameter Constraints

We also consider the behavior of steady state virus quantity of the system δT^* with on-treatment, to examine the relation between drug efficacy and reproductive number. When $u(t) = 1,\ t \geq t_0$, the amount of virus presence at steady state, denoted by $\bar{V}_d$, is

$$\bar{V}_d = \frac{\rho}{k}\left(R_0 - \frac{1}{(1-\theta)}\right). \tag{2.49}$$

From the Eq.(2.49), we find that increasing drug efficacy causes the infection rate k to decrease, which in turn increases the number of available target cells. Denoting μ the fraction of the pre-treatment steady state viral load ($\bar{V}$ in (2.9)) present for a given drug efficacy, if drug therapy reduces the viral load by n-logs, μ would be 10^{-n} and this can be written as

$$\mu = \frac{\bar{V}_d}{\bar{V}} = \frac{R_0 - \frac{1}{(1-\theta)}}{R_0 - 1}, \tag{2.50}$$

and solving for θ gives

$$\theta = 1 - \frac{1}{R_0 - f(R_0 - 1)}, \tag{2.51}$$

which can be interpreted as a required drug efficacy for viral load drop by desired proportionality μ. Perelson et al.[116, 112] refer to the drug efficacy,

which corresponds to $\bar{V}_d = 0$ or equivalently $\mu = 0$ as the 'critical efficacy' and let denote it by θ_0. Then

$$\theta_0 = 1 - \frac{1}{R_0}, \tag{2.52}$$

and we note that the infected steady state, $\bar{V}_d$, becomes negative for $\theta > \theta_0$, i.e., the drug will extinguish the viral population. Although the results of the model indicate that extinction should occur, it appears that the viral population is not extinguished in any patients studied and several clinical results indicate that extinction of the viral population does not occur under HAART(Chun et al.,[25]; Dornadula et al., [41]; Furtado et al., [54]; Natarajan et al., [105]; Zhang et al., [168]; Sharkey et al., [142]). Perelson suggest that one must conclude that no patients have experienced drug efficacies greater than or equal to the critical efficacy. Thus, models with a concave down relationship between steady state viral load during treatment and efficacy contradict clinical results, which implement that the three component model (2.2) is poorly suited for modeling low steady state viral loads.This gives you an opportunity to search for advanced models that do not have these flaws and as a result gained insight into mechanisms that do or do not play a role in maintaining low virus loads in drug treatments.

According to [75], because T cell counts and viral loads in HIV-infected patients generally change very slowly before ART is initiated, it is reasonable to assume that these and other related system variables are at a quasi-steady state before treatment. This condition the can be used to identify relations existing among parameters and thus to limit the ranges of values parameter can take. At pre-treatment, quasi-steady state $kTV - \delta T^* = 0$ and $N\delta T^* - cV = 0$. Further, $T^*_{ps} = \frac{cV_{ps}}{N\delta}$, where the subscript ps us used to denote a pre-treatment quasi-steady state value, correspond to a fraction of plasma virus produced by

productively infected cells. Then this yields the following parameter constraint:

$$k = \frac{c}{NT_{ps}}. \tag{2.53}$$

Although above basic three component model can be used to describe the acute HIV infection. If the infection becomes worse than a certain period of time, however, the applicability of the three component models is lost. More complex models which can describe the spread of HIV within the body and its development toward AIDS, are then required. In this paper, we consider HIV models which account for the latently infected cell population and chronical infection, which are related with two phase of viral decay and are recognized as the major reason for successive viral rebound even with HAART.

2.1.2 Chronical infection model

We now investigate more sophisticated versions of three component HIV model with respect to persistence of low-level viral load. Drug perturbation studies have found that as plasma HIV-1 decays under drug therapy, there are several observable phases of the decay. The most rapid occurs as free virus is cleared from the blood (due to the rate constant c) and establishes a quasi-steady state with the number of infected cells. The next phase is due to the decline to productively infected cells, and has been used to determine the rate constant δ. This phase is characterized by an exponential fall in viral load, and has been termed the 'first'(observable) phase. A later (second) phase has been observed, and this has been attributed to the decay of 'chronically' infected cells, or cells which produce much smaller amounts of virus than the main population of infected cells, and, perhaps as a consequence, die at a much slower rate. Of concern for HIV-infected patients experiencing recurrent episodes of transient viremia include the potential effects on the chronic infection that

may serve as viral reservoirs. It is known that the effects on chronically infected cells are more lingering than the productively infected cells. A standard representation presented by Perelson et al.,[112] of a system with this second type of infected cell population is as follow.

$$\begin{aligned}
\frac{dT}{dt} &= \lambda - \rho T - kTV, \qquad T(t_0) = T_0 \\
\frac{dT^*}{dt} &= (1-\epsilon_c)kTV - \delta T^*, \qquad T^*(t_0) = T_0^* \\
\frac{dT_c^*}{dt} &= \epsilon_c kTV - \mu T_c^*, \qquad T_c^*(t_0) = T_{c,0}^* \\
\frac{dV}{dt} &= N\delta T^* + N_c \mu T_c^* - cV, \qquad V(t_0) = V_0.
\end{aligned} \tag{2.54}$$

In this model, Perelson et al.,[112] allow heterogeneity in target cells by allowing 2 co-circulating populations of target cells. They assume that most infected cells are short-lived($I(t)$), a small proportion is assumed to be chronically infected($I_c(t)$). Chronically infected cells are assumed to have lower mortality and to produce virus at a slower rate than short-lived infected cells. The antigen activates a fraction of CD4+ T cells at a rate ϵ_c and leads to HIV production from these two types of infected populations and is cleared from the body at a constant rate per viral particle. The chronically infected cells die with a rate constant μ, and N_c is an average number of virions produced in the lifetime of chronically infected cells

Variable/Parameter	Units	Description
T_c^*	$cells/ml$	Chronically infected $CD4^+$ T cell density.
$\epsilon_c \in [0,1]$	-	fraction of uninfected T cells that upon infection become chronical.
μ	day^{-1}	death rate of chronically infected cell(lysis).
N_c	$\frac{copies}{cell}$	Number of free virus produced by a chronically infected T cell.

Table 2.2: A description of variables and parameters of the chronic infection model

We now derive the reproductive number for the system (2.54). Following the assumption applied in the derivation of reproductive number for the previous model (2.2), we consider the constant population number of healthy T cell is constant in uninfected period, so that we have $T(t) = \frac{\lambda}{\rho}$. Let us denote the population of PI cell and CI cell in a unit volume at time $t = 0$ by T_1^* and $T_{c,1}^*$, respectively. From the second and the third equations of (2.54), two types of infected cell population can be obtained by $T^*(t) = T_1^* e^{-\delta(t-t_0)}$ and $T_c^*(t) = T_{c,1}^* e^{-\mu(t-t_0)}$ in uninfected period. Setting $t_0 = 0$ and $V_0 = 0$, we solve for $V(t)$ by substituting $T^*(t)$ and $T_c^*(t)$ into the fourth equation of (2.54) and this gives

$$V(t) = \frac{N\delta T_1^*}{c-\delta}(-e^{-\delta t} - e^{-ct}) + \frac{N_c \mu T_{c,1}^*}{c-\mu}(-e^{-\mu t} - e^{-ct}). \tag{2.55}$$

By the definition of the reproductive number, the secondary population of PI T cell with $T_1^* = 1$ and $T_{c,1}^* = 0$, is obtained by $\frac{(1-\epsilon_c)\lambda k}{\rho}\left(\frac{N}{c}\right)$. In the same way, the secondary population density of the CI T cell with $T_{c,1}^* = 1$ is given by $\frac{\epsilon_c(\lambda k)}{\rho}\left(\frac{N_c}{c}\right)$. Then the overall reproductive number derived from the model (2.54) is given by

$$R_0^c = \frac{\lambda k\left((1-\epsilon_c)N + \epsilon_c N_c\right)}{c\rho}. \tag{2.56}$$

We note that $R_0^c = R_0$ if the proportionality of chronic infection is zero, i.e., $\epsilon_c = 0$.

Proposition 2.1.13. *The system* (2.54) *is locally input–to–state stable in some neighborhood of* $(T(t), T^*(t), T_c^*(t), V(t), u(t))^T = \left(\frac{\lambda}{\rho R_0^c}, \frac{\lambda(1-\epsilon_c)}{\delta}\left(1 - \frac{1}{R_0^c}\right), \frac{\lambda\epsilon_c}{\mu}\left(1 - \frac{1}{R_0^c}\right), \frac{\rho(R_0^c-1)}{k}, 0\right)^T$. *Moreover,a viral persistence equilibrium point* $\left(\frac{\lambda}{\rho R_0^c}, \frac{\lambda(1-\epsilon_c)}{\delta}\left(1 - \frac{1}{R_0^c}\right), \frac{\lambda\epsilon_c}{\mu}\left(1 - \frac{1}{R_0^c}\right), \frac{\rho(R_0^c-1)}{k}\right)^T$ *of the system* (2.54) *is stable when* $a_3 > 0,\ a_1a_2a_3 > a_3^2 + a_1^2a_4$ *for the coefficients in 2.58, and* $R_{c,0} > \frac{1}{k\lambda}$.

Proof. In order to apply Theorem 2.1.7, a proper lyapunov function U sat-

isfying (2.12) is required. For this purpose, we consider a system when the input $u(t) = 0$, called the unforced system of (2.54). Then an equilibrium point $(\frac{\lambda}{\rho R_0^c}, \frac{\lambda(1-\epsilon_c)}{\delta}\left(1-\frac{1}{R_0^c}\right), \left(\frac{\lambda\epsilon_c}{\mu}\right)\left(1-\frac{1}{R_0^c}\right), \frac{\rho(R_0^c-1)}{k})^T$ is obtained from the unforced system of (2.54). By using the change of variables

$$\widetilde{T}(t) = T(t) - \frac{\lambda}{\rho R_0^c}, \quad \widetilde{T^*}(t) = T^*(t) - \frac{\lambda(1-\epsilon_c)}{\delta}\left(1-\frac{1}{R_0^c}\right),$$
$$\widetilde{T_c^*}(t) = T_c^*(t) - \left(\frac{\lambda\epsilon_c}{\mu}\right)\left(1-\frac{1}{R_0^c}\right), \quad \widetilde{V}(t) = V(t) - \frac{\rho(R_0^c-1)}{k},$$

the unforced system becomes

$$\begin{aligned}
\frac{d\widetilde{T}(t)}{dt} &= -(\rho R_0^c)\widetilde{T}(t) - \left(\frac{\lambda k}{\rho R_0^c}\right)\widetilde{V}(t) - k\widetilde{T}(t)\widetilde{V}(t),\\
\frac{d\widetilde{T^*}(t)}{dt} &= (1-\epsilon_c)\left\{k\widetilde{T}(t)\widetilde{V}(t) + \rho(R_0^c-1)\widetilde{T}(t) + \left(\frac{\lambda k}{\rho R_0^c}\right)\widetilde{V}(t)\right\} - \delta\widetilde{T^*}(t),\\
\frac{d\widetilde{T_c^*}(t)}{dt} &= \epsilon_c\left\{k\widetilde{T}(t)\widetilde{V}(t) + \rho(R_0^c-1)\widetilde{T}(t) + \left(\frac{\lambda k}{\rho R_0^c}\right)\widetilde{V}(t)\right\} - \mu\widetilde{T_c^*}(t),\\
\frac{d\widetilde{V}(t)}{dt} &= N\delta\widetilde{T^*}(t) + N_c\mu\widetilde{T_c^*}(t) - c\widetilde{V}(t).
\end{aligned} \tag{2.57}$$

For notational convenience, we denote the variables with $\widetilde{\mathbf{x}} = (\widetilde{T}(t), \widetilde{T^*}(t), \widetilde{T_c^*}(t), \widetilde{V}(t))^T$. Then the linearized system of(2.57) at the viral persistence equilibrium point can be expressed as

$$\dot{\widetilde{\mathbf{x}}} = \mathbf{A}\widetilde{\mathbf{x}} + \mathbf{h}(\widetilde{\mathbf{x}}),$$

where the Jacobian matrix $\mathbf{A}$ and the nonlinear part $\mathbf{h}(\widetilde{\mathbf{x}})$ are given by

$$\mathbf{A} = \begin{pmatrix} -\rho R_0^c & 0 & 0 & -\left(\frac{\lambda k}{\rho R_0^c}\right) \\ \rho(1-\epsilon_c)(R_0^c-1) & -\delta & 0 & \frac{\lambda k(1-\epsilon_c)}{\rho R_0^c} \\ \rho\epsilon_c(R_0^c-1) & 0 & -\mu & \frac{\lambda k \epsilon_c}{\rho R_0^c} \\ 0 & N\delta & N_c\mu & -c \end{pmatrix}, \mathbf{h}(\widetilde{\mathbf{x}}) = k\widetilde{T}(t)\widetilde{V}(t) \begin{pmatrix} -1 \\ (1-\epsilon_c) \\ \epsilon_c \\ 0 \end{pmatrix}.$$

From the Routh-Hurwitz criteria, all eigenvalues of $\mathbf{A}$ have negative real parts when

$$\begin{aligned} a_1 &= R_0^c\rho + c + \delta + \mu, \\ a_2 &= R_0^c\rho(c+\delta+\mu) + (c\delta + c\mu + \delta\mu) - \frac{\lambda k M}{\rho R_0^c},\ M = (1-\epsilon_c)N\delta + N_c\epsilon_c\mu, \\ a_3 &= R_0^c\rho(c\delta + c\mu + \delta\mu) - c\delta\mu - \frac{(k\lambda)^2 M}{R_0^c}, \\ a_4 &= \mu\delta c\rho(k\lambda R_0^c - 1), \end{aligned} \tag{2.58}$$

satisfy condition(2.18c), where $\{a_i\}_{i=1}^4$ is the corresponding coefficients referred in Theorem 2.1.9. We note that all model parameters are assumed to be positive, and the viral persistence equilibrium point of the linear system $\dot{\widetilde{\mathbf{x}}} = \mathbf{A}\widetilde{\mathbf{x}}$ is uniformly asymptotically stable only when $a_3 > 0,\ a_1a_2a_3 > a_3^2 + a_1^2a_4$, and $R_0^c > \frac{1}{k\lambda}$.

Theorem 2.1.8 gives a symmetric positive definite matrix $\mathbf{P}$, given by

$$\mathbf{p} = \frac{1}{2c\rho(1-R_0^c)} \begin{pmatrix} \frac{1}{\rho} & -\frac{Nk\lambda}{\rho} & -\frac{(N_ck\lambda)}{\rho} & -\frac{(k\lambda)}{\rho} \\ 0 & \frac{(c\rho - N_c\epsilon_c k\lambda)}{\delta} & \frac{N_ck\lambda(1-\epsilon_c)}{\delta} & \frac{k\lambda(1-\epsilon_c)}{\delta} \\ 0 & \frac{(N\epsilon_c k\lambda)}{\mu} & \frac{(c\rho - Nk\lambda + N\epsilon_c k\lambda)}{\mu} & \frac{(\epsilon_c k\lambda)}{\mu} \\ 0 & N\rho & N_c\rho & \rho \end{pmatrix}.$$

For the linear system $\dot{\widetilde{\mathbf{x}}} = \mathbf{A}\widetilde{\mathbf{x}}$, we consider the Lyapunov function $U(\widetilde{\mathbf{x}}) =$

$\widetilde{\mathbf{x}}^T\mathbf{P}\widetilde{\mathbf{x}}$ and we have the inequalities (2.25).

Let us split the system (2.54) by

$$\dot{\widetilde{\mathbf{x}}} = \mathbf{A}\widetilde{\mathbf{x}} + \mathbf{h}(\widetilde{\mathbf{x}}) + \mathbf{g}(u(t)), \tag{2.59}$$

where $\mathbf{g}(u(t))$ with the input function $u(t)$ is given by

$$\mathbf{g}(u(t)) = k\theta\left(\widetilde{T}(t) + \frac{\lambda}{\rho R_0^c}\right)\left(\widetilde{V}(t) + \frac{\rho(R_0^c - 1)}{k}\right)\begin{pmatrix} u(t) \\ -(1-\epsilon_c)u(t) \\ -\epsilon_c u(t) \\ 0 \end{pmatrix}.$$

Now, we are going to show that the Lyapunov function $U(\widetilde{\mathbf{x}})$ for the linear system $\dot{\widetilde{\mathbf{x}}} = \mathbf{A}\widetilde{\mathbf{x}}$ is indeed the proper function the system (2.78) satisfying (2.12).

By using (2.25b), we obtain

$$\dot{U}(\widetilde{\mathbf{x}}) = \nabla_{\widetilde{\mathbf{x}}}U \cdot \dot{\widetilde{\mathbf{x}}} \leq -||\widetilde{\mathbf{x}}||^2 + ||\nabla_{\widetilde{\mathbf{x}}}U||\ ||\mathbf{h}(\widetilde{\mathbf{x}})|| + ||\nabla_{\widetilde{\mathbf{x}}}U||\ ||\mathbf{g}(u(t))||. \tag{2.60}$$

Note that $0 < \epsilon_c < 1$, since the nonlinear part $\mathbf{h}(\widetilde{\mathbf{x}})$ satisfy $\lim_{||\widetilde{\mathbf{x}}||\to 0} ||\mathbf{h}(\widetilde{\mathbf{x}})|| = 0$, for any $\epsilon > 0$, there exists a constant $r > 0$ such that

$$||\mathbf{h}(\widetilde{\mathbf{x}})|| < \epsilon \quad \text{as} \quad ||\widetilde{\mathbf{x}}|| < r. \tag{2.61}$$

Moreover, $\mathbf{g}(u(t))$ with the input function $u(t)$ satisfies the following inequality:

$$||\mathbf{g}(u(t))|| < \theta\left(\rho R_0^c \widetilde{T}(t) + \frac{k\lambda\widetilde{V}(t)}{\rho R_0^c} + \lambda + \epsilon\right)||u(t)||. \tag{2.62}$$

Substituting (2.61) and (2.62) into (2.60), and using the inequality (2.25c), we have

$$\begin{aligned}\dot{U}(\widetilde{\mathbf{x}}) < & -||\widetilde{\mathbf{x}}||^2 + 2\xi_{\max}(\mathbf{P})\theta\left(\rho R_0^c + \frac{k\lambda}{\rho R_0^c}\right)||u(t)||||\widetilde{\mathbf{x}}||^2 \\ & + 2\xi_{\max}(\mathbf{P})||\widetilde{\mathbf{x}}||\left(\epsilon + (\lambda+\epsilon)||u(t)||\right).\end{aligned} \tag{2.63}$$

Let $D_{r_u} = \{u(t) \in \mathbb{R} \mid ||u(t)|| < r_u\}$ and $D_r = \{\widetilde{\mathbf{x}} \in \mathbb{R}^3 \mid ||\widetilde{\mathbf{x}}|| < r\}$. We choose constant r_u and r satisfying

$$\left(\frac{2\xi_{\max}(\mathbf{p})r\left(\theta\left(\rho R_0^c + \frac{k\lambda}{\rho R_0^c}\right)r_u r + (\epsilon + (\lambda+\epsilon)r_u)\right)}{z}\right)^{1/2} < r\left(\frac{\xi_{\min}(\mathbf{P})}{\xi_{\max}(\mathbf{P})}\right)^{1/2}, \tag{2.64a}$$

for $0 < z < 1$, in order to estimate the bounds on the initial state and input (the constants k_1 and k_2 in Definition 2.1.6 and Theorem 2.1.7).
By recalling (2.63), we get

$$\begin{aligned}\dot{U}(\widetilde{\mathbf{x}}) < & -(1-z)||\widetilde{\mathbf{x}}||^2 - z||\widetilde{\mathbf{x}}||^2 \\ & + 2\xi_{\max}(\mathbf{p})r\left(\theta\left(\rho R_0^c + \frac{k\lambda}{\rho R_0^c}\right)||u(t)||r + (\epsilon + (\lambda+\epsilon)||u(t)||)\right), \\ \leq & -(1-z)||\widetilde{\mathbf{x}}||^2, \quad (0 < z < 1),\end{aligned} \tag{2.65}$$

where $\left(\frac{2\xi_{\max}(\mathbf{p})r\left(\theta\left(\rho R_0^c + \frac{k\lambda}{\rho R_0^c}\right)||u(t)||r + (\epsilon+(\lambda+\epsilon)||u(t)||)\right)}{z}\right)^{1/2} \leq ||\widetilde{\mathbf{x}}|| < r$. From (2.25c) and (2.65), we finally find the explicit forms of class $\mathcal{K}$ functions on

$D_r \times D_{r_u}$,

$$\alpha_1(||\widetilde{\mathbf{x}}||) = \xi_{\min}(\mathbf{P})||\widetilde{\mathbf{x}}||^2, \quad \alpha_2(||\widetilde{\mathbf{x}}||) = \xi_{\max}(\mathbf{P})||\widetilde{\mathbf{x}}||^2, \quad \alpha_3(||\widetilde{\mathbf{x}}||) = (1-z)||\widetilde{\mathbf{x}}||^2,$$

$$\omega(||u||) = \left(\frac{2\xi_{\max}(\mathbf{p}) r \left(\theta \left(\rho R_0^c + \frac{k\lambda}{\rho R_0^c} \right) ||u(t)||r + (\epsilon + (\lambda + \epsilon)||u(t)||) \right)}{z} \right)^{1/2}.$$

Therefore, the split system is locally input–to–state stable by Theorem 2.1.7 with

$$\begin{aligned} k_1 &= \alpha_2^{-1}(\alpha_1(r)) = r \left(\frac{\xi_{\min}(\mathbf{P})}{\xi_{\max}(\mathbf{P})} \right)^{1/2}, \\ k_2 &= \omega^{-1}(\min\{k_1, \omega(r_u)\}) = r_u, \\ \gamma(a) &= \alpha_1^{-1} \circ \alpha_2 \circ \omega(a) \\ &= \left(\frac{2\xi_{\max}^2(\mathbf{p}) r \left(\theta \left(\rho R_0^c + \frac{k\lambda}{\rho R_0^c} \right) ar + (\epsilon + (\lambda + \epsilon)a) \right)}{z\xi_{\min}(\mathbf{p})} \right)^{1/2}. \end{aligned}$$

□

We then discuss the positivity and boundedness of solutions to system (2.54).

Proposition 2.1.14. *Suppose* $\mathbf{x}$ *satisfy* (2.54) *and* $T_0 > 0, T_0^* > 0, T_{c,0}^* > 0$ *and* $V_0 > 0$. *Then* $T(t), T^*(t), T_c^*(t)$, *and* $V(t)$ *are bounded and remain in positive for all* $t > 0$.

Proof. Recall that all parameters $\mathbf{p}$ in the system (2.54) are positive. We first establish the property for some time interval $[0, t_1]$, then extend the proof to an arbitrary interval. Since we assumed positivity of initial conditions, there must be some $t_1 > 0$ such that $T(t), T^*(t), T_c^*(t)$, and $V(t)$ are positive. On

this interval,

$$\frac{dT(t)}{dt} = \lambda - \rho T(t) - (1 - \theta u(t))kT(t)V(t) \leq \lambda. \tag{2.66}$$

Solving for $T(t)$ gives

$$T(t) \leq T_0 + \lambda t \leq C_1(1 + t), \tag{2.67}$$

where the constant C_1 satisfying $C_1 \leq \max\{\lambda, T_0\}$. In particular, there is constant bound for T which is uniform in time. Next, we can place lower bounds on $\frac{dT^*}{dt}$, $\frac{dT_c^*}{dt}$ and $\frac{dV}{dt}$. On the interval $(0, t_1]$, we have

$$\begin{aligned}
\frac{dT^*(t)}{dt} &= (1 - \epsilon_c)(1 - \theta u(t))kT(t)V(t) - \delta T^*(t) \geq -\delta T^*(t), \\
\frac{dT_c^*(t)}{dt} &= \epsilon_c(1 - \theta u(t))kT(t)V(t) - \mu T_c^*(t) \geq -\mu T_c^*(t), \\
\frac{dV(t)}{dt} &= N\delta T^*(t) + N_c\mu T_c^*(t) - cV(t) \geq -cV(t).
\end{aligned}$$

Using separation of variables, we re–write these differential inequalities to find

$$T^*(t) \geq T_0^* e^{-\delta t} > 0,\ T_c^*(t) \geq T_{c,0}^* e^{-\mu t} > 0, \quad \text{and} \quad V(t) \geq V_0 e^{-ct} > 0. \tag{2.68}$$

Recall that $u(t) \in [0, 1]$ for $t \geq 0$, a summation of $\frac{dT^*(t)}{dt}$, $\frac{dT_c^*(t)}{dt}$ with $\frac{dV(t)}{dt}$ has bound as follow.

$$\begin{aligned}
\frac{d}{dt}(T^* + T_c^* + V)(t) =& (1 - \theta u(t))kT(t)V(t) + (N - 1)\delta T^*(t) \\
&+ (N_c - 1)\mu T_c^*(t) - cV(t) \\
\leq& kT(t)V(t) + N\delta T^*(t) + N_c\mu T_c^*(t), \quad t \in [0, t_1].
\end{aligned}$$

Due to the bound on $T(t)$, a substitution gives

$$\begin{aligned}\frac{d}{dt}(T^* + T_c^* + V)(t) &\leq kC_1(1+t)V(t) + N\delta T^*(t) + N_c\mu T_c^*(t) \\ &\leq C_2(1+t)(T^* + T_c^* + V)(t),\end{aligned} \tag{2.69}$$

where $C_2 \geq \max\{kC_1, N\delta, N_c\mu\}$. Solving the differential equation (2.69) yields

$$T^*(t) + T_c^*(t) + V(t) \leq C_3 e^{t^2}$$

for $t \in [0, t_1]$ where C_3 depends upon $C_2, T_0^*, T_{c,0}^*$ and V_0 only. Since $T^*(t)$ and $T_c^*(t)$ are positive from (2.68), we can place an upper bound on $V(t)$ by $V(t) \leq C_3 e^{t^2}$.

Moreover, since $V(t)$ is also positive, it follows that both of $T^*(t)$ and $T_c^*(t)$ must be as well, hence, $T^*(t) \leq C_3 e^{t^2},\ T_c^*(t) \leq C_3 e^{t^2}$. With these bounds in place, we can now examin $T(t)$ and bound it from below using

$$\begin{aligned}\frac{dT(t)}{dt} &\geq -\rho T(t) - kT(t)V(t) \geq -\rho T(t) - kC_3 e^{t^2} T(t) \\ &\geq -C_4(1 + e^{t^2})T(t), \quad t \in [0, t_1],\end{aligned} \tag{2.70}$$

where $C_4 \geq \max\{\rho, kC_3\}$. Shifting the last term to the other side of the in equation (2.70) gives

$$\frac{dT(t)}{dt} + C_4(1 + e^{t^2})T(t) \geq 0,$$

and we find that for $t \in [0, t_1]$,

$$T(t) \geq T_0 \exp(-C_4 \int_0^t (1 + e^{\tau^2}) d\tau) > 0.$$

By applying the contradiction referred to in the Proposition 2.1.12 for the

model (2.2), we can conclude that for any $t_1 > 0$, $T(t), T^*(t), T_c^*(t), V(t)$ are bounded and remain positive for all $t \in [0, t_1]$. □

2.1.3 Latent infection model

As previously mentioned in 2.2, HIV-1 belongs to a class of retroviruses and the viral DNA copy on this process is called "provirus" and the status of infected T cell is distinguished by a provirus activity in cell. When the provirus is duplicated with cell DNA and reproduce themselves, then the host T cell population are in a productively infected status. The virion, however, can remain latent within a T cell while not being reproduced, giving no sign of its presence for months or years. Because of their latent state, these cells are not likely to be subject to immunosurveillance by HIV-specific T cells. Perhaps as a consequence, these cells persist during drug therapy (Chun[24]; Finzi [49];Wong [162]), either by replenishment from ongoing replication or an extremely long half-life.

Usually the resting memory $CD4^+$ T cell population harbor HIV-RNA as provirus, so they are usually called as latently infected cell. Occasional antigen-driven stimulation activates them to induce viral gene expression and it leads to viral replication and temporal expansion of rhe reservoirs. After all, this causes successive viral rebound even with potent ART. Latently infected cells thus pose a serious obstacle to eradicating the virus, suggesting that this population of cells could play a crucial role in maintaining a low steady state viral load during therapy. In 1997, Perelson [112] suggested that the second phase in the decay profile is probably due to sources such as activation of latently infected lymphocyte or release of trapped virions. They declared that decay of productively infected T cell population leave the secondary sourved as the major source which is reflected in the slope of the second-phase decline.

Assuming the overall drug efficacy θ implented in 2.1.2, a basic model of latent cell activation was proposed by Rong and Perelson et al.[134] as follow:

$$\begin{aligned}
\frac{dT}{dt} &= \lambda - \rho T - (1-\theta u(t))kTV, \quad T(0) = T_0 \\
\frac{dT^*}{dt} &= (1-\epsilon)(1-\theta u(t))kTV - \delta T^* + r_L L, \quad T^*(0) = T_0^* \\
\frac{dL}{dt} &= \epsilon(1-\theta u(t))kTV - (\delta_L + r_L)L, \quad L(0) = L_0 \\
\frac{dV}{dt} &= N\delta T^* - cV, \quad V(0) = V_0.
\end{aligned} \tag{2.71}$$

This model includes $L(t)$ representing a concentration of latently infected resting CD4$^+$ T cells that harbour virus which are not transcriptased yet, then they become infected and produce low level of virus[168]. The formation of latently infected resting cells was modelled by a proportionality, ϵ, of viral infections of target healthy T cells results in latency. Unlike with three component model(2.2), the productively infected cells are produced not only by infection of target cells but the activation of latently infected cells at rate $r_L L$ caused by interaction with their relevant antigen or other stimuli. Here the heterogeneity in the activation rate among latently infected cells[152, 151] are not taken into account and instead the average rate is assumed. They explicitly describe the death of latently infected cells by defining kinetic constants δ_L for the rate of death. A details for state and parameters of equation (2.71) are listed in 2.3.

Var/Par	Unit	Description
L	$cells/ml$	latently infected CD4$^+$ T cell density.
r_L	day^{-1}	activation rate of latently infected T cell.
$\epsilon \in [0,1]$	-	fraction of uninfected T cells that upon infection become latent.
δ_L	day^{-1}	death rate of activated resting memory cell(natural death).

Table 2.3: A description of variables and parameters of the latent cell activation model

To derive the reproductive number for model equations (2.71), To derive the reproductive number for latent model, we again assume the constant population density of the uninfected lymphocyte cell during the uninfected period, so that $T(t) = \frac{\lambda}{\rho}$. Let us denote the population of PI T cell and LI T cell in a unit volume at time $t = 0$ by T_1^* and L_1, respectively. From the second and third equations of (2.71), the population densities of both lymphocyte cells at time t are given by $L(t) = L_1 e^{-(r_L+\delta_L)t}$ and $T^*(t) = T_1^* e^{-\delta t} + BL_1(e^{-(r_L+\delta_L)t} - e^{-\delta t})$, where $B = \frac{r_L}{\delta-(r_L+\delta_L)}$. Substituting $T^*(t)$ and $L(t)$ into the fourth equation of (2.71) and multiplying integrating factor yield a analytic solution for the virus state $V(t)$ as follow:

$$V(t) = \frac{N\delta BL_1}{c-(r_L+\delta_L)}(e^{-(r_L+\delta_L)t} - e^{-ct}) + \frac{N\delta(T_1^* - BL_1)}{c-\delta}(e^{-\delta t} - e^{-ct}). \quad (2.72)$$

By the definition of the reproductive number, the secondary population of PI T cell with $T_1^* = 1$ and $L_1 = 0$, is obtained by $\frac{(1-\epsilon)\lambda k}{\rho}\left(\frac{N}{c}\right)$. With $T_1^* = 0$ and $L_1 = 1$, the secondary population density of the chronically infected T cell can be given by

$$\begin{aligned}
&\int_0^\infty \epsilon k T(t) V(t) dt \\
&= \frac{\epsilon\lambda k}{\rho}\left[\frac{N\delta B}{c-(r_L+\delta_L)}\int_0^\infty \left(e^{-(r_L+\delta_L)t} - e^{-ct}\right) dt - \frac{N\delta B}{c-\delta}\int_0^\infty \left(e^{-\delta t} - e^{-ct}\right) dt\right] \\
&= \frac{\epsilon\lambda k(N\delta B)}{\rho}\left[\frac{1}{c-(r_L+\delta_L)}\left(\frac{1}{r_L+\delta_L} - \frac{1}{c}\right) - \frac{1}{c-\delta}\left(\frac{1}{\delta} - \frac{1}{c}\right)\right] \\
&= \frac{\epsilon\lambda k(N\delta B)}{c\rho}\left[\frac{1}{(r_L+\delta_L)} - \frac{1}{\delta}\right] = \frac{\lambda kN)}{c\rho}\left(\frac{\epsilon r_L}{r_L+\delta_L}\right).
\end{aligned} \quad (2.73)$$

Then the overall reproductive number of infected lymphocytes in the system (2.71), denoted by R_0^L, is

$$R_0^L = \left((1-\epsilon) + \frac{\epsilon r_L}{r_L+\delta_L}\right) R_0. \quad (2.74)$$

and we note that $R_0^L = R_0$ if the proportionality of the latent infection is zero,

i.e., $\epsilon = 0$.

Proposition 2.1.15. *The system* (2.71) *is locally input–to–state stable in some neighborhood of* $(T(t), T^*(t), L(t), V(t), u(t))^T = \big(\frac{\lambda}{\rho R_{L,0}}, \frac{\lambda(R_{L,0}-1)}{\delta R_0}, \frac{\epsilon\lambda}{(r_L+\delta_L)}\left(1-\frac{1}{R_{L,0}}\right), \frac{\rho(R_{L,0}-1)}{k}, 0\big)^T$. *Moreover, a viral persistence equilibrium point* $\big(\frac{\lambda}{\rho R_{L,0}}, \frac{\lambda(R_{L,0}-1)}{\delta R_0}, \frac{\epsilon\lambda}{(r_L+\delta_L)}\left(1-\frac{1}{R_{L,0}}\right), \frac{\rho(R_{L,0}-1)}{k}\big)^T$ *of the system* (2.71) *is stable when* $a_3 > 0$, $a_1a_2a_3 > a_3^2 + a_1^2a_4$ *for the coefficients in 2.77, and* $R_{L,0} > 1$.

Proof. In order to apply Theorem 2.1.7, we need to find a proper lyapunov function U satisfying (2.12). For this purpose, we consider a system in the absence of the forcing input, i.e., $u(t) = 0$, which is called an unforced system of (2.71). Then it has equilibrium point $\big(\frac{\lambda}{\rho R_{L,0}}, \frac{\lambda(R_{L,0}-1)}{\delta R_0}, \frac{\epsilon\lambda}{(r_L+\delta_L)}\left(1-\frac{1}{R_{L,0}}\right), \frac{\rho(R_{L,0}-1)}{k}\big)^T$ which is called as viral extinction equilibrium. By using the change of variables

$$\widetilde{T}(t) = T(t) - \frac{\lambda}{\rho R_{L,0}}, \quad \widetilde{T^*}(t) = T^*(t) - \frac{\lambda(R_{L,0}-1)}{\delta R_0},$$
$$\widetilde{L}(t) = L(t) - \frac{\epsilon\lambda}{(r_L+\delta_L)}\left(1-\frac{1}{R_{L,0}}\right), \quad \widetilde{V}(t) = V(t) - \frac{\rho(R_{L,0}-1)}{k},$$

the unforced system is transformed into

$$\begin{aligned}
\frac{d\widetilde{T}(t)}{dt} &= -(\rho R_{L,0})\widetilde{T}(t) - \frac{\lambda k}{\rho R_{L,0}}\widetilde{V}(t) - k\widetilde{T}(t)\widetilde{V}(t),\\
\frac{d\widetilde{T^*}(t)}{dt} &= (1-\epsilon_L)\left\{\rho(R_{L,0}-1)\widetilde{T}(t) + \frac{\lambda k}{\rho R_{L,0}}\widetilde{V}(t) + k\widetilde{T}(t)\widetilde{V}(t)\right\}\\
&\quad - \delta\widetilde{T^*}(t) + r_L\widetilde{L}(t),\\
\frac{d\widetilde{L}(t)}{dt} &= \epsilon_L\left\{\rho(R_{L,0}-1)\widetilde{T}(t) + \frac{\lambda k}{\rho R_{L,0}}\widetilde{V}(t) + k\widetilde{T}(t)\widetilde{V}(t)\right\} - (r_L+\delta_L)\widetilde{L}(t),\\
\frac{d\widetilde{V}(t)}{dt} &= N\delta\widetilde{T}(t) - c\widetilde{V}(t).
\end{aligned} \tag{2.75}$$

For clear notation, we introduce $\widetilde{\mathbf{x}} = (\widetilde{T}(t), \widetilde{T^*}(t), \widetilde{L}(t), \widetilde{V}(t))^T$, then the linearized system of (2.75) at the viral persistence equilibrium point is

$$\dot{\widetilde{\mathbf{x}}} = \mathbf{A}\widetilde{\mathbf{x}} + \mathbf{h}(\widetilde{\mathbf{x}}), \tag{2.76}$$

where the Jacobian matrix $\mathbf{A}$ and the nonlinear part $\mathbf{h}(\widetilde{\mathbf{x}})$ are given by

$$\mathbf{A} = \begin{pmatrix}
-(\rho R_{L,0}) & 0 & 0 & -\frac{\lambda k}{\rho R_{L,0}}\\
(1-\epsilon_L)\rho(R_{L,0}-1) & -\delta & r_L & \frac{\lambda k(1-\epsilon_L)}{\rho R_{L,0}}\\
\epsilon_L\rho(R_{L,0}-1) & 0 & -(r_L+\delta_L) & \frac{\lambda k\epsilon_L}{\rho R_{L,0}}\\
0 & N\delta & 0 & -c
\end{pmatrix},$$

$$\mathbf{h}(\widetilde{\mathbf{x}}) = k\widetilde{T}(t)V(t)\begin{pmatrix} -1\\ 1-\epsilon_L\\ \epsilon_L\\ 0 \end{pmatrix}.$$

From the Routh-Hurwitz criteria, all eigenvalues of $\mathbf{A}$ have negative real parts

when

$$
\begin{aligned}
a_1 &= R_{L,0}\rho + r_L + c + \delta + \delta_L,\\
a_2 &= R_{L,0}\rho(r_L + c + \delta + \delta_L) + (r_L c + r_L\delta + c\delta + c\delta_L + \delta\delta_L) - \frac{c\delta(1-\epsilon)R_0}{R_{L,0}},\\
a_3 &= R_{L,0}\rho(r_L c + r_L\delta + c\delta + c\delta_L + \delta\delta_L) + 2c\delta(r_L + \delta_L) - \frac{c\rho\delta(1-\epsilon)R_0}{R_{L,0}},\\
a_4 &= c\rho\delta(r_L + \delta_L)(R_{L,0} - 1).
\end{aligned}
\tag{2.77}
$$

satisfy condition(2.18c), where $\{a_i\}_{i=1}^4$ is the corresponding coefficients referred in Theorem 2.1.9. Hence the persistence equilibrium point of the linear system $\dot{\widetilde{\mathbf{x}}} = \mathbf{A}\widetilde{\mathbf{x}}$ is uniformly asymptotically stable only when $a_3 > 0,\ a_1a_2a_3 > a_3^2 + a_1^2a_4$, and $R_{L,0} > 1$.

Theorem 2.1.8 gives a symmetric positive definite matrix $\mathbf{P}$, given by

$$
\mathbf{P} = \frac{1}{2A}\begin{pmatrix}
\frac{(R_{L,0}-R_0)B+R_0\delta_L\epsilon}{\rho} & -\frac{R_0B}{\rho} & -\frac{r_LR_0}{\rho} & -\frac{R_0B}{\rho N}\\
-\frac{(R_{L,0}-R_{L,0}^2)B+(R_{L,0}^2-R_0)(\delta_L\epsilon)}{\delta} & \frac{R_{L,0}^2B}{\delta} & \frac{(R_{L,0}^2r_L)}{\delta} & \frac{R_0(B-\delta_L\epsilon)}{N\delta}\\
\epsilon R_{L,0}(R_{L,0}-1) & \epsilon R_0 & R_{L,0}^2 - R_0(1-\epsilon) & \frac{\epsilon R_0}{N}\\
\frac{N[(R_{L,0}^2-R_{L,0})(B-\delta_L\epsilon)}{c} & \frac{NR_{L,0}^2B}{c} & \frac{(NR_{L,0}^2r_L)}{c} & \frac{R_{L,0}^2B}{c},
\end{pmatrix}
$$

where $R_{L,0}$ is the reproductive number derived from the latent cell activation model (2.71) and $A = (R_{L,0}^2 - R_0)(r_L + \delta_L) + (\delta_L\epsilon)R_0$ and $B = r_L + \delta_L$. For the linear system $\dot{\widetilde{\mathbf{x}}} = \mathbf{A}\widetilde{\mathbf{x}}$, we consider the Lyapunov function $U(\widetilde{\mathbf{x}}) = \widetilde{\mathbf{x}}^T\mathbf{P}\widetilde{\mathbf{x}}$ and we have the inequalities (2.25). Let us split the system (2.71) by

$$
\dot{\widetilde{\mathbf{x}}} = \mathbf{A}\widetilde{\mathbf{x}} + \mathbf{h}(\widetilde{\mathbf{x}}) + \mathbf{g}(u(t)),
\tag{2.78}
$$

where $\mathbf{g}(u(t))$ with the input function $u(t)$ is given by

$$\mathbf{g}(u(t)) = k\theta \left(\widetilde{T}(t) + \frac{\lambda}{\rho R_{L,0}}\right)\left(\widetilde{V}(t) + \frac{\rho(R_{L,0}-1)}{k}\right)\begin{pmatrix} u(t) \\ -(1-\epsilon)u(t) \\ -\epsilon u(t) \\ 0 \end{pmatrix}.$$

Now, we are going to show that the Lyapunov function $U(\widetilde{\mathbf{x}})$ for the linear system $\dot{\widetilde{\mathbf{x}}} = \mathbf{A}\widetilde{\mathbf{x}}$ is indeed the proper function the system (2.78) satisfying (2.12).

By using (2.25b), we obtain

$$\dot{U}(\widetilde{\mathbf{x}}) = \nabla_{\widetilde{\mathbf{x}}} U \cdot \dot{\widetilde{\mathbf{x}}} \leq -||\widetilde{\mathbf{x}}||^2 + ||\nabla_{\widetilde{\mathbf{x}}} U||\ ||\mathbf{h}(\widetilde{\mathbf{x}})|| + ||\nabla_{\widetilde{\mathbf{x}}} U||\ ||\mathbf{g}(u(t))||. \quad (2.79)$$

Note that $0 < \epsilon < 1$, since the nonlinear part $\mathbf{h}(\widetilde{\mathbf{x}})$ satisfy $\lim_{||\widetilde{\mathbf{x}}||\to 0} ||\mathbf{h}(\widetilde{\mathbf{x}})|| = 0$, for any $\nu > 0$, there exists a constant $r > 0$ such that

$$||\mathbf{h}(\widetilde{\mathbf{x}})|| < \nu \quad \text{as} \quad ||\widetilde{\mathbf{x}}|| < r. \quad (2.80)$$

Moreover, $\mathbf{g}(u(t))$ with the input function $u(t)$ satisfies the following inequality:

$$||\mathbf{g}(u(t))|| < \theta\left(\rho R_{L,0}\widetilde{T}(t) + \left(\frac{k\lambda}{\rho R_{L,0}}\right)\widetilde{V}(t) + \lambda + \nu\right)||u(t)||. \quad (2.81)$$

Substituting (2.80) and (2.81) into (2.79), and using the inequality (2.25c), we have

$$\begin{aligned}\dot{U}(\widetilde{\mathbf{x}}) < &- ||\widetilde{\mathbf{x}}||^2 + 2\theta\xi_{\max}(\mathbf{p})\left(\rho R_{L,0} + \frac{k\lambda}{\rho R_{L,0}}\right)||u(t)||||\widetilde{\mathbf{x}}||^2 \\ &+ 2\xi_{\max}(\mathbf{P})||\widetilde{\mathbf{x}}||\left(\nu + (\lambda+\nu)||u(t)||\right).\end{aligned} \quad (2.82)$$

Let $D_{r_u} = \{u(t) \in \mathbb{R} \mid ||u(t)|| < r_u\}$ and $D_r = \{\widetilde{\mathbf{x}} \in \mathbb{R}^3 \mid ||\widetilde{\mathbf{x}}|| < r\}$. We choose constant r_u and r satisfying

$$\left[2\xi_{\max}(\mathbf{p})r\left\{\left(\rho R_{L,0} + \frac{k\lambda}{\rho R_{L,0}}\right)\theta r_u r + (\nu + (\lambda+\nu)r_u)\right\}\right]^{1/2} < r\left(\frac{z\ \xi_{\min}(\mathbf{P})}{\xi_{\max}(\mathbf{P})}\right)^{1/2}$$

for $0 < z < 1$, in order to estimate the bounds on the initial state and input (the constants k_1 and k_2 in Definition 2.1.6 and Theorem 2.1.7). By recalling (2.82), we get

$$\begin{aligned}\dot{U}(\widetilde{\mathbf{x}}) &< -(1-z)||\widetilde{\mathbf{x}}||^2 - z||\widetilde{\mathbf{x}}||^2 \\ &\quad + 2\xi_{\max}(\mathbf{p})r\left(\theta\left(\rho R_{L,0} + \frac{k\lambda}{\rho R_{L,0}}\right)||u(t)||r + (\nu + (\lambda+\nu)||u(t)||)\right) \\ &\leq -(1-z)||\widetilde{\mathbf{x}}||^2, \quad (0 < z < 1),\end{aligned} \tag{2.83}$$

where

$$\left(2\xi_{\max}(\mathbf{p})rz^{-1}\left(\left(\rho R_{L,0} + \frac{k\lambda}{\rho R_{L,0}}\right)\theta||u(t)||r + (\nu + (\lambda+\nu)||u(t)||)\right)\right)^{1/2}$$
$$\leq ||\widetilde{\mathbf{x}}|| < r.$$

From (2.25c) and (2.83), we finally find the explicit forms of class $\mathcal{K}$ functions on $D_r \times D_{r_u}$,

$$\alpha_1(||\widetilde{\mathbf{x}}||) = \xi_{\min}(\mathbf{P})||\widetilde{\mathbf{x}}||^2, \quad \alpha_2(||\widetilde{\mathbf{x}}||) = \xi_{\max}(\mathbf{P})||\widetilde{\mathbf{x}}||^2, \quad \alpha_3(||\widetilde{\mathbf{x}}||) = (1-z)||\widetilde{\mathbf{x}}||^2,$$
$$\omega(||u||) = \left(\frac{2\xi_{\max}(\mathbf{p})r\left(\theta\left(\rho R_{L,0} + \frac{k\lambda}{\rho R_{L,0}}\right)||u(t)||r + (\nu + (\lambda+\nu)||u(t)||)\right)}{z}\right)^{1/2}.$$

Therefore, the split system is locally input–to–state stable by Theorem 2.1.7

with

$$
\begin{aligned}
k_1 &= \alpha_2^{-1}(\alpha_1(r)) = r\left(\frac{\xi_{\min}(\mathbf{P})}{\xi_{\max}(\mathbf{P})}\right)^{1/2}, \\
k_2 &= \omega^{-1}(\min\{k_1, \omega(r_u)\}) = r_u, \\
\gamma(a) &= \alpha_1^{-1} \circ \alpha_2 \circ \omega(a) \\
&= \left(\frac{2\xi_{\max}^2(\mathbf{p}) r\left(\left(\rho R_{L,0} + \frac{k\lambda}{\rho R_{L,0}}\right)\theta a r + \lambda a + \nu(1+a)\right)}{z\xi_{\min}(\mathbf{p})}\right)^{1/2}
\end{aligned}
$$

□

Following proposition discuss the positivity and boundedness of solutions to system (2.71).

Proposition 2.1.16. *Suppose* $\mathbf{x}$ *satisfy* (2.71) *and* $T_0 > 0, T_0^* > 0, L_0 > 0$ *and* $V_0 > 0$. *Then* $T(t), T^*(t), L(t)$, *and* $V(t)$ *are bounded and remain in positive for all* $t > 0$.

Proof. Recall that all parameters $\mathbf{p}$ in the system (2.71) are positive. We first establish the property for some time interval $[0, t_1]$, then extend the proof to an arbitrary interval. Since we assumed positivity of initial conditions, there must be some $t_1 > 0$ such that $T(t), T^*(t), L(t)$, and $V(t)$ are positive. On this interval,

$$\frac{dT(t)}{dt} = \lambda - \rho T(t) - (1 - \theta u(t)) k T(t) V(t) \leq \lambda,$$

and this gives

$$T(t) \leq T_0 + \lambda t \leq C_1(1 + t),$$

for some constant C_1 satisfying $C_1 \leq \max\{\lambda, T_0\}$. In particular, there is constant bound for $T(t)$ which is uniform in time. Next, we can place lower bounds

on $\frac{dT^*}{dt}$, $\frac{dL}{dt}$ and $\frac{dV}{dt}$. On the interval $(0, t_1]$, we have

$$\frac{dT^*(t)}{dt} \geq -\delta T^*(t), \quad \frac{dV(t)}{dt} \geq -cV(t),$$
$$\frac{dL(t)}{dt} = \epsilon_c(1-\theta u(t))kT(t)V(t) - (r_L+\delta_L)L(t) \geq -(r_L+\delta_L)L(t).$$

Using separation of variables, we re–write these differential inequalities to find

$$T^*(t) \geq T_0^* e^{-\delta t} > 0, \ L(t) \geq L_0 e^{-(r_L+\delta_L)t} > 0, \text{ and } V(t) \geq V_0 e^{-ct} > 0. \quad (2.84)$$

Recall that $u(t) \in [0,1]$ for $t \geq 0$, a summation of $\frac{dT^*(t)}{dt}, \frac{dL(t)}{dt}$ with $\frac{dV(t)}{dt}$ has bound as follow.

$$\frac{d}{dt}(T^* + L + V)(t) \leq kT(t)V(t) + N\delta T^*(t) + r_L L(t), \quad t \in [0, t_1].$$

Due to the bound on $T(t)$, a substitution gives

$$\begin{aligned} \frac{d}{dt}(T^* + L + V)(t) &\leq kC_1(1+t)V(t) + N\delta T^*(t) + r_L L(t) \\ &\leq C_2(1+t)(T^* + L + V)(t), \end{aligned} \quad (2.85)$$

where $C_2 \geq \max\{kC_1, N\delta, r_L\}$. Solving the differential equation (2.85) yields

$$T^*(t) + L(t) + V(t) \leq C_3 e^{t^2}$$

for $t \in [0, t_1]$ where C_3 depends upon C_2, T_0^*, L_0 and V_0 only. Since $T^*(t)$ and $L(t)$ are positive from (2.84), we can place an upper bound on $V(t)$ by $V(t) \leq C_3 e^{t^2}$. Moreover, since $V(t)$ is also positive, it follows that both of $T^*(t)$ and $L(t)$ must be as well, hence, $T^*(t) \leq C_3 e^{t^2}$, $L(t) \leq C_3 e^{t^2}$. With

these bounds in place, we can now examin $T(t)$ and bound it from below using

$$\begin{aligned}\frac{dT(t)}{dt} &\geq -\rho T(t) - kT(t)V(t) \geq -\rho T(t) - kC_3 e^{t^2} T(t) \\ &\geq -C_4(1 + e^{t^2})T(t), \quad t \in [0, t_1],\end{aligned} \tag{2.86}$$

for some constant C_4 satisfying $C_4 \geq \max\{\rho, kC_3\}$. Then from the (2.86), we find that

$$T(t) \geq T_0 \exp(-C_4 \int_0^t (1 + e^{\tau^2}) d\tau) > 0$$

for $t \in [0, t_1]$. Applying the contradiction referred to in the Proposition 2.1.12 gives a conclusion that $T(t), T^*(t), L(t), V(t)$ are bounded and remain positive for all $t > 0$. □

2.2 Parameter estimation

The HIV model is a system of differential equations with a set of parameters. Mathematical problems with such parameter-dependent differential equations can be lead to inverse problem which require parameter estimation based on the measurements of output variable. With several HIV models surveyed in Section 2.1, we are particularly interested in finding a parameter set that minimize the chi-square value between observed data in [139] and numerical solutions. We first describe the characteristics of the data set, including the treatment regimens undergone by various patients. We examine longitudinal viral load data from 9 patients, which shows viral rebound while therapeutic Interruption. This data set includes samples below the limit of detection of the assay used. From this data, we quantify the rate of viral expansion during primary HIV infection. In this section, We describe the characteristics of the data set, including the treatment regimens undergone by various patients. We also describe inverse problem formulations and corresponding computational

approaches, together with a parameter sensitivity analysis.

2.2.1 Description of measurement data and their clinical result

The data for our study come from over 8 adults with asymptomatic HIV-1 infection. These subjects were enrolled in a trial study of Ruiz *et al.*[139] based at University Hospital Germans Trias i Pujol in Barcelona,Spain.The subjects of this study contains the patients who had laboratory documented evidence of HIV-1 infection, a CD4 : CD8 ratio greater than 1 for a minimum of 6 months, and plasma HIV-RNA levels of less than 50 $copies/ml$ (the limit of detection of the assay) for at least 2 years before study entry. Thus it makes its measurement particularly useful for understanding viral dynamics which highly related to existence of latent reservoir or chronic infection.

A total of 9 patients were included in the study, of whom intermittently discontinued their ART regimens in a structured manner, remaining off therapy until two consecutive viral load measurements above 3000 $copies/ml$ were obtained, or for a maximum of 30 days. ART was re-initiated for 90 days until the next interruption cycle begin. This administration manner is called a Structured therapeutic Interruption(STI). It is shown that the re-initiation of ART successfully drove plasma viraemia to below the level of detectability (50 $copies/ml$) in all interrupter patients data. A primary goal of clinical studies is to investigate the clinical,virological and immunological consequences driven by treatment interruption approaches in chronically HIV-infected patients. According to [139], the aim of this clinical study is to develop advanced drug regimen which can overcome a major limitation of current ART that significant restoration of HIV specific CD8+ T cell is not induced except at primary infection and decrease in parallel to virus clearance in plasma.

During the entire follow-up period, all patients in the study underwent

combination therapy with three or more ART drugs, although the precise regime varied from patient to patient as dictated by the treating physician. All subjects we considered were exposed to three consecutive cycles of STI, and viral load rebound was evident in all treatment discontinuations. The measurement of interrupter subject 6,9 and 12, who have problems of detection, shortage of the number of data points and drug adherence, respectively, are excluded in this paper. No side-effects were observed throughout the study period.

Viral load measurements were quantified with RNA Polymerase Chain Reaction(PCR) analysis three times weekly during the interruptions, yielding measurements in viral RNA copies per milliliter(ml). Characteristics of patients are summarized in Table 2.4 referred to [139], and differences in the baseline(BL) $CD4^+$ and $CD8^+$ T cell subsets counts (initial counts) were measured between individuals before the first interruption(before treatment initiation), which implements that the subject's cell density and immune response are different from each other before virologic suppression. Table2.4 also summarizes the data set for all 9 patients, including the clinical identification number assigned to the patient, number of longitudinal viral load measurements, total number of days on and off treatment. Each of terms "IVDU", "Hetero" and "Homo" indicates an intravenous drug user, heterosexual and homosexual, respectively. Values of "ratio" in the last column denote a proportionalities of treatment administration days, assuming that $t_f = 380$. Patient-specific treatment schedules underwent in [139] are depicted together with numerical results in Section2.3.

According to the data analysis done by authors of [139], they found that the mean time before the plasma viral load increased to more than 50 $copies/ml$ was significantly shorter in the second and third STI (11.1 days and 12.3 days,

Patient	Age (years)	Risk factor	CD4 count at BL ($cells/mm^3$)	CD8 count at BL ($cells/mm^3$)	DN of VL	on/off (days)	ratio (%)
1	33	IVDU	2870	1107	36	292/ 58	0.77
2	37	IVDU	742	616	36	301/ 51	0.79
3	29	IVDU	1673	1032	37	303/ 49	0.80
4	32	Hetero	1141	809	39	313/ 46	0.82
5	41	IVDU	1189	1094	32	295/ 56	0.78
7	28	Hetero	1311	897	21	283/ 67	0.74
10	38	Homo	1486	957	25	298/ 57	0.78
11	38	Homo	1002	729	32	301/ 52	0.79

Table 2.4: [139] Characteristics and summary of 9 patients with viral load measurements in their longitudinal data, ordered by patient identification number.(BL,baseline; DN of VL,data number of viral load.)

respectively) than in the first (14.4 days). Extrapolating back to the beginning of each interruption cycle, they conclude that the shorter time before virus rebounded to above detectable levels was associated with a higher initial viral load. Then they hypothesize that this is caused by successive STI cycles re-seeding reservoirs of virus within the body. When they investigate changes in T cell subsets after three STI, they found that, at baseline, CD4 and CD8 T cell subsets were not significantly different with other group of patients, of whom continued on their previous ART during the whole study follow-up. Overall, the authors found that treatment interruptions were not associated with significant changes in CD4 or CD8 cell counts, but the reduction in viral replication by the third STI cycle is unlikely to be caused by lower target cell densities.

2.2.2 An algorithm for parameter estimation

Among several integration methods for the numerical solution of ordinary differential equation, we have used the Adams-type method [34] to obtain the numerical solutions of HIV models and compare the result with our new

model, a fractional-order HIV model in Chapter 3. Three well-known mathematicians Kai Diethelm, Neville J. Ford and Alan D. Freed [34] successfully present the numerical approximation of Volterra intergral equation by using a piecewise linear interpolation polynomial and introduced a fractional Adams-type predictor-corrector method for solving initial value problem for fractional-order differential equations, proving that the order of convergence of the numerical method is $\min\{2, 1+\alpha\}$ for $0 < \alpha \leq 2$ if ${}^{\mathrm{C}}D_t^{\alpha} y \in C^2[0, t_f]$. An arithmetic complexity of their algorithm with steps N is $O(N^2)$, whereas a comparable algorithm for a classical IVP with integer order only give rise to $O(N)$. The challenge of the computational complexity is essentially because fractional derivatives are non-local operators. A detail of the algorithm for this numerical method will be given in 3.4.

A quasi-optimal parameters are estimated by using a nonlinear weighted least squares method, the Levenberg-Marquardt(LM) algorithm [51]. The LM algorithm is one of the popular gradient-based optimization methods, where the performance index is the mean squared error. The LM algorithm is a variation of Newton's method that was designed for minimizing functions that are sums of squares of other nonlinear functions. This method combines the advantageous functionality of two fundamental methods, namely steepest descent and Newton-Raphson; both use numerical derivative information. It provides a nice compromise between the speed of Newton's method and the guaranteed convergence of steepest descent. We have applied for the numerical solution for various states of Three-component, Latent cell activation and chronic infection model. The measurement data of HIV-RNA used for parameter estimation were given with a $\log_{10}$ scaled quantities and we denote by $\{(t_j, y_j)\}_{j=1}^{n}$ the data pairs where n indicates the number of available data points. The low-level viremia measurements below the limit of assay detections, are served as limit

value(50 $copies/mL$), and these data are not used for the estimation. Model fit will be to the base-10 logarithm of the quantities of unscaled viral states solution, (V), which is comparative to data given. A patient-specific underwent ART records during the observation period $[t_0, t_f]$ are also provided in the reference and these are used for input of control variable $u(t),\ t \in [t_0, t_f]$ in solving the HIV dynamics system numerically. Given a vector of model dynamics parameters $\mathbf{p}$ and specified initial condition for the states x_0, we calculate numerical solutions for model using Adams method with derivative order 1.

It is important but difficult to determine an initial guess for each parameter in the nonlinear model due to the high dependency, and we use a nonlinear least square method with a sufficiently many initial guesses, and the quasi optimal parameters were then obtained by taking the minimum of all local minima calculated with these initial guesses. Designate the m model parameters in each model by

$$\mathbf{p} := (\lambda, \rho, k, \delta, N, c, \theta_{rt}, \theta_p \ + \ \text{dependent on model})^T \in \mathbb{R}_+^m,$$

we assume that the parameter vector $\mathbf{p}$ is in the range

$$\mathcal{P} := \Pi_{j=1}^m [p_j^{\min}, p_j^{\max}] \in \mathbb{R}_+^m, \tag{2.87}$$

where $p_j^{\min}$ and $p_j^{\max}$ are the lower and upper bound of the parameter $p_j, j = 1, \ldots, m$. We divide the m-orthotope $\mathcal{P}$ into equal-sized suborthotopes with 20^m vertices to choose one candidate initial guess. One needs some restrictions on parameter values considering the defined biological meanings. Denote by $V(t; \mathbf{p}), t \in [t_0, t_f]$ the viral states solution of each model depending on the parameters $\mathbf{p}$. Then our objective is to find optimal $\mathbf{p}$ for the nonlinear least

squares problem:

$$\min_{\mathbf{p}\in\mathbb{R}^m_+} \chi^2(\mathbf{p}), \tag{2.88}$$

where the objective function $\chi^2(\mathbf{p})$ denotes a sum of squared deviations of data to model,

$$\chi^2(\mathbf{p}) = \sum_{j=1}^{n} \left(r_j(\mathbf{p})\right)^2 = \mathbf{r}(\mathbf{p})^T \mathbf{r}(\mathbf{p}), \tag{2.89}$$

for a residual map $\mathbf{r} : \mathbb{R}^m \to \mathbb{R}^n$ whose components are given by

$$r_j(\mathbf{p}) = y_j - \log_{10}\left(V(t_j;\mathbf{p})\right) = \ \ j = 1, \cdots, n. \tag{2.90}$$

The partial derivatives of $f(t, x; \mathbf{p})$ with respect to every single element of the parameter vector $\mathbf{p}$ are required for the nonlinear least-squares method and the Levenberg-Marquardt algorithm. We differentiate subject model equations with respect to $\mathbf{p}$, interchanges the time and parameter derivatives. Here, the number of data point we consider in parameter estimation is greater than the number of parameter, m. We fix a standard deviation to 1 for all data points, assuming that the log-scaled measurements are normally distributed. The local minima of this minimization problem (2.88) are progressively sought by using the Levenberg-Marquardt method, while the state solutions of each model are obtained by using the Adams-type predictor-corrector method for the updated parameter set $\mathbf{p}$ in successive iterations.

Following the general stop-iteration criterion in optimization procedure, we assume that the local optimum is approached when subsequent changes in the parameter values do not improve the chi-square value or change in parameters is small enough. We let the iteration stop if the relative change in the chi-square values between current and previous iteration is small enough; $\frac{|\chi^2_k - \chi^2_{k-1}|}{|\chi^2_{k-1}|} < 1e-04$,where χ^2_k denotes a chi-square values obtained in $k-$th

iteration. When the variation in parameters is small then $1e-15$, we also terminate the iteration and regard current candidate parameter optimal one best describe the target data set.

Scaled system

Scale is important in that one must decide whether to model at the micro level, e.g., of viral RNA, or more at the systemic level. It is recommended by Adams[34] to solve the HIV dynamics system numerically by using a log-transformed system. They suggest that this procedure resolve a problem of states becoming unrealistically negative during solution due to round-off error. It also enables efficient handling of extremely small values or values that vary over several orders of magnitude during the simulations

Using the transformation $x = \log_{10}(\bar{x})$, with the original system $\dot{\bar{x}} = \bar{g}_i(t, \bar{x}; \mathbf{p})$ we obtain the system

$$\frac{dx_i}{dt} = \frac{10^{-x_i}}{ln(10)} \bar{g}_i(t, 10^x; \mathbf{p}), \quad i = 1, 2, \ldots, N_x, \tag{2.91}$$

which is the log-transformed analog of the reduced system with the number of state variable, N_x. Given a vector of model dynamics parameter $\mathbf{p}$ and specified initial conditions $\bar{x}_0$, we calculate numerical solutions for the model.

2.2.3 Initial guess for initial state density and model parameters

Recall that the RNA quantities of all patients in the data for our study had been undetectable(< 50 *copies*$/m\ell$) for at least two years before the STI. Then, one of our goals is to use patient data from primary infection periods with models to predict positive initial viral load(V_0) which is transient low-level viremia observed in well-suppressed patients on potent treatment, and use this value as an initial guess for initial condition for viral state($V(t_0)$) load.

In case of three component model, we can get analytic solution for $V(t)$ until the first peak(which is pre-treatment period) of viral load occurred as follow.

$$V(t) = V_0 e^{-ct} + \frac{(B - AN)}{(c - \delta)}(e^{-\delta t} - e^{-ct}) + \frac{AN}{c}(1 - e^{-ct}) \tag{2.92}$$

where $A = kT_0V_0$ and $B = N\delta T_0^*$, for $T_0 = \frac{\lambda}{\rho + kV_0}$and $T_0^* = \frac{kT_0V_0}{\delta}$ using the formula of nontrivial steady state. The initial density based on above equation, however, can not be used for initial guess of V_0, since the number of data existing before the first treatment is smaller than the number of parameters to be estimated in the equation (2.92).

We, therefore, following the approach of [131], we can estimate primary viral expansion rate by using the consecutive measurements of HIV-1 RNA before initiation of the first treatment. Denoting this period of early infection by $\mathcal{T}_1$, the viral loads are assumed to be in an exponential growth phase during this time and follow the equation $V_I(t) = V_{I,0}e^{r(t-t_0)},\ t \in \mathcal{T}_1$, where r denotes a primary HIV replication rate after the patients are newly diagnosed. For a fixed growth rate r, we also calculate a doubling time given by $t_d(= \frac{\ln(2)}{r})$, which denotes a time it takes for the amount of viral load to double at a certain point in time. The estimated values of V_0, r and t_d are listed in Table 2.5 for each patients. The initial viral doubling time has a median of 1.4 days with an interquartile range of 0.78 to 2.64 days. We can observe how fast the viral load increases and how variable this parameter is among individuals during primary infection. To specify a informative search range for each of the unknown parameters and initial states conditions, we refer values similar to those reported or justified in the literature. The parameter indicated in Table2.6 are taken directly from the literature and principally extracted from the Callaway–Perelson [22] and Kirschner [77] papers. The superscripts * de-

Patient	Primary HIV replication rate, r	Doubling time t_d	Estimated V_0 $(copies/ml)$
1	0.467	1.49	5.78E-02
2	0.477	1.45	1.96E-01
3	0.638	1.09	2.49E-02
4	0.657	1.06	1.02E+00
5	0.312	2.22	9.64E-01
6	0.263	2.64	7.09E-01
7	0.315	2.20	4.73E-02
8	0.881	0.786	4.72E+00
10	0.562	1.23	3.69E-04
11	0.676	1.02	4.11E-02

Table 2.5: Estimated values for primary infection and initial viral load.

notes parameters the author indicated were estimated from human data and ** denotes those estimated from macaque data. Based on these values, we set a range for initial guess in each of parameters.

parameter	value	Range of initial guess
λ	$[10^2, 10^3]$[22]	$[10^2, 10^3]$
ρ	0.01^{**}[22], 0.02[77]	$[0.01, 0.5]$
k	8.0×10^{-7}[22], 2.4×10^{-5}[77]	$[5.0 \times 10^{-7}, 5.0 \times 10^{-5}]$
δ	0.7^{*}[116, 22], 0.24[22]	$[0.1, 0.9]$
N	100^{*}[22], 2000[62],1200[77]	$[100, 5000]$
c	13[47, 102, 22], 23 [129]	$[5, 30]$
θ	$\in [0, 1]$	$[0.1, 0.9]$
ϵ	0.001[22]	$[0.01, 0.1]$
r_L	3×10^{-3}[77], 0.1[135]	$[5.0 \times 10^{-3}, 1.0 \times 10^{-1}]$
δ_L	0.001[22], 0.02[77], 0.004[48]	$[5.0 \times 10^{-3}, 5.0 \times 10^{-2}]$
ϵ_c	0.01 [115]	$[5.0 \times 10^{-3}, 1.0 \times 10^{-1}]$
μ	$[0.03, 0.12]$[77], 0.078[115], 0.07[112]	$[0.01, 0.1]$
N_c	1000[115]	$[1000, 5000]$

Table 2.6: Reference parameters and range of initial guess for estimation.

2.2.4 Analysis of parameter sensitivity

Modeling biological phenomena for any dynamic system needs to take into account the nature of connection between the parameters of the dynamic system and the observed solution in the model. This function of these parameters is reflecting the characteristics of studies phenomena such that death rate of productively infected lymphocyte or reproduction number of viral load in the HIV model. Therefore, it is valuable to know about how perturbations in these parameters present themselves in the solution.

To estimate model parameters and initial states to which the model solution is most sensitive, we present and analyze the parameter sensitivity results for Three-component, Latent cell activation, Chronic infection model. Using a semi-relative sensitive analysis[148] with our subject data, this process yields sensitivity information as a function of time over the interval of interest. By quantifying overall measure of the sensitivity of the state solution to each parameter, then we rank the resulting scalars to determine the most sensitive parameters to infectious virus state.

Computing sensitivity of model outputs to dynamic parameters both yields information about identifiability and helps construct the relationship between estimated parameters and error estimated in an inverse problem process. For three ordinary differential equation model we discuss previously, semi-relative sensitivities can be computed explicitly by differentiating the dynamical system with respect to model parameters. To describe this methodology, suppose we wish to determine the relative sensitivity of observed model quantities x to particular parameters $p_j,\ j = 1, 2, \ldots, m$. The semi-relative sensitivity of the model solution to parameter p_j is given by

$$\frac{\partial x(t; \mathbf{p})}{\partial p_j}. \tag{2.93}$$

Note that a parameter p_j can be a model parameter or an initial condition. Denoting the system of model equations by

$$\frac{dx}{dt} = f(t, x, ; \mathbf{p}), \quad x(0) = x_0, \tag{2.94}$$

we formally differentiate with respect to each p_j and interchange the order of the time and parameter derivatives[12, 53]. In the case of r parameters and n model state variables, we thus obtain an $(n \times r)-$dimensional system of differential equations for the sensitivities $x_{\mathbf{p}}(t; \mathbf{p}) = \frac{\partial x}{\partial \mathbf{p}}(t; \mathbf{p})$, where $\mathbf{p}$ is the vector of parameters considered:

$$\frac{d}{dt}\left(\frac{\partial x}{\partial \mathbf{p}}(t)\right) = \frac{\partial f}{\partial x}\frac{\partial x}{\partial \mathbf{p}}(t) + \frac{\partial f}{\partial \mathbf{p}} \tag{2.95}$$

with initial condition

$$\frac{\partial x}{\partial \mathbf{p}}(0) = \frac{\partial x_0}{\partial \mathbf{p}}. \tag{2.96}$$

The initial condition matrix has zero entries since the initial conditions are independent of the model parameters, except when initial states values are included in the vector of parameters to be estimated. In the latter case, the sensitivity initial condition for a model state with respect to its own initial value is 1. Note that $\frac{\partial f}{\partial x}$ is the Jacobian of the ODE system,and $\frac{\partial f}{\partial \mathbf{p}}$ is similarly a matrix containing the derivatives of the right side with respect to the parameters considered.

2.3 Numerical result

2.3.1 Sensitivity equations

We solve the system (2.95) and with initial condition(2.96) for $x_{\mathbf{p}}(t; \mathbf{p})$ by coupling it with the original differential equation system to obtain an

$(nr+n)-$dimensional system which we again solve numerically with applied integration method. This process yields sensitivity information as a function of time over the interval of integration considered. To understand overall which model dynamic parameters and initial conditions most influence the outputs of the system we take the L^2 norm of these over time. In particular with HIV model we considered, given treatment protocol, observation times, and parameters for specific patient k, we compute the influence of each parameter p_j on viral RNA response over time. We examine results for relative sensitivity for viral RNA to each of the number of subject models and corresponding initial conditions. In case of three-component HIV model(2.2), the sensitivity equations are as follow:

$$
\begin{aligned}
\frac{\partial DT(t)}{\partial \lambda} =& 1-\rho\frac{\partial DT(t)}{\partial \lambda}-(1-\theta u(t))k\left(V(t)\frac{\partial DT(t)}{\partial \lambda}+T(t)\frac{\partial DV(t)}{\partial \lambda}\right),\ \frac{\partial T(t)}{\partial \lambda}\Big|_{t=0}=0,\\
\frac{\partial DT(t)}{\partial \rho} =& -T(t)-\rho\frac{\partial DT(t)}{\partial \rho}-(1-\theta u(t))k\left(V(t)\frac{\partial DT(t)}{\partial \rho}+T(t)\frac{\partial DV(t)}{\partial \rho}\right)\\
&,\ \frac{\partial T(t)}{\partial \rho}\Big|_{t=0}=0,\\
\frac{\partial DT(t)}{\partial k} =& -(1-\theta u(t))T(t)V(t)-\rho\frac{\partial DT(t)}{\partial k}\\
&-(1-\theta u(t))k\left(V(t)\frac{\partial DT(t)}{\partial k}+T(t)\frac{\partial DV(t)}{\partial k}\right),\ \frac{\partial T(t)}{\partial k}\Big|_{t=0}=0,\\
\frac{\partial DT(t)}{\partial \theta} =& ku(t)TV-\rho\frac{\partial DT(t)}{\partial \theta}-(1-\theta u(t))k\left(V(t)\frac{\partial DT(t)}{\partial \theta}+T(t)\frac{\partial DV(t)}{\partial \theta}\right)\\
&,\ \frac{\partial T(t)}{\partial \theta}\Big|_{t=0}=0,\\
\frac{\partial DT(t)}{\partial T_0} =& -(\rho+(1-\theta u(t))kV(t))\frac{\partial DT(t)}{\partial T_0}-(1-\theta u(t))kT(t)\frac{\partial DV(t)}{\partial T_0},\ \frac{\partial T(t)}{\partial T_0}\Big|_{t=0}=1,\\
\frac{\partial DT(t)}{\partial p_j} =& -(\rho+(1-\theta u(t))kV(t))\frac{\partial DT(t)}{\partial p_j}-(1-\theta u(t))kT(t)\frac{\partial DV(t)}{\partial p_j},\ \frac{\partial T(t)}{\partial p_j}\Big|_{t=0}=0,\\
&\text{for } p_j=\delta,N,c,T_0^*,V_0.
\end{aligned}
$$

$$
\begin{aligned}
\frac{\partial DT^*(t)}{\partial \theta} =& -u(t)kT(T)V(t) + (1-\theta u(t))k\left(V(t)\frac{\partial T(t)}{\partial \theta} + T(t)\frac{\partial V(t)}{\partial \theta}\right) \\
& -\delta\frac{\partial T^*(t)}{\partial \theta},\ \frac{\partial T^*(t)}{\partial \theta}\Big|_{t=0} = 0, \\
\frac{\partial DT^*(t)}{\partial k} =& (1-\theta u(t))T(t)V(t) + (1-\theta u(t))k\left(V(t)\frac{\partial T(t)}{\partial k} + T(t)\frac{\partial V(t)}{\partial k}\right) \\
& -\delta\frac{\partial T^*(t)}{\partial k},\ \frac{\partial T^*(t)}{\partial k}\Big|_{t=0} = 0, \\
\frac{\partial DT^*(t)}{\partial \delta} =& -T^*(t) + (1-\theta u(t))k\left(V(t)\frac{\partial T(t)}{\partial \delta} + T(t)\frac{\partial V(t)}{\partial \delta}\right) - \delta\frac{\partial T^*(t)}{\partial \delta} \\
& ,\ \frac{\partial T^*(t)}{\partial \delta}\Big|_{t=0} = 0, \\
\frac{\partial DT^*(t)}{\partial T_0^*} =& (1-\theta u(t))k\left(V(t)\frac{\partial T(t)}{\partial T_0^*} + T(t)\frac{\partial V(t)}{\partial T_0^*}\right) - \delta\frac{\partial T^*(t)}{\partial T_0^*},\ \frac{\partial T^*(t)}{\partial T_0^*}\Big|_{t=0} = 1, \\
\frac{\partial DT^*(t)}{\partial p_j} =& (1-\theta u(t))k\left(V(t)\frac{\partial T(t)}{\partial p_j} + T(t)\frac{\partial V(t)}{\partial p_j}\right) - \delta\frac{\partial T^*(t)}{\partial p_j},\ \frac{\partial T^*(t)}{\partial p_j}\Big|_{t=0} = 0, \\
& \text{for } p_j = \lambda, \rho, N, c, T_0, V_0.
\end{aligned}
$$

$$
\begin{aligned}
\frac{\partial DV(t)}{\partial N} =& \delta T^*(t) + +N\delta\frac{\partial T^*(t)}{\partial N} - c\frac{\partial V(t)}{\partial N},\ \frac{\partial V(t)}{\partial N}\Big|_{t=0} = 0, \\
\frac{\partial DV(t)}{\partial \delta} =& NT^*(t) + N\delta\frac{\partial T^*(t)}{\partial \delta} - c\frac{\partial V(t)}{\partial \delta},\ \frac{\partial V(t)}{\partial \delta}\Big|_{t=0} = 0, \\
\frac{\partial DV(t)}{\partial c} =& -V(t) + N\delta\frac{\partial T^*(t)}{\partial c} - c\frac{\partial V(t)}{\partial c},\ \frac{\partial V(t)}{\partial c}\Big|_{t=0} = 0, \\
\frac{\partial DV(t)}{\partial V_0} =& N\delta\frac{\partial T^*(t)}{\partial V_0} - c\frac{\partial V(t)}{\partial V_0},\ \frac{\partial V(t)}{\partial V_0}\Big|_{t=0} = 1, \\
\frac{\partial DV(t)}{\partial p_j} =& N\delta\frac{\partial T^*(t)}{\partial p_j} - c\frac{\partial V(t)}{\partial p_j},\ \frac{\partial V(t)}{\partial p_j}\Big|_{t=0} = 0,\ \text{for } p_j = \lambda, \rho, k, \theta, T_0, T_0^*.
\end{aligned}
$$

In case of chronic model(2.54) and latent reservoir model(2.71), we apply as done for the three component model(2.2) as described above. The ranked sensitivity of the parameters $\mathbf{p}$ for virus states $V(t)$ and other states are given in Table 2.8. These results are dependent on the relative magnitude of the parameters considered and therefore vary among the models. This sensitivity analysis will inform the inverse problem process, as one should not expect to estimate a parameter to which the model solutions are insensitive. We can verify that the model output $V(t)$ are most sensitive to the parameters a

infection rate k and secondarily to the parameters death rate of target cell ρ or a total drug efficacy θ, and it is consistent with the underlying biological phenomena.

2.3.2 Numerical simulation

In this section, we provide the numerical solution of the model systems we considered. We apply plasma HIV-RNA measurement of 9 patients in this model and estimate patient-specific model parameters. For each of these initial guesses, LM method is employed to estimate optimal parameters then the minima of these optimal parameters which generate a smallest χ^2-value are taken as our global optimal values. To evaluate the goodness of fit for each patient data, we use relative ℓ_2 error obtained by $\sqrt{\chi^2}/\sqrt{\sum_k {y_k}^2}$. In this section, we present the numerical results for parameters estimation by applying on the 9 patients data using the method described in § 2.2.1. We evaluate the goodness of fit for each patient data by calculating relative ℓ_2 error. The estimated quasi-optimal model parameters $\mathbf{p}$ and indicators for goodness of fit for each patient are listed in 2.7. We also calculate the values of R_0 for each patient using the estimated model parameters and comparison is listed in Tabal2.11. We check that all patients have R_0 greater than 1 so that viral infection spread as expected, which correspondence to the pattern of measurement. A patient of whom viral dynamics show the highest R_0 is patient 2 with Three component model (2.2), whereas patient 8 has highest R_0 both with chronic (2.54) and latent models (2.71).The patient who has highest average value of R_0 with three models are patient 8(2.22) and 2(1.72). We also observe that the patients whose risk factor is Homosexual are in the highest level in the comparison of the infection rate values, Heterosexual patients are in the middle level, and last patients with IVDU are in the lowest level. Through

a semi-relative sensitive calculation[148] implemented in Subsection2.3.1, we attempt to estimate those parameters to which the model solution is most sensitive. This process yields sensitivity information as a function of time over the interval of interest. We wish to have some overall measure of the sensitivity of the model solution(V) to the parameters and initial states combination, we take a norm($L_2 - norm$) in time and then rank the resulting scalars to determine the most sensitive parameters. We find that these comparisons are similar using the two or sup norm, and report using the two norm here. For comparative analysis for sensitivity parameter among the nine patients, we use the time span long enough to contains the observation period of all patients. Table 2.8 contain the ranked semi-relative sensitivities and parameter for viral RNA load and results in the tables are calculated for each patients considered. With the underwent treatment schedule for each patients in the reference[139], we find that the model solutions(V) are most sensitive to the parameters k, ρ, T_0, θ and secondarily to the parameters T_0^* and δ for most patients with the chronic infection model. We note that the model solutions are highly sensitive to drug efficacy θ. In case of three-component model(2.2), we find that the model solutions(V) are sensitive to the parameters k, ρ, θ and secondarily to the parameters c, δ and T_0 for most patients, as listed in Table2.8. With latent cell activation model(2.71), we have interest in the result in Table that the model solutions(V) are sensitive not only to the infection rate(k),death rate of target lymphocyte population ρ, but also sensitive to r_L and δ_L which are the activated rate and death rate of latently infected cell. Considering the suggestion of Perelson et al.[112] that the second phase in the viral decay profile is due to the activation of latently infected lymphocyte, we deduce that the the existence of long-term latent reservoirs in patients can be significantly influential reason for viral persistence. These

results are dependent on the relative magnitude of the parameters considered. This sensitivity analysis will inform the inverse problem process, as one should not expect to estimate a parameter to which the model solutions are insensitive. From the Table2.8 which estimated sensitivity parameters of latent cell activation model, we had interested that the virus had a high sensitivity to parameters associated with decay of latent cells, δ_L.

Figure 2.1-2.2 show the patients' measurements of HIV-RNA in a logarithmic scale with simulated viral load trajectory with underwent clinical STI therapy. As we can see, the numerical results fit the RNA measurement well, especially it was well matched to the rate of increase or decrease of the viral load around the peak point when there is viral blip. In the process of the plasma virus droving to below the detectable level due to initiation of treatment, we observe that the HIV-RNA measurement of the patient $3, 4$ and 8 does not continue to decrease exponentially, but once in second phase, the rate of decrease is rebounding and our model states. The authors of [139] hypothesizes that it is caused by consecutive STI cycles re-seeding reservoirs of virus within the body. We note that our model is exactly covering the physiological phenomena as shown in the numerical results of patient $3, 4$ and 11. In this section, we present some numerical results obtained from the HIV models we considered. We apply plasma HIV-RNA measurement of 9 patients in this model and estimate patient-specific model parameters. For each of these initial guesses, Levenberg–Marquardt method is employed to estimate optimal parameters then the minima of these optimal parameters which generate a smallest χ^2-value are taken as our global optimal values. To evaluate the goodness of fit for each patient data, we use relative L_2 error obtained by $\sqrt{\chi^2}/\sqrt{\sum_k {y_k}^2}$. A parameter sensitivity is computed by taking ℓ_2 norm of states partial derivatives with respect to each parameter in $\mathbf{p}$. In this section,

we present the numerical results for parameters estimation by applying on the 9 patients data using the method described in § 2.2. We evaluate the goodness of fit for each patient data by calculating relative ℓ_2 error. The estimated quasi-optimal model parameters $\mathbf{p}$ and indicators for goodness of fit for each patient are listed in 2.7. Figure 2.1-2.2 show the patients' measurements of HIV-RNA in a logarithmic scale with simulated viral load trajectory with underwent clinical STI therapy. As we can see, the numerical results fit the RNA measurement well, especially it was well matched to the rate of increase or decrease of the viral load around the peak point when there is viral blip. In the process of the plasma virus droving to below the detectable level due to initiation of treatment, we observe that the HIV-RNA measurement of the patient 3 and 4 does not continue to decrease exponentially, but once in second phase, the rate of decrease is rebounding and our model states. The authors of [139] hypothesizes that it is caused by consecutive STI cycles re-seeding reservoirs of virus within the body. We note that our model is exactly covering the physiological phenomena as shown in the numerical results of patient 3, 4 and 11.

2.4 Conclusion

In Section 2.1, we proved that three component, Chronic infection and latent reservoir models have bounded and positive solutions under certain parameters constraint. In Section 2.2, by using Levenberg-Marquardt algorithm for nonlinear least square method, we estimated patient-specific values for model parameters and initial states best describe the successive viral rebound data under STI control. We also found that the infectivity k is the most sensitive in the HIV infection dynamics by performing semi-relative sensitivity analysis. In Section 2.3, we presented our numerical results for various states

P	Estimated parameters						
	λ	ρ	k	δ	N	c	θ
1	4.46E+02	1.85E-01	3.68E-06	9.56E-01	1.93E+03	1.06E+01	4.47E-01
2	2.11E+02	3.48E-01	6.78E-06	4.45E-01	2.62E+03	6.20E+00	5.09E-01
3	1.54E+02	3.12E-01	8.76E-06	7.88E-01	3.00E+03	8.24E+00	4.16E-01
4	4.19E+02	2.41E-01	6.48E-06	9.83E-01	2.09E+03	1.41E+01	4.29E-01
5	3.41E+02	2.25E-01	7.74E-06	7.00E-01	1.83E+03	1.48E+01	3.67E-01
7	3.45E+02	2.28E-01	7.94E-06	1.52E-01	1.97E+03	1.36E+01	5.55E-01
8	1.91E+02	5.93E-01	8.92E-06	6.17E-01	4.39E+03	8.04E+00	4.19E-01
10	3.26E+02	2.49E-01	8.52E-06	7.41E-01	1.83E+03	1.52E+01	3.04E-01
11	3.31E+02	2.49E-01	8.44E-06	8.96E-01	1.85E+03	1.51E+01	3.20E-01

Patient	Estimated parameters			Relative ℓ_2 error
	T_0	T_0^*	V_0	
1	2.06E+03	3.57E-04	2.33E-01	1.42E-01
2	1.22E+01	8.19E-02	4.48E+02	1.45E-01
3	8.02E+02	6.99E-04	2.38E-02	1.94E-01
4	2.10E+03	4.46E-02	3.36E+01	1.57E-01
5	1.18E+03	1.26E-02	1.63E+01	1.83E-01
7	3.16E+03	8.83E-02	4.90E+01	1.64E-01
8	1.86E+03	1.40E-03	8.45E+00	2.54E-01
10	2.95E+03	3.77E-05	3.00E-02	1.51E-01
11	1.41E+01	3.48E+00	4.02E+04	1.41E-01

Table 2.7: Estimated parameters and goodness of fit for the three component model.

Patient	Sensitive parameter p_i (Three component model)					
	Rank 1	Rank 2	Rank 3	Rank 4	Rank 5	Rank 6
1	k	ρ	θ	δ	c	T_0
2	k	ρ	c	θ	δ	$p1$
3	k	ρ	θ	c	δ	T_0
4	k	ρ	θ	c	δ	T_0
5	k	ρ	θ	c	δ	T_0
7	k	ρ	θ	δ	c	T_0
8	k	ρ	θ	c	δ	T_0
10	k	ρ	θ	T_0	δ	c
11	k	ρ	θ	c	δ	$p1$

Patient	Sensitive parameter p_i (Chronic infection model)					
	Rank 1	Rank 2	Rank 3	Rank 4	Rank 5	Rank 6
1	k	ρ	θ	ϵ_c	μ	δ
2	k	θ	ρ	μ	ϵ_c	δ
3	k	θ	ρ	ϵ_c	μ	δ
4	k	ρ	θ	ϵ_c	μ	δ
5	k	ρ	c	θ	μ	ϵ_c
7	k	ρ	θ	μ	ϵ_c	c
8	k	θ	ρ	ϵ_c	μ	δ
10	k	ρ	θ	c	ϵ_c	δ
11	k	θ	ρ	μ	ϵ_c	δ

Patient	Sensitive parameter p_i (Latent cell activation model)					
	Rank 1	Rank 2	Rank 3	Rank 4	Rank 5	Rank 6
1	k	ρ	δ_L	r_L	ϵ	δ
2	k	δ_L	ρ	r_L	θ	δ
3	k	ρ	δ_L	r_L	ϵ	δ
4	k	r_L	δ_L	c	ρ	ϵ
5	k	ρ	δ_L	r_L	ϵ	δ
7	k	r_L	ρ	δ_L	ϵ	δ
8	k	r_L	ρ	δ_L	θ	ϵ
10	k	ρ	δ_L	r_L	c	ϵ
11	k	ρ	δ_L	r_L	ϵ	δ

Table 2.8: Ranked semi-relative sensitivity of the model state $V(t)$ to parameters ($\mathbf{p}$) estimated from each patient with three different models.

Patient	Estimated parameters					
	λ	ρ	k	δ	N	c
1	4.49E+02	1.93E-01	3.55E-06	9.39E-01	1.94E+03	1.06E+01
2	2.21E+02	3.64E-01	6.67E-06	4.44E-01	2.73E+03	5.86E+00
3	1.70E+02	3.50E-01	7.76E-06	9.67E-01	3.31E+03	7.52E+00
4	4.17E+02	2.47E-01	6.34E-06	9.95E-01	2.08E+03	1.42E+01
5	3.61E+02	2.48E-01	6.97E-06	9.91E-01	1.93E+03	1.44E+01
7	3.49E+02	2.66E-01	6.80E-06	9.37E-01	1.98E+03	1.38E+01
8	2.26E+02	6.57E-01	7.93E-06	9.99E-01	5.13E+03	6.60E+00
10	3.55E+02	2.53E-01	8.10E-06	8.80E-01	1.98E+03	1.41E+01
11	2.49E+02	2.67E-01	6.03E-06	7.20E-01	2.46E+03	8.08E+00
	θ	ϵ_c	μ	N_c		
1	6.71E-01	2.59E-02	7.15E-02	1.85E+03		
2	6.59E-01	7.19E-02	5.99E-02	2.72E+03		
3	7.88E-01	6.73E-02	6.32E-02	3.11E+03		
4	4.96E-01	1.38E-02	2.63E-02	1.26E+03		
5	5.70E-01	4.66E-02	3.66E-02	1.49E+03		
7	6.92E-01	1.48E-02	1.81E-02	9.55E+02		
8	7.22E-01	1.42E-02	5.50E-02	5.10E+03		
10	5.80E-01	1.97E-02	8.25E-02	1.50E+03		
11	8.77E-01	9.46E-02	6.79E-02	3.31E+03		

Patient	Estimated parameters				Relative ℓ_2 error
	T_0	T_0^*	V_0	$T_{c,0}^*$	
1	2.32E+03	2.85E-02	3.33E+00	9.97E-03	1.30E-01
2	6.05E+02	2.32E-02	2.75E+00	1.33E-02	1.30E-01
3	4.85E+02	9.49E-03	2.60E+00	1.04E-02	1.65E-01
4	1.68E+03	3.42E-02	3.23E+00	1.81E-02	1.39E-01
5	1.42E+03	1.14E-02	1.15E+00	1.18E-02	9.82E-02
7	1.30E+03	2.87E-02	3.06E+00	2.23E-02	1.88E-01
8	3.44E+02	6.82E-03	2.53E+00	1.79E-03	1.81E-01
10	1.40E+03	3.60E-02	3.19E+00	8.69E-03	3.37E-01
11	2.90E+02	7.13E-02	1.54E+02	3.77E-02	1.01E-01

Table 2.9: Estimated parameters and goodness of fit for the chronic infection model.

Patient	Estimated parameters					
	λ	ρ	k	δ	N	c
1	4.62E+02	1.84E-01	3.67E-06	7.38E-01	1.98E+03	1.02E+01
2	2.25E+02	3.50E-01	7.15E-06	5.05E-01	2.73E+03	6.04E+00
3	1.69E+02	3.36E-01	8.09E-06	9.52E-01	3.30E+03	7.70E+00
4	4.35E+02	2.36E-01	6.37E-06	9.65E-01	2.12E+03	1.41E+01
5	3.64E+02	2.46E-01	7.00E-06	9.97E-01	1.94E+03	1.43E+01
7	3.53E+02	2.56E-01	6.99E-06	9.58E-01	1.89E+03	1.39E+01
8	4.38E+02	1.24E-01	7.68E-06	7.67E-01	2.06E+03	1.43E+01
10	3.60E+02	2.46E-01	7.64E-06	9.19E-01	1.82E+03	1.39E+01
11	2.55E+02	2.62E-01	6.14E-06	7.66E-01	2.52E+03	7.93E+00
	θ	r_L	ϵ	δ_L		
1	7.28E-01	5.12E-02	4.03E-02	4.05E-02		
2	7.08E-01	7.04E-02	1.99E-01	1.28E-02		
3	9.87E-01	6.05E-02	8.72E-02	7.86E-03		
4	4.88E-01	9.05E-05	3.44E-02	8.29E-03		
5	6.40E-01	3.15E-02	6.12E-02	1.08E-02		
7	6.42E-01	2.60E-03	3.69E-02	1.66E-02		
8	6.90E-01	5.27E-04	2.34E-01	3.63E-02		
10	5.32E-01	4.13E-02	4.50E-02	2.01E-02		
11	8.13E-01	7.58E-02	1.84E-01	1.31E-02		

Patient	Estimated parameters				Relative ℓ_2 error
	T_0	T_0^*	V_0	L_0	
1	2.72E+03	1.66E-04	1.64E-01	1.68E-03	9.67E-02
2	6.37E+02	7.00E-03	1.82E+00	9.65E-03	1.27E-01
3	5.16E+02	3.76E-04	2.38E-01	1.56E-03	1.44E-01
4	1.84E+03	1.01E-01	1.10E+01	1.90E-04	1.24E-01
5	1.45E+03	1.14E-02	2.09E+00	2.14E-02	9.36E-02
7	1.54E+03	1.19E-03	1.21E+00	9.56E-02	1.17E-01
8	2.02E+03	9.16E-02	1.01E+01	5.48E+00	1.58E-01
10	1.82E+03	2.27E-03	3.93E-01	9.75E-07	2.04E-01
11	1.04E+03	7.48E-04	6.04E+00	1.18E-03	1.04E-01

Table 2.10: Estimated parameters and goodness of fit for the latent cell activation model ($N_p = 14$).

Patient	Three-component(2.2)	Chronic(2.54)	Latent(2.71)
1	1.61	1.47	1.71
2	1.75	1.75	1.67
3	1.58	1.55	1.59
4	1.66	1.54	1.70
5	1.45	1.30	1.31
7	1.74	1.25	1.27
8	1.57	2.09	3.00
10	1.34	1.56	1.40
11	1.37	1.56	1.55

Table 2.11: Comparison on reproductive number(R_0) for three models.

with estimated parameters for each of the models. We conform that the patient data showing successive viral rebound during interruption of HAART can be better described by the HIV models which include the lymphocyte subpopulations providing residual virus replication. Our results support a clinical finding that latent infection of CD4 T cells provides a mechanism.

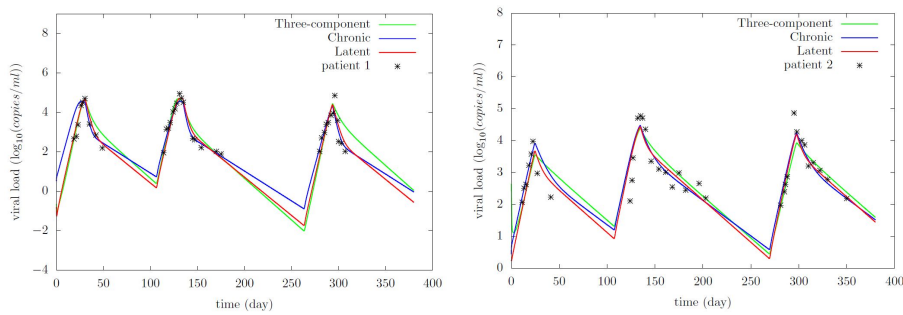

(a) Patient 1

(b) Patient 2

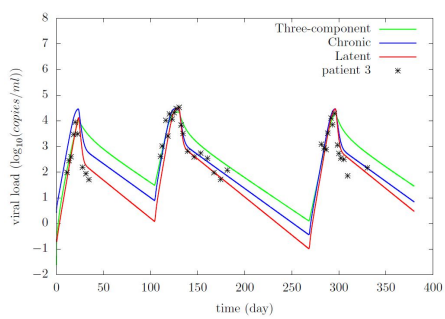

(c) Patient 3

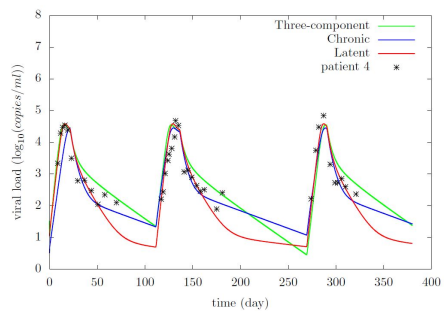

(d) Patient 4

Figure 2.1: Plot of clinical data and numerical results of each dynamics model.

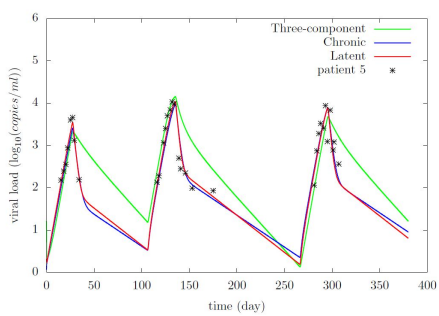

(a) Patient 5

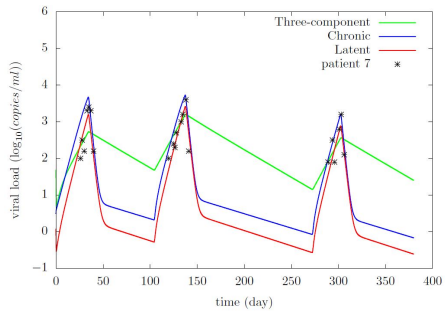

(b) Patient 7

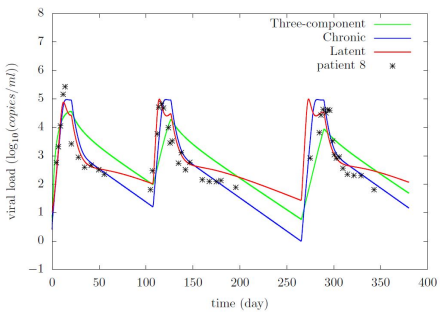

(c) Patient 8

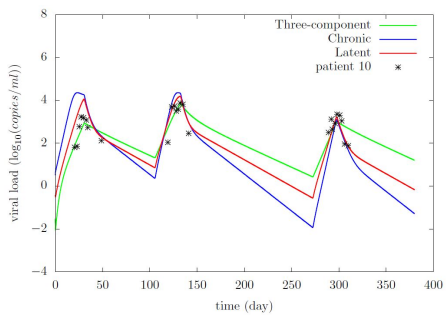

(d) Patient 10

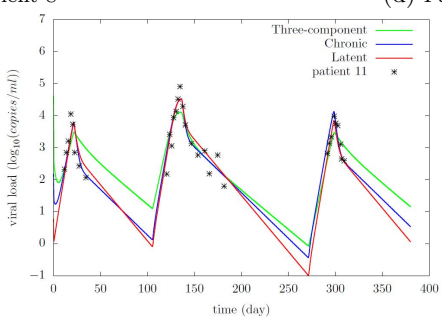

(e) Patient 11

Figure 2.2: Plot of clinical data and numerical results of each dynamics model.

Chapter 3

A fractional-order model for HIV infection

Fractional differential equations provide an excellent mathematical tool for the description of memory and hereditary properties of various materials and processes. These operators are non-local which is the most significant advantage in applications. The standard derivative of a function includes information about the value of the function at certain earlier time points only, while the fractional derivative encapsulates information about the function's behaviour from the earliest point in time up to the present. This advantages of fractional differential equations become apparent in the description of rheological properties of the blood. Considering several researches finding relationship of blood cell abnormalities and changes in rheological properties to HIV infection, we introduce a fractional derivative of order $0 < \alpha < 1$ to models of HIV infection dynamics in lymphocyte population.

3.1 The fractional calculus

The *fractional calculus* is a name for the theory of integrals and derivatives of arbitrary order, which unify and generalize the notions of integer-order differentiation and $n-$fold integration. Considering the infinite sequence of $n-$fold integrals and $n-$fold derivatives:

$$\ldots, \quad \int_{t_0}^{t} d\tau_2 \int_{t_0}^{\tau_2} f(\tau_1) d\tau_1, \quad \int_{t_0}^{t} f(\tau_1) d\tau_1, \quad f(t), \quad , \frac{df(t)}{dt}, \quad \frac{d^2 f(t)}{dt^2}, \quad .. \tag{3.1}$$

Newton and Leibniz developed the notions of differentiation and integration of integer order. The symbol

$$\frac{d^n y}{dx^n} \tag{3.2}$$

invented by Leibniz denotes the nth derivative of a function y with respect to x. In 1819, the Lacroix [39] firstly mentioned a derivative of arbitrary order in his text. He developed nth derivative of $y = x^m$, for a positive integer m,

$$\frac{d^n y}{dx^n} = \frac{m!}{(m-n)!} x^{m-n}, \tag{3.3}$$

where $n(\leq m)$ is an integer. By using the gamma function defined by

$$\Gamma(x) = \int_0^{\infty} t^{x-1} e^{-t} dt, \tag{3.4}$$

he obtain a formula for the fractional derivative as follow:

$$\frac{d^\alpha y}{dx^\alpha} = \frac{\Gamma(\beta+1)}{\Gamma(\beta-\alpha+1)} x^{\beta-\alpha}, \tag{3.5}$$

In 1822, Fourier [52] obtained an integral representations for f and its derivatives:

$$f(x) = \frac{1}{2\pi} \int_{-\infty}^{\infty} f(\eta) d\eta \int_{-\infty}^{\infty} cos(p(x-\eta) dp, \tag{3.6}$$

with

$$\frac{d^n}{dx^n} f(x) = \frac{1}{2\pi} \int_{-\infty}^{\infty} f(\eta) d\eta \int_{-\infty}^{\infty} p^n \cos(p(x-\eta) + \frac{1}{2} n\pi) dp, \tag{3.7}$$

for an integer n. The first application of fractional operations was made by Abel in 1823 who applied the fractional calculus in the solution of an integral equation based on the tautochronous problem. The solution is originated from the fact that the derivative of a constant function is not always equal to zero.

After that, many famous mathematicians have devoted their energies to fractional calculus over the years, and some definitions of fractional derivative have been contributed [57, 100, 123]. The reason of using fractional order differential equations is that they are naturally related to systems with memory which exists in most biological systems. Also they are closely related to fractals which are abundant in biological systems. The definition of fractional derivative involves an integration which is non local operator (as it is defined on an interval) so fractional derivative is a non local operator. In other word, calculating time fractional derivative of a function $f(t)$ at some time $t = t_1$ requires all the previous history, i.e. all $f(t)$ from $t = 0$ to $t = t_1$ The results derived of the fractional systems are of a more general nature. However, the fundamental solutions of these equations still exhibit useful scaling properties that make them attractive for applications. We would like to put your attention that time fractional derivatives change also the solutions we usually get in standard system. The concept of fractional or non-integer order derivation and

integration can be traced back to the genesis of integer order calculus itself. Most of the mathematical theory applicable to the study of noninteger order calculus was developed through the end of 19th century. However it is in the past hundred years that the most intriguing leaps in engineering and scientific application have been found. The calculation technique has in some cases had to change to meet the requirement of physical reality. The derivatives are understood in the Caputo sense. The general response expression contains a parameter describing the order of the fractional derivative that can be varied to obtain various responses.

3.2 Motivation

Mathematical models have been proved valuable in understanding the dynamics of HIV infection. Perelson [114, 115], Kirschner and De Boer [76] proposed an ODE model of cell-free viral spread of HIV in a well-mixed compartment such as the bloodstream. These models has been important in the field of mathematical modelling of HIV infection, and many other models have been proposed, which take the model of them as their inspiration. However, the large amount of work done on modelling the HIV infection has been restricted to integer-order ordinary differential equations [31, 107].

The theory of fractional differential operators generalizes the notion of standard operators of integer orders to fractional orders. Such differential operators appear in modeling diverse physical problems involving e.g., porous or fractured media [16], viscoelastic materials [94], viscous fluid flows subject to wall-friction effects[153], bioengineering applications [93], and anomalous transport [98]. Fractional derivatives are a very natural and common tool in the classical models of viscoelasticity. Recently, fractional calculus has also been widely applied in many fields([3, 4, 6, 28, 44, 60, 72, 83, 123]) of biology

and many mathematicians and applied researched have tried to model real processes using the fractional calculus. Machado and Cunha analyzed the fractionalorder dynamics in botanical electrical impedances [66, 67]. Petrovic, Spasic and Atanackovic developed a fractional-order mathematical model of a human root dentin [117]. In biology, it has been deduced that the membranes of cells of biological organism have fractional-order electrical conductance [28] and then are classified in groups of non-integer order models. Fractional derivatives embody essential features of cell rheological behavior and have enjoyed greatest success in the field of rheology [38]. Also, it has been shown that modelling the behavior of brainstem vestibule-oculumotor neurons by fractional ordinary differential equations (FODE) has more advantages than classical integer-order modelling [6]. FODE are naturally related to systems with memory which exists in most biological systems. Also, they are closely related to fractals, which are abundant in biological systems [4]. Some researchers also found that fractional ordinary differential equations are naturally related to systems with memory which exists in most biological systems. It has been deduced that the membrane of cells or biological organism have fractional-order electrical conductance [60]. With this reason, some mathematical models which describe cells behavior are classified into groups of non-integer-order models. In the field of rheology, fractional-order derivatives embody essential features of cell rheological behavior and have enjoyed greatest success [123]. Fractional-order equations are also closely related to fractals, which are abundant in biological systems. Erythrocytes in static human blood form loose aggregates with distinctive morphology similar to stacks of coins. This aggregation is often called rouleaux formation and is caused by various macromolecules present in the plasma, especially fibrinogen. Red cell aggregation affects low shear blood viscosity and microvascular flow dynamics. Rampling et al.,[96] also found

that RBC aggregation is particularly apparent under conditions of low flow, namely, low shear stress. The rouleaux formation can dramatically decrease blood flow velocity leading to compromised tissue perfusion and oxygen delivery leading eventually to organ ischemia.[127] Some researchers have studied the relationship of blood cell abnormalities and changes in rheological properties to HIV infection [21]. Many changes in the blood component properties such as deformability, aggregability, viscoelasticity are investigated during the asymptomatic period in the HIV infected patients[61, 103]. Recent studies of Gallegos et al. [55] found that red blood cell(RBC) deformability significantly decreased in HIV infected individuals, which suggested that increased aggregation and decreased erythrocyte deformability are features of HIV disease but unrelated to the severity of the immunodeficiency. Some influencing factors on the dynamics of blood flow have been founded in HIV infection [46, 75]. The first one is an anatomic abnormality of the microvasculature in HIV disease. The hematological factors, which contain increased erythrocyte aggregation, increased leukocyte rigidity and decreased erythrocyte deformability, are also detected in HIV-infected individuals. These factors are directly associated with increased plasma fibrinogen, which is a determinant factor in the HIV infection. Therefore, it has been deduced that an increased RBC aggregation has been associated with the severity of HIV disease.

Therefore, one of the challenges in HIV research has been to unravel the multifactorial structure of the disease, which leads to changes in hemorheological parameters[10]. The existence of hemorheological parameters in HIV system and fractional derivatives embody essential features of cell rheological behavior. There are a few research which introduce fractional-order into the traditional HIV models ([7, 36, 37, 56]), however, none of them carefully controlled the time unit with respect to differential operator and did data as-

similation with patient measurement. In this paper, we propose a system of fractional-order differential equations for modelling HIV infection of lymphocyte population in plasma. We introduce a model that contains fractional-order differential equations of order $0 < \alpha < 1$ into Latent reservoir model. In section 3.3, we give derivation and analysis of the fractional-order system in HIV infection model. Section is devoted for the description for numerical method for solving FODE, including how to determine the optimal initial guess for the new model parameters. The model parameters including optimal fractional order are estimated for 10 patient measurements and comparison on integer-order model are presented in . From these results, we not only confirm that our analysis is correct, but verify that a parameter representing the rheological behavior in plasma is significantly correlated with critical parameter relating with lymphocyte population.

3.3 Model derivation

We first give the definition of fractional-order integration and fractional-order differentiation [123]. There are several approaches to the generalization of the notion of differentiation to fractional orders e.g. Riemann-Liouville, Caputo and Generalized Functions approach. For the concept of fractional derivative, we will adopt Caputo's definition which has the advantage of dealing with initial value problem in proper. Recall Euler's Gamma function (also called Euler's integral of the second kind) as follows:

$$\Gamma(x) = \int_0^\infty t^{x-1} e^{-t} dt. \tag{3.8}$$

We then begin by clarifying the definitions of fractional–order integration and differentiation; see, for instance, [57]. Denote by $\mathbb{R}_+$ and $\mathbb{R}_+^n$ the set of strictly

positive real numbers and set of points with positive components in $\mathbb{R}^n$, respectively.

Definition 3.3.1. *Let $\alpha \in \mathbb{R}_+$. A function $J_a^\alpha f(t)$, defined by*

$$J_a^\alpha f(t) = \frac{1}{\Gamma(\alpha)} \int_a^t (t-u)^{\alpha-1} f(u) du, \tag{3.9}$$

is called the Riemann–Liouville fractional integral of order α of a function $f : \mathbb{R}_+ \to \mathbb{R}_+^n$.

Definition 3.3.2. *Let $\alpha \in \mathbb{R}_+$ and $m = \lceil \alpha \rceil$. The Caputo fractional derivative of order α of a continuous function $f : \mathbb{R}_+ \to \mathbb{R}_+^n$ is given by*

$${}_C D_a^\alpha f(t) = J_a^{m-\alpha} D^m f(t), \tag{3.10}$$

where $\lceil . \rceil$ is the ceiling function satisfying $\lceil x \rceil = \min\{z \in \mathbb{Z} : z \geq x\}$, and $D = \frac{d}{dt}$.

The Laplace transform of Caputo fractional derivative (3.10) is given as follows:

$$\mathcal{L}({}_C D_a^\alpha f(t)) = \int_0^\infty {}_C D_a^\alpha f(t) e^{-st} dt = s^\alpha \mathcal{L}(f(t)) - s^{\alpha-1} f(0), \quad 0 < \alpha \leq 1. \tag{3.11}$$

Now we introduce fractional-order differentiation of order $\alpha \in (0, 1)$ into the ODE model of latent cell activation, proposed by Rong et al.[134]. The new system is described by the following set of equations:

$$\begin{aligned}
&D_0^\alpha T(t) = \tau^{1-\alpha}(\lambda - (1-\theta u(t))kV(t)T(t)) - \rho^\alpha T(t), \quad T(0) = T_0 \\
&D_0^\alpha T^*(t) = \tau^{1-\alpha}(1-\epsilon)(1-\theta u(t))kT(t)V(t) - \delta^\alpha T^*(t) + r_L^\alpha L(t), \quad T^*(0) = T_0^* \\
&D_0^\alpha L(t) = \tau^{1-\alpha}\epsilon(1-\theta u(t))kT(t)V(t) - (\delta_L^\alpha + r_L^\alpha)L(t), \quad L(0) = L_0 \\
&D_0^\alpha V(t) = N\delta^\alpha T^*(t) - c^\alpha V(t), \qquad V(0) = V_0,
\end{aligned} \tag{3.12}$$

where the parameters are equal to the one listed in the previous model in (2.3) except $\tau(day)$ is time constant required to preserve units. Here, $\alpha \in (0, 1)$ is restricted such that fractional derivative can be approximately described the rate of change in cell counts or viral copies.

Remark 3.3.3. *$u(t)$ is an input variable while $T(t), T^*(t), L(t)$ and $V(t)$ are output variables. In this system, these output variables affect each other physiologically which behaves in a nonlinear fashion, and $u(t)$ is considered as bounded and piecewise C^1 function.*

Remark 3.3.4. *In* (3.12)*, we can consider that the parameter $\tau^{1-\alpha}$ takes a role of balancing the cell reflects the effect of the rheological behavior properties ,especially RBC aggregation, resulting in the dynamics of blood flow of the HIV infected individuals. This means that $\tau^{1-\alpha}$ can be considered as a parameter that describes the effect of the rheological behavior in the lymphocyte cell production from thymus. This means that increase in RBC aggregation and decrease in deformability lead to low flow rate of blood, then the cell production in thymus(λ) can be decrease. Then the more the need of the active rate ($\tau^{1-\alpha}$) to maintain the balance of it. The greater the effect on the flow of the bloodstream, the less susceptibility to increase or decrease in lymphocyte cell and virus population.*

For the notational simplification, denote $C^1(\mathbb{R}_+, \mathbb{R}^4)$ by the Banach space of continuously differentiable functions mapping $\mathbb{R}_+$ into $\mathbb{R}^4$,
$\mathbf{x}(t) = (T(t), T^*(t), L(t), V(t))^T \in C^1(\mathbb{R}_+, \mathbb{R}^4)$. Then (3.12) can be re-written as

$$ {}_C D_0^{\alpha} \mathbf{x}(t) = \mathbf{f}(t, \mathbf{x}; \mathbf{p}), \quad \mathbf{x}(0) = (T_0, T_0^*, L_0, V_0)^T \tag{3.13} $$

where we denote the right hand side in (3.13) by

$$\mathbf{f}(t,\mathbf{x};\mathbf{p}) = \begin{pmatrix} -\tau^{1-\alpha}(1-\theta u(t))kx_1(t)x_4(t) - \rho^\alpha x_1(t) \\ \tau^{1-\alpha}(1-\epsilon)(1-\theta u(t))kx_1(t)x_4(t) - \delta^\alpha x_2(t) + r_L^\alpha x_3(t) \\ \tau^{1-\alpha}\epsilon(1-\theta u(t))kx_1(t)x_4(t) - (\delta_L^\alpha + r_L^\alpha)x_3(t) \\ N\delta^\alpha x_2(t) - c^\alpha x_4(t) \end{pmatrix} + \begin{pmatrix} \tau^{1-\alpha}\lambda \\ 0 \\ 0 \\ 0 \end{pmatrix}, \quad (3.14)$$

where $\mathbf{p} = \{\lambda, \rho, k, \delta, N, c, \theta, \epsilon, r_L, \delta_L, \tau^{1-\alpha}, \alpha\}$ is a set of parameters contained. Note that the system is called the off–treatment system of (3.34) when the input $u(t) = 0$. Throughout this section, we denote the ℓ_2 norm by $||\cdot||$, and eigenvalues of matrix $\mathbf{A}$ by $spec(\mathbf{A})$.

To discuss the non–negativity and boundedness of the solution of (3.12), we need the following preliminaries.

Theorem 3.3.5. (Theorem 2.1., Remark 2.3., and Theorem 3.1. in [85]) *Consider the following initial value problem for Caputo fractional differential equations*

$$\begin{cases} {}_C D_{t_0}^\alpha \mathbf{x} = \mathbf{f}(t,\mathbf{x}), \quad 0 < \alpha \leq 1, \\ \mathbf{x}(t_0) = \mathbf{x}_0, \end{cases} \quad (3.15)$$

where the function $\mathbf{f}(t,\mathbf{x}) : \mathbb{R} \times \mathbb{R}^d \to \mathbb{R}^d$ *is a vector field and the dimension* $d \geq 1$. *Choose any* $a, b \in \mathbb{R}_+$, *and let*

$$\mathcal{T} = [t_0 - a, t_0 + a],$$
$$\mathcal{B} = \{\mathbf{x} \in \mathbb{R}^d | \, ||\mathbf{x} - \mathbf{x}_0|| \leq b\},$$
$$\mathcal{D} = \{(t,\mathbf{x}) \in \mathbb{R} \times \mathbb{R}^d \,|\, t \in \mathcal{T}, \mathbf{x} \in \mathcal{B}\}.$$

Assume that the function $\mathbf{f}(t,\mathbf{x}) : \mathcal{D} \to \mathbb{R}^d$ *satisfies the following conditions:*

1. $\mathbf{f}(t,\mathbf{x})$ *is Lebesgue measurable with respect to* t *on* $\mathcal{T}$*;*

2. $\mathbf{f}(t,\mathbf{x})$ *is continuous with respect to* $\mathbf{x}$ *on* $\mathcal{B}$*;*

3. there exists a bounded real–valued function $M(t)$ such that

$$||\mathbf{f}(t,\mathbf{x})|| \leq M(t),$$

for almost every $t \in \mathcal{T}$ and all $\mathbf{x} \in \mathcal{B}$.

Then, there at least exists a solution of the initial value problem (3.15) *on the interval $[t_0 - h, t_0 + h]$ for some positive number h satisfying*

$$\mathbf{x}(t) = \mathbf{x}_0 + J_{t_0}^{\alpha}\left(\mathbf{f}(t,\mathbf{x})\right).$$

Moreover, if the function $\mathbf{f}(t,\mathbf{x})$ satisfies the above first two conditions 1 and 2 in the global space $\mathbb{R} \times \mathbb{R}^d$ and

$$||\mathbf{f}(t,\mathbf{x})|| \leq \lambda||\mathbf{x}|| + w, \tag{3.16}$$

for almost every $t \in \mathbb{R}$ and all $\mathbf{x} \in \mathbb{R}^d$ where λ, w are two positive constants, then, there exists a function $\mathbf{x}(t)$ on $(-\infty, \infty)$ satisfying the initial condition in (3.15)*. If $\nabla_{\mathbf{x}}\mathbf{f}(t,\mathbf{x})$ is further assumed to be continuous with respect to $\mathbf{x}$, this gives the uniqueness of the solution $\mathbf{x}(t)$ in* (3.15)*.*

Lemma 3.3.6. Generalized Mean value Theorem in [111] *Let $0 < \alpha \leq 1$. Suppose that $f \in C[a,b]$ and ${}_C D_a^{\alpha} f \in C(a,b]$. Then, for all $t \in (a,b]$, there exist $\xi \in (a,t)$ such that*

$$f(t) = f(a) + \frac{1}{\Gamma(\alpha)}({}_C D_a^{\alpha} f)(\xi)(t-a)^{\alpha}. \tag{3.17}$$

Corollary 3.3.7. (Corollary 1. in [37])

Let $0 < \alpha \leq 1$. Suppose that $f \in C[a,b]$ and ${}_C D_a^{\alpha} f \in C(a,b]$. If ${}_C D_a^{\alpha} f(t) \geq 0,\ \forall t \in (a,b)$, then f is a non–decreasing function. If ${}_C D_a^{\alpha} f(t) \leq 0, \forall t \in (a,b)$,

then f is a non–increasing function.

Lemma 3.3.8. (Fractional Comparison Principle in [84])

Let $x(0) = y(0)$ and ${}_C D_0^{\alpha} x(t) \leq {}_C D_0^{\alpha} y(t)$, where $0 < \alpha \leq 1$. Then $x(t) \leq y(t)$.

Definition 3.3.9. *For $\alpha > 0$, the Mittag–Leffler function E_{α} is defined by*

$$E_{\alpha}(z) := \sum_{j=0}^{\infty} \frac{z^j}{\Gamma(j\alpha + 1)}. \tag{3.18}$$

Moreover, it is an entire function if $\alpha > 0$.

The Mittag–Leffler function with two parameters defined by

$$E_{\alpha,\beta}(z) := \sum_{j=0}^{\infty} \frac{z^j}{\Gamma(j\alpha + \beta)} \tag{3.19}$$

is an entire function whenever $\alpha > 0, \beta > 0$ and $z \in \mathbb{C}$. The Laplace transform of the Mittag–Leffler function with two parameters[123] is given by

$$\mathcal{L}(t^{\beta-1} E_{\alpha,\beta}(-\lambda t^{\alpha})) = \frac{s^{\alpha-\beta}}{s^{\alpha} + \lambda}, \quad Re(s) > |\lambda|^{1/\alpha}. \tag{3.20}$$

The following lemmas are useful in the proof of the non–negativity, boundedness, and stability of the solution (3.13).

Lemma 3.3.10. (Page 210 in [1]) *Suppose that $0 < \alpha < 2$, $\beta \in \mathbb{R}$, and $\mu \in \left(\frac{\alpha\pi}{2}, min\{\pi, \alpha\pi\}\right)$. Then for an arbitrary integer $N \geq 1$, the following asymptotic expansion holds:*

$$E_{\alpha,\beta}(z) = -\sum_{j=1}^{N} \frac{1}{\Gamma(-j\alpha + \beta) z^j} + \mathcal{O}\left(\frac{1}{z^{N+1}}\right), \text{ as } |z| \to \infty, \ \mu \leq |arg(z)| \leq \pi. \tag{3.21}$$

From the above lemma the following result follows:

Lemma 3.3.11. (Theorem 1.6. in [123]) *Suppose that* $0 < \alpha < 2$, $\beta \in \mathbb{R}$, *and* $\mu \in \left(\frac{\alpha\pi}{2}, min\{\pi, \alpha\pi\}\right)$. *Then there exists* $M > 0$ *such that*

$$|E_{\alpha,\beta}(z)| \leq \frac{M}{1+|z|}, \quad \mu \leq |arg(z)| \leq \pi.$$

Lemma 3.3.12. (Corollary 1. in [157]) *Suppose that* $\mathbf{A} \in \mathbb{C}^{n\times n}$, $0 < \alpha < 2$, $\beta \in \mathbb{R}$, *and* $\mu \in \left(\frac{\alpha\pi}{2}, min\{\pi, \alpha\pi\}\right)$. *Then there exists* $C > 0$ *such that*

$$||E_{\alpha,\beta}(\mathbf{A})|| \leq \frac{C}{1+||\mathbf{A}||},$$

where $\mu \leq |arg(spec(\mathbf{A}))| \leq \pi$.

By the help of Lemmas, we now prove the existence of the solution in (3.13).

Proposition 3.3.13. *There is a solution* $\mathbf{x}(t)$ *in* (3.13) *that remains in* $\mathbb{R}^4_+$ *and bounded.*

Proof. Note that $\mathbf{f}(t, \mathbf{x}; \mathbf{p})$ in (3.13) satisfies clearly the conditions 1 and 2 of Theorem 3.3.5 in $\mathbb{R}_+ \cup \{0\} \times \mathbb{R}^4$, we now show that it satisfies the condition (3.16). Due to the boundedness of $|u(t)| \leq 1$, ${}_C D_0^\alpha x_1(t)$ satisfies

$$\begin{aligned} ||{}_C D_0^\alpha x_1(t)|| &\leq \tau^{1-\alpha}\lambda - \rho^\alpha x_1(t) \\ &\leq \rho^\alpha ||x_1(t)|| + \tau^{1-\alpha}\lambda. \end{aligned} \tag{3.22}$$

Then, Theorem 3.3.5 gives the existence and uniqueness of solutions $x_1(t)$ on $t \in (0, \infty)$. In addition, we have

$$\begin{aligned} {}_C D_0^\alpha x_1(t) &\leq -\rho^\alpha x_1(t) + \tau^{1-\alpha}\lambda \\ &= -\rho^\alpha \left(x_1(t) - \frac{\tau^{1-\alpha}\lambda}{\rho^\alpha} \right) \end{aligned} \tag{3.23}$$

Let $K_1(t) = x_1(t) - \frac{\tau^{1-\alpha}\lambda}{\rho^\alpha}$. Then, using the the linearity of Caputo derivative, (3.30) can be rewritten as follows:

$$ {}_C D_0^\alpha K_1(t) \leq -\rho^\alpha K_1(t). $$

By applying Lemma 3.3.8, we have

$$ K_1(t) \leq K_1(0) E_{\alpha,1}(-\rho^\alpha t^\alpha), \quad \forall t > 0, \tag{3.24} $$

and thus we have $\limsup_{t\to\infty} x_1(t) \leq \frac{\tau^{1-\alpha}\lambda}{\rho^\alpha}$ by Lemma 3.3.11, and it follows that there exists a constant $R_1 > 0$ such that $||x_1(t)|| \leq R_1$. The non–negativity of the solution $x_1(t)$ can be guaranteed from

$$ {}_C D_0^\alpha x_1(t) \mid_{x_1(t)=0} = \tau^{1-\alpha}\lambda \geq 0, \tag{3.25} $$

and Corollary 3.3.7. Thus the solution $x_1(t)$ remains in $\mathbb{R}_+$.

Secondly, we let $x_\ell(t) = \epsilon x_1(t) + x_3(t)$. Then, by using the non-negativity and boundedness of the solution $x_1(t)$, ${}_C D_0^\alpha x_\ell(t)$ satisfies

$$ \begin{aligned} ||{}_C D_0^\alpha x_\ell(t)|| &\leq \epsilon(\tau^{1-\alpha}\lambda - \rho^\alpha x_1(t)) - (r_L^\alpha + \delta_L^\alpha) x_3(t) \\ &\leq M_1^\alpha ||x_\ell(t)|| + \tau^{1-\alpha}\epsilon\lambda, \end{aligned} \tag{3.26} $$

where $M_1 = \max\{\rho, r_L, \delta_L\}$. Then, Theorem 3.3.5 gives the existence and uniqueness of solutions $x_3(t)$ on $(0, \infty)$.

In addition, we have

$$ \begin{aligned} {}_C D_0^\alpha x_\ell(t) &\leq -M_1^\alpha x_\ell(t) + \tau^{1-\alpha}\epsilon\lambda \\ &= -M_1^\alpha \left(x_\ell(t) - \frac{\tau^{1-\alpha}\epsilon\lambda}{M_1^\alpha} \right) \end{aligned} \tag{3.27} $$

Let $K_2(t) = x_\ell(t) - \frac{\tau^{1-\alpha}\epsilon\lambda}{M_1^\alpha}$. Then, using the linearity of Caputo derivative, (3.30) can be rewritten as follows:

$$ {}_C D_0^\alpha K_2(t) \leq -M_1^\alpha K_2(t). $$

By applying Lemma 3.3.8, we have

$$ K_2(t) \leq K_2(0) E_{\alpha,1}(-M_1^\alpha t^\alpha), \quad \forall t > 0, \tag{3.28} $$

and thus we have $\limsup_{t\to\infty} \; x_\ell(t) \leq \frac{\tau^{1-\alpha}\epsilon\lambda}{M_1^\alpha}$ by Lemma 3.3.11, and it follows that there exists a constant $R_2 > 0$ such that $||x_3(t)|| \leq R_2$. We also find that the solution $x_3(t)$ remains in $\mathbb{R}_+$. from ${}_C D_0^\alpha x_3(t) \mid_{x_3(t)=0} = 0$ and Corollary 3.3.7.

In the same way done for $x_2(t)$, we can show that the existence of the soluton $x_2(t)$ by considering $x_r(t) = (1-\epsilon)x_1(t) + x_2(t)$. Then we can see that ${}_C D_0^\alpha x_r(t)$ satisfying

$$ ||{}_C D_0^\alpha x_r(t)|| \leq M_2^\alpha ||x_r(t)|| + \tau^{1-\alpha}(1-\epsilon)\lambda, \tag{3.29} $$

where $M_2 = \max\{\rho, \delta\}$ by using the help of x_1 and $x_3(t)$. Then,the existence and uniqueness of solutions $x_2(t)$ on $(0, \infty)$ can be proved from Theorem 3.3.5.

In addition, we have

$$ \begin{aligned} {}_C D_0^\alpha x_r(t) &\leq -M_2^\alpha x_r(t) + \tau^{1-\alpha}(1-\epsilon)\lambda \\ &= -M_2^\alpha \left(x_r(t) - \frac{\tau^{1-\alpha}(1-\epsilon)\lambda}{M_2^\alpha} \right) \end{aligned} \tag{3.30} $$

BY using the the linearity of Caputo derivative,and Lemma 3.3.8, we have

$$K_3(t) \leq K_3(0)E_{\alpha,1}(-M_2^{\alpha}t^{\alpha}), \quad \forall t > 0, \tag{3.31}$$

,where $K_3(t) = x_r(t) - \frac{\tau^{1-\alpha}(1-\epsilon)\lambda}{M_2^{\alpha}}$, and thus we have $\limsup_{t\to\infty} \; x_r(t) \leq \frac{\tau^{1-\alpha}(1-\epsilon)\lambda}{M_2^{\alpha}}$ by Lemma 3.3.11, and it follows that there exists a constant $R_3 > 0$ such that $||x_2(t)|| \leq R_3$. The solution $x_2(t)$ remains in $\mathbb{R}_+$ due to the ${}_CD_0^{\alpha}x_2(t) \mid_{x_2(t)=0}= 0$ and Corollary 3.3.7.

From (3.12), ${}_CD_0^{\alpha}x_4(t)$ in (3.13) satisfies

$$\begin{aligned} ||{}_CD_0^{\alpha}x_4(t)|| &\leq c^{\alpha}||x_4(t)|| + N\delta^{\alpha}||x_2(t)|| \\ &\leq c^{\alpha}||x_4(t)|| + N\delta^{\alpha}R_3, \end{aligned} \tag{3.32}$$

which gives the sufficient condition for global existence and uniqueness of solution $x_4(t)$ by (3.16) in Theorem 3.3.5. Hence, $x_4(t)$ has a solution on $(0, \infty)$.

Then the existing solution $\mathbf{x}(t)$ for (3.13) has the form of

$$\mathbf{x}(t) = \mathbf{x}(0) + J_0^{\alpha}\left(\mathbf{f}(t, \mathbf{x}; \mathbf{p})\right). \tag{3.33}$$

The non–negativity of all solution $\mathbf{x}(t)$ can be guaranteed from

$${}_CD_0^{\alpha}\mathbf{x}(t) \mid_{\mathbf{x}(t)=0}= \begin{pmatrix} \tau^{1-\alpha}\lambda \\ 0 \\ 0 \\ 0 \end{pmatrix} \geq \begin{pmatrix} 0 \\ 0 \\ 0 \\ 0 \end{pmatrix}, \tag{3.34}$$

and Corollary 3.3.7. Thus the solution remains in $\mathbb{R}^4_+$.

From (3.12), we have

$$ {}_C D_0^{\alpha} x_4(t) \leq -c^{\alpha} x_4(t) + N\delta^{\alpha} R_3. \tag{3.35} $$

Let $K_4(t) = x_4(t) - NR_3 \left(\frac{\delta}{c}\right)^{\alpha}$, Then (3.35) gives

$$ {}_C D_0^{\alpha} K_4(t) \leq -c^{\alpha} K_4(t). $$

and we have

$$ K_4(t) \leq K_4(0) E_{\alpha,1}(-c^{\alpha} t^{\alpha}) \quad \forall t > 0. \tag{3.36} $$

from Lemma 3.3.8. Therefore, we have $\limsup_{t\to\infty} \; x_4(t) \leq NR_3 \left(\frac{\delta}{c}\right)^{\alpha}$ by Lemma 3.3.11. □

3.4 Numerical methods

There are a number of numerical and analytical methods developed for various types of FDEs, for example, variational iterative method, fractional differential transform method, a domain decomposition method, homotopy perturbation method and power series method. In [34], Kai Diethelm, Neville J. Ford and Alan D. Freed introduced Adams-type predictor-corrector method for solving both linear and nonlinear fractional differential equations. In the numerical algorithm the authors converted the considered equations into the Volterra integral equation and then approximated the integral by using a piecewise linear interpolation polynomial. It is used for both linear and nonlinear problems, and can be extended to multi-term fractional-order differential equations. We use this method for numerical solution of the nonlinear system (3.12) by replacing original system into systems of equivalent Volterra integral

equations. We again use the nonlinear least square method implemented in 2.2 to estimated optimal values for model parameters and initial states, and particulary optimal fractional order α in this section. In 3.4.1, we introduce briefly the fractional Adams-type predictor-corrector method as an integration method for fractional-order differential equation. In order to use the nonlinear weighted least–squares method and the Levenberg–Marquardt algorithm, sensitivity equations are discussed in 3.4.2.

3.4.1 The fractional Adams method

The fractional Adams-type predictor-corrector method[34] is an effective technique for solving fractional-order differential equations. Consider the following fractional-order differential equation

$$D^{\alpha}_{t_0}(t) = f(t, x(t)), \quad x(t_0) = x_0. \tag{3.37}$$

Assume that the function f is continuous and satisfies a Lipschitz condition with respect to its second argument with Lipschitz constant L on a suitable set. Then there exists a unique solution x of the initial value problem (3.37) on some interval $[t_0, t_f]$ by the existence and uniqueness theorem for the Caputo's type of fractional-order differential equation.

It is well-known that (3.37) is equivalent to the Volterra integral equation can be interpreted as a Volterra integral equation[34]

$$x(t) = \sum_{k=0}^{\lceil\alpha\rceil-1} x_0^{(k)} \frac{t^k}{k!} + \frac{1}{\Gamma(\alpha)} \int_0^t (t-u)^{\alpha-1} f(u, x(u)) du \tag{3.38}$$

in the sense that a continuous function is a solution of the initial value problem (3.37) if and only if it is a solution of (3.38). In case of our model (3.12), we have $\lceil\alpha\rceil = 1$.

Setting $h = (t_f - t_0)/N,\ t_j = jh,\ j = 0, 1, \ldots, N$, where N is a positive integer. The integral of nonlinear term in (3.38) can be approximated by the following linear interpolation:

$$\int_{t_0}^{t_{k+1}} (t-u)^{\alpha-1} f(u, x(u))du \approx \int_{t_0}^{t_{k+1}} (t-u)^{\alpha-1} \tilde{f}_{k+1}(u, x(u))du, \qquad (3.39)$$

where $\tilde{f}_{k+1}$ is the piecewise linear interpolant for f with equispaced nodes and knots chosen at $t_j,\ j = 0, 1, \ldots, k+1$. An explicit calculation yields that we can write the integral on the right-hand side of (3.39) as

$$\int_{t_0}^{t_{k+1}} (t-u)^{\alpha-1} \tilde{f}_{k+1}(u, x(u))du = \sum_{j=0}^{k+1} a_{j,k+1} f(t_j, x(t_j)), \qquad (3.40)$$

where

$$a_{j,k+1} = \frac{h^\alpha}{\alpha(\alpha+1)} \times \begin{cases} k^{\alpha+1} - (k-\alpha)(k+1)^\alpha, & j = 0 \\ (k-j+2)^{\alpha+1} + (k-j)^{\alpha+1} - 2(k-j+1)^{\alpha+1}, & 1 \le j \le k, \\ 1, & j = k+1. \end{cases} \qquad (3.41)$$

Using the above discretization, the integrand in (3.38) can be approximated as follows:

$$\begin{aligned} x(t_{k+1}) &\approx x_{k+1} \\ &= x_0 + \frac{1}{\Gamma(\alpha)} \left(\sum_{j=0}^{k} a_{j,k+1} f(t_j, x(t_j)) + a_{k+1,k+1} f(t_{k+1}, x_{k+1}^P) \right), \end{aligned} \qquad (3.42)$$

where each of x_{k+1} and x_{k+1}^P is an approximation and a predictor at time t_{k+1}. respectively. The predictor x_{k+1}^P is determined by replacing the integral

on the right-hand side of (3.38) following the product rectangle rule, i.e.,

$$\int_{t_0}^{t_{k+1}} (t-u)^{\alpha-1} f(u, x(u))du \approx \sum_{j=0}^{k} b_{j,k+1} f(t_j, x(t_j)), \tag{3.43}$$

where now

$$b_{j,k+1} = \frac{h^\alpha}{\alpha} \left((k+1-j)^\alpha - (k-j)^\alpha \right). \tag{3.44}$$

Therefore, the predictor x_{k+1}^P is obtained as follows:

$$x_{k+1}^P = x_0 + \frac{1}{\Gamma(\alpha)} \sum_{j=0}^{k} b_{j,k+1} f(t_j, x(t_j)). \tag{3.45}$$

We see that we first have to calculate the predictor x_{k+1}^P according to (3.45), then we evaluate $f(t_{k+1}, x_{k+1}^P)$, use this to determine the corrector x_{k+1} by means of (3.42), and finally evaluate $f(t_{k+1}, x_{k+1})$ which is then used in the next iteration.(PECE: predict, evaluate, correct, evaluate). By using the derived discrete scheme, we find the numerical solution for the system (3.12).

Following theorem is for the order of convergence of this numerical method. Some information on the errors of the quadrature formulas that have used in the derivation of the predictor and the corrector are required ,respectively. They first give a statement on the product rectangle rule that have used for the predictor.

Theorem 3.4.1. *(Theorem 2.4 of [35]) (a)Let* $g \in \mathbf{C}^1[0, t_f]$. *Then,*

$$\left| \int_0^{t_{n+1}} (t_{n+1}-u)^{\alpha-1} g(u)du - \sum_{j=0}^{n} b_{j,n+1} g(t_j) \right| \leq \frac{1}{\alpha} \left\| g\prime \right\|_\infty t_{n+1}^\alpha h.$$

(b)Let $g(t) = t^p$ for some $p \in (0,1)$. Then,

$$\Big| \int_0^{t_{n+1}} (t_{n+1} - u)^{\alpha-1} g(u)du - \sum_{j=0}^{n} b_{j,n+1} g(t_j) \Big| \leq C(\alpha, p) t_{n+1}^{\alpha+p-1} h.$$

where $C(\alpha, p)$ is a constant that depends only on α and p.

Theorem 3.4.2. *(Theorem 2.5 of [35]) (a)Let $g \in \mathbf{C}^2[0, t_f]$ then there is a constant C_α depending only on α such that*

$$\Big| \int_0^{t_{n+1}} (t_{n+1} - u)^{\alpha-1} g(u)du - \sum_{j=0}^{n+1} a_{j,n+1} g(t_j) \Big| \leq C_\alpha \left\| g'' \right\|_\infty t_{n+1}^{\alpha} h^2.$$

(a)Let $g \in \mathbf{C}^1[0, t_f]$ and assume that g' fulfils a Lipschitz condition of order μ for some $\mu \in (0,1)$. Then, there exist positive constants $B_{\alpha,\mu}$(depending only on α and μ) and $M(g, \mu)$ (depending only on g and μ) such that

$$\Big| \int_0^{t_{n+1}} (t_{n+1} - u)^{\alpha-1} g(u)du - \sum_{j=0}^{n+1} a_{j,n+1} g(t_j) \Big| \leq B_{\alpha,\mu} M(g, \mu) t_{n+1}^{\alpha} h^{1+\mu}.$$

(b)Let $g(t) = t^p$ for some $p \in (0,2)$ and $Q = \min(2, p+1)$. Then,

$$\Big| \int_0^{t_{n+1}} (t_{n+1} - u)^{\alpha-1} g(u)du - \sum_{j=0}^{n+1} a_{j,n+1} g(t_j) \Big| \leq C_{\alpha,p} t_{n+1}^{\alpha+p-Q} h^Q.$$

where $C_{\alpha,p}$ is a constant that depends only on α and p.

Lemma 3.4.3. *(Lemma 3.1 of [35]) Assume that the solution y of the initial value problem*(3.37) *is such that*

$$\Big| \int_0^{t_{n+1}} (t_{n+1} - u)^{\alpha-1} D^\alpha y(u)du - \sum_{j=0}^{n} b_{j,n+1} D^\alpha y(t_j) \Big| \leq C_1 t_{n+1}^{\gamma_1} h^{\delta_1}$$

and

$$\Big| \int_0^{t_{n+1}} (t_{n+1}-u)^{\alpha-1} D^\alpha y(u) du - \sum_{j=0}^{n+1} a_{j,n+1} D^\alpha y(t_j) \Big| \le C_2 t_{n+1}^{\gamma_2} h^{\delta_2}$$

with some $\gamma_1, \gamma_2 \ge 0$ *and* $\delta_1, \delta_2 \ge 0$. *Then for some suitable chosen* $t_f > 0$, *we have*

$$\max_{0 \le j \le N} |y(t_j) - y_h(t_j)| = O(h^q),$$

where $q = \min\{\delta_1 + \alpha, \delta_2\}$.

Theorem 3.4.4. (Theorem 3.2 in [35]) *Assume that the function* $f(t, x(t))$ *in* (3.37) *is of class* $C^2[0, t_f]$ *for some suitable* t_f. *Then,*

$$\max_{0 \le j \le N} |x(t_j) - x_j| = \begin{cases} O(h^2), & \text{if } 1 \le \alpha < 2 \\ O(h^{1+\alpha}), & \text{if } 0 < \alpha < 1. \end{cases}$$

Proof. We may apply lemma 3.4.3 with $\gamma_1 = \gamma_2 = \alpha > 0,\ \delta_1 = 1$ and $\delta_2 = 2$. Thus we find an $O(h^q)$ error bound where

$$q = \min\{1+\alpha, 2\} = \begin{cases} 2, & \text{if} \quad \alpha \ge 1, \\ 1+\alpha, & \text{if} \quad \alpha < 1. \end{cases}$$

□

Note that in a certain sense the theorem above deals with the "optimal" situation: the function that we approximate in our process is $f(\cdot, y(\cdot)) = D^\alpha y$. In order to obtain very good error bounds, we need to make sure that the quadrature errors for this function are (asymptotically) as small as possible. A sufficient condition for this to hold is, as is well known from quadrature theory, that this function is in C^2 on the interval of integration, i.e., $D^\alpha y$ is at least

two times continuously differentiable on $[0, t_f]$. So this theorem shows us what kind of performance the Adams method can give under optimal circumstances, and it also states sufficient conditions for such results to hold. We then obtain the numerical solution for each state variables by discretizing (3.12) using the form of (3.42) and (3.45).

3.4.2 Sensitivity equations

The nonlinear weighted least–squares method and the Levenberg–Marquardt algorithm require the partial derivatives of each states variable with respect to every single element of the parameter vector $\mathbf{p}$. In order to obtain the derivatives, we need to calculate the first derivatives of the model prediction $\mathbf{f}(t, \mathbf{x}(t); \mathbf{p})$ with respect to every single element of the parameter vector $\mathbf{p}$. And then interchanging the order of time and parameter derivatives, the fractional Adams method is applied. Therefore, we obtain the partial derivatives of $\mathbf{x}(t)$ with respect to every single element of the parameter vector $\mathbf{p}$. Our model (3.12) is not dynamically linear system, and therefore it is not possible to calculate the exact derivatives since the dependency of $f(t, \mathbf{x}(t); \mathbf{p})$ on parameters $\mathbf{p}$ is unknown. In particular, partial derivatives of (3.12) with respect to each parameters including fractional order α are obtained as follows. For

certain parameter $p_j \in \mathbf{p}$, we have

$$\begin{aligned}
\frac{\partial D_0^\alpha T(t)}{\partial p_j} =& -(\tau^{1-\alpha}(1-\theta u)kV + \rho^\alpha)\frac{\partial T}{\partial p_j} - \tau^{1-\alpha}(1-\theta u)kT\frac{\partial V}{\partial p_j} \\
&+ \begin{cases}
\tau^{1-\alpha} & \text{if } p_j = \lambda \\
-\alpha\rho^{\alpha-1}T(t) & \text{if } p_j = \rho \\
-\tau^{1-\alpha}((1-\theta u(t))V(t)T(t)) & \text{if } p_j = k \\
\tau^{1-\alpha}(u(t)kV(t)T(t)) & \text{if } p_j = \theta \\
(\lambda - (1-\theta u(t))kV(t)T(t)) & \text{if } p_j = \tau^{1-\alpha} \\
-\tau^{1-\alpha}\ln(\tau)\Big(\lambda - (1-\theta u(t))kV(t)T(t)\Big) & \text{if } p_j = \alpha \\
-\rho^\alpha \ln(\rho)T(t) & \\
0 & \text{otherwise,}
\end{cases} \\
, \frac{\partial T}{\partial p_j}\Big|_{t=0} =& \begin{cases}
1 & \text{if } p_j = T_0 \\
0 & \text{otherwise.}
\end{cases}
\end{aligned}$$

$$\begin{aligned}
\frac{\partial D_0^\alpha L(t)}{\partial p_j} =& \tau^{1-\alpha}\epsilon(1-\theta u(t))k\left(V(t)\frac{\partial T(t)}{\partial p_j} + T(t)\frac{\partial V}{\partial p_j}\right) - (\delta_L^\alpha + r_L^\alpha)\frac{\partial L}{\partial p_j} \\
&+ \begin{cases}
\epsilon(1-\theta u(t))kT(t)V(t) & \text{if } p_j = \tau^{1-\alpha} \\
\tau^{1-\alpha}(1-\theta u(t))kT(t)V(t) & \text{if } p_j = \epsilon \\
\tau^{1-\alpha}\epsilon(-u(t))k & \text{if } p_j = \theta \\
\tau^{1-\alpha}\epsilon(1-\theta u(t))T(t)V(t) & \text{if } p_j = k \\
-\alpha\delta_L^{\alpha-1}L(t) & \text{if } p_j = \delta_L \\
-\alpha r_L^{\alpha-1}L(t) & \text{if } p_j = r_L \\
-\left(\delta_L^\alpha \ln(\delta_L(t)) + r^\alpha \ln(r)\right)L & \text{if } p_j = \alpha \\
0 & \text{otherwise}
\end{cases} \\
, \frac{\partial L(t)}{\partial p_j}\Big|_{t=0} =& \begin{cases}
1 & \text{if } p_j = L_0 \\
0 & \text{otherwise.}
\end{cases}
\end{aligned}$$

$$\frac{\partial D_0^\alpha T^*(t)}{\partial p_j} = k\tau^{1-\alpha}(1-\epsilon)(1-\theta u(t))\left(V(t)\frac{\partial T(t)}{\partial p_j} + T(t)\frac{\partial V(t)}{\partial p_j}\right) - \delta^\alpha \frac{\partial T^*}{\partial p_j} + r_L^\alpha \frac{\partial L}{\partial p_j}$$

$$+ \begin{cases} -\tau^{1-\alpha}(1-\theta u(t))kT(t)V(t) & \text{if } p_j = \epsilon \\ \tau^{1-\alpha}(1-\epsilon)(-u(t))kT(t)V(t) & \text{if } p_j = \theta \\ \tau^{1-\alpha}(1-\epsilon)(1-\theta u(t))T(t)V(t) & \text{if } p_j = k \\ -\alpha * \delta^{\alpha-1}T^*(t) & \text{if } p_j = \delta \\ -\alpha * \rho^{\alpha-1}T(t) & \text{if } p_j = r_L \\ (1-\epsilon)(1-\theta u(t))kT(t)V(t) & \text{if } p_j = \tau^{1-\alpha} \\ -\tau^{1-\alpha}\ln(\tau)(1-\epsilon)(1-\theta_1 u(t))kT(t)V(t) & \text{if } p_j = \alpha \\ -\delta^\alpha \ln(\delta)T^*(t) + r^\alpha \ln(r)L(t) & \\ 0 & \text{otherwise,} \end{cases}$$

$$, \frac{\partial T^*}{\partial p_j}\Big|_{t=0} = \begin{cases} 1 & \text{if } p_j = T_0^* \\ 0 & \text{otherwise.} \end{cases}$$

$$\frac{\partial D_0^\alpha V(t)}{\partial p_j} = -c^\alpha \frac{\partial V(t)}{\partial p_j} + N\delta^\alpha \frac{\partial T^*(t)}{\partial p_j}$$

$$+ \begin{cases} N\alpha\delta^{\alpha-1}T^*(t) & \text{if } p_j = \delta \\ \delta^\alpha T^*(t) & \text{if } p_j = N \\ -\alpha c^{\alpha-1}V(t) & \text{if } p_j = c \\ N\delta^\alpha \ln(\delta)T^*(t) - c^\alpha \ln(c)V(t) & \text{if } p_j = \alpha \\ 0 & \text{otherwise,} \end{cases}$$

$$, \frac{\partial V(t)}{\partial p_j}\Big|_{t=0} = \begin{cases} 1 & \text{if } p_j = V_0 \\ 0 & \text{otherwise.} \end{cases}$$

3.4.3 Initial guess for paramters and the fractional order

For determining an initial guess for each parameters and initial states in the nonlinear equation (3.12), we consider a nuber of initialization approaches for obtaining optimal model parameters. We again divide the range of each parameter used in 2.2, which cover the reference values in Table2.6 into 20 equal-sized vertices to choose one candidate initial guess. One needs some restrictions on parameter values considering the defined biological meanings, for example, the parameters for the drug efficacy(θ), the death rate of lymphocyte(λ, ρ, δ_L) and proportionality(ϵ, ϵ_C) should be in the range $[0, 1]$. To find the optimal fractional order, the same process is performed in the range $[0.1, 1.0]$ of the fractional order α. We surely contains the case of $\alpha = 1.00$ since we can accept of optimality of fractional-order model with α than the integer model. From these, we choose the parameters generating the smallest chi-square value, which is given by $\chi^2 = \sum_{j=1}^{n}(y_j - \log_{10}(V(t_j; \mathbf{p})))^2$, where n is the number of data, y_j and $V(t_j; \mathbf{p})$ are measurement data and the numerical solution for the set of parameter $\mathbf{p}$ at time t_j, respectively. To evaluate the goodness of fit for each patient data, we use relative ℓ_2 error calculated by $\sqrt{\chi^2}/\sqrt{\sum_k {y_k}^2}$. The rest of this process is the same as for initial model.

3.5 Numerical results: model fits and sample predictions

In this section, we present some numerical results obtained from the fractional-order HIV model with latent reservoir. As we done with the integer-order HIV models in the previous chapter, we use the calibrated individual patient data to carry out inverse problem to obtain patient-specific parameter estimated in the fracitonal-order model.

Figure 3.1-3.2 show the measurements of plasma HIV viral load with numerical solution of the model(3.12) given by the estimated parameters.In Table 3.1, the estimated model parameters with optimal fractional order α, the relative ℓ_2 error for each patient are given. In Table 3.1, the optimal fractional order, the estimated parameter and initial conditions for states, and the relative ℓ_2 error for each patients are given. Compared to the values in Table3.3, the fractional model produces the smaller chi-square value than the model restricted to $\alpha = 1$ so that the viral rebound pattern of patient data can be descried by the fractional derivative better for all 9 patients. In Section3.3, we note that the parameter $\tau^{1-\alpha}$ estimated in Table 3.1 can be physiologically interpreted as the effect of rheological behavior to the infection process of HIV in plasma. The value of the $\tau^{1-\alpha}$ is determined to maintain the balance of virus-lymphocyte cell populations, depending on the growth rate of target cell(λ), infection rate(k).

We also performed a sensitivity analysis for estimated parameters with fractiona-order latent cell activation model, and the results are ranked in order in Table 3.2. Having similar parameters with high sensitivity observed in the integer model (2.71),i.e., k, δ_L, ρ and r_L, the notable point in this result is that the fractional order α and the balancing $\tau^{1-\alpha}$ belong to parameters with relatively high sensitivity among 16 parameters.

In the period of treatment, the decay dynamics of viral load are better fitted to the fractional model than the integer model, especially for patients 2,4 and 11 in Figure3.1 and Figure3.2. It can be seen that the response rate to the factors affecting the increase or decrease of the population is slower than that of the integer difference derivatives, which is consistent with the new model.Overall in most cases, having three interruptions yields a good prediction of long-term vial dynamics. For all nine patients, the fractional

model fit better than the model restricted to $\alpha = 1$, especially in the viral decay interval.

Red blood cell (RBC) deformability is a major determinant of the ability of the RBC to pass repeatedly through the microcirculation. A decrease in RBC deformability leads to tissue perfusion and organ dysfunction. According to Athanassiou et al.,[10], the rigidity of RBCs in HIV seropositive patients was significantly higher than that of the healthy individuals. Moreover, a index of rigidity(IR) was observed RBC deformability is decreased in HIV disease, in a degree mainly related to $CD4^{+}$cell depletion. This means that a low IR value indicates a higher flow rate of the blood, and it is related with high CD4 cell counts. The lower the value of α, the slower the blood flow velocity is depicted. To demonstrate the results of previous studies, we investigated the relationship between the density of CD4 cells in patients with relatively low α values.

Considering above clinical findings, we compare the the total population values estimated from each model during the same observation time. From the comparison on lymphocyte density listed in Table 3.4, for all patients, we find that the total value of target cell $T(t)$ for same observation time period is smaller when $0 < \alpha < 1$, which means that patient actually shows slower blood flow velocity and has higher value of index of rigidity(IR),than the case of $\alpha = 1$. Thus, the numerical results are coincide with the result of previous research on RBC deformability within HIV-infected patients, which denotes a high value of index of rigidity(IR) indicates a higher flow rate of the blood the fractional order model and consider the rheological factor. In case of reproductive number compared in Table3.5, the fracitonal model provides higher values for patients 2,3,5,8,11 and smaller value for patients 1,4,7,10 than the integer model. Recall the findings of Gallegos et al. [55] that increased aggre-

gation and decreased erythrocyte deformability are unrelated to the severity of the immunodeficiency, we can see that there is no influence on secondary reproductive number of productively infected lymphocyte population(T^*).

Patient	Estimated parameters					
	λ	ρ	k	δ	N	c
1	4.53E+02	1.81E-01	3.67E-06	7.01E-01	1.98E+03	1.00E+01
2	2.27E+02	3.53E-01	7.03E-06	4.19E-01	2.75E+03	5.98E+00
3	1.67E+02	3.34E-01	8.16E-06	8.70E-01	3.30E+03	7.61E+00
4	4.38E+02	2.38E-01	6.31E-06	9.12E-01	2.11E+03	1.41E+01
5	3.69E+02	2.42E-01	7.17E-06	8.23E-01	1.94E+03	1.42E+01
6	3.64E+02	2.53E-01	7.27E-06	6.17E-01	1.60E+03	1.43E+01
7	3.55E+02	2.58E-01	7.16E-06	8.39E-01	1.91E+03	1.37E+01
8	3.99E+02	1.80E-01	7.89E-06	7.74E-01	2.12E+03	1.40E+01
10	3.55E+02	2.51E-01	7.54E-06	8.69E-01	1.80E+03	1.41E+01
11	2.62E+02	2.64E-01	5.85E-06	5.45E-01	2.57E+03	7.75E+00
	θ	r_L	ϵ	δ_L	α	$\tau^{1-\alpha}$
1	8.87E-01	4.32E-02	7.08E-02	3.74E-02	9.78E-01	1.009E+00
2	7.33E-01	5.62E-02	1.33E-01	1.06E-02	9.80E-01	1.009E+00
3	9.86E-01	5.62E-02	9.49E-02	5.32E-03	9.84E-01	1.011E+00
4	4.84E-01	1.37E-04	5.11E-02	3.27E-03	9.70E-01	9.919E-01
5	7.91E-01	2.97E-02	9.57E-02	1.29E-02	9.48E-01	1.020E+00
6	6.01E-01	1.65E-03	3.02E-02	1.10E-02	9.70E-01	1.097E+00
7	6.92E-01	1.92E-03	7.47E-02	1.68E-02	9.58E-01	1.004E+00
8	6.82E-01	9.05E-04	2.11E-01	2.25E-02	9.84E-01	1.087E+00
10	6.12E-01	5.09E-02	3.99E-02	2.67E-02	9.48E-01	1.103E+00
11	8.99E-01	5.81E-02	1.12E-01	8.52E-03	9.80E-01	1.009E+00

Patient	Estimated parameters				Relative ℓ_2 error
	T_0	I_0	V_0	L_0	
1	2.74E+03	6.13E-04	7.76E-02	5.46E-06	9.15E-02
2	6.21E+02	8.34E-03	4.96E+00	1.30E-02	1.23E-01
3	5.52E+02	3.68E-04	6.85E-02	2.12E-04	1.42E-01
4	1.84E+03	9.66E-02	8.37E+00	3.20E-02	1.14E-01
5	1.01E+03	1.02E-02	1.01E+00	1.01E-01	9.33E-02
7	9.40E+02	9.86E-03	8.94E-01	9.41E-02	1.15E-01
8	2.06E+03	9.00E-02	8.86E+00	1.99E+00	1.52E-01
10	1.56E+03	5.47E-06	4.74E-04	1.02E-06	1.48E-01
11	5.33E+02	2.97E-02	6.04E+01	5.46E-02	9.41E-02

Table 3.1: Optimal order ($0 < \alpha < 1$), estimated parameters, and relative ℓ_2 error for each patient

Patient	Sensitive parameter p_i					
	Rank 1	Rank 2	Rank 3	Rank 4	Rank 5	Rank 6
1	k	δ_L	ρ	r_L	$\tau^{1-\alpha}$	δ
2	k	δ_L	ρ	r_L	$\tau^{1-\alpha}$	α
3	k	δ_L	r_L	$\tau^{1-\alpha}$	ρ	α
4	k	r_L	δ_L	ρ	$\tau^{1-\alpha}$	θ
5	k	δ_L	ρ	$\tau^{1-\alpha}$	r_L	α
7	k	r_L	ρ	δ_L	$\tau^{1-\alpha}$	α
8	k	r_L	α	δ_L	ρ	θ
10	k	α	ρ	δ_L	$\tau^{1-\alpha}$	r_L
11	k	δ_L	r_L	ρ	$\tau^{1-\alpha}$	α

Table 3.2: [Fractional-order Latent cell activation model] Ranked semi-relative sensitivity of the model state ($V(t)$) to parameters ($\mathbf{p}$) estimated from each patient with fractional-order latent cell activation model.

Patient	Estimated parameters				Relative ℓ_2 error
	T_0	T_0^*	V_0	L_0	
1	2.72E+03	1.66E-04	1.64E-01	1.68E-03	9.67E-02
2	6.37E+02	7.00E-03	1.82E+00	9.65E-03	1.27E-01
3	5.16E+02	3.76E-04	2.38E-01	1.56E-03	1.44E-01
4	1.84E+03	1.01E-01	1.10E+01	1.90E-04	1.24E-01
5	1.45E+03	1.14E-02	2.09E+00	2.14E-02	9.36E-02
7	1.54E+03	1.19E-03	1.21E+00	9.56E-02	1.17E-01
8	2.02E+03	9.16E-02	1.01E+01	5.48E+00	1.58E-01
10	1.82E+03	2.27E-03	3.93E-01	9.75E-07	2.04E-01
11	1.04E+03	7.48E-04	6.04E+00	1.18E-03	1.04E-01

Table 3.3: Estimated initial conditions for states and relative ℓ_2 error for each patient when $\alpha = 1.00$.

Patient	$\alpha = 1.00$	$0 < \alpha < 1$		
	$\int T(t)dt$	$\int T(t)dt$	α	$\tau^{1-\alpha}$
1	9.27E+05	9.08E+05	9.782E-01	1.009E+00
2	2.41E+05	2.38E+05	9.80E-01	1.009E+00
3	1.87E+05	1.87E+05	9.84E-01	1.011E+00
4	6.63E+05	6.28E+05	9.70E-01	9.919E-01
5	5.55E+05	5.33E+05	9.48E-01	1.020E+00
7	5.23E+05	4.94E+05	9.58E-01	1.004E+00
8	1.16E+06	7.99E+05	9.84E-01	1.087E+00
10	5.50E+05	5.49E+05	9.48E-01	1.103E+00
11	3.65E+05	3.64E+05	9.80E-01	1.009E+00

Table 3.4: A comparison on the total population number of target cells $CD4^+$ during observaton between the case o $\alpha = 1.00$ and $0 < \alpha < 1$

Patient	$\alpha = 1.00$	$0 < \alpha < 1$
1	1.71	1.69
2	1.67	1.83
3	1.59	1.62
4	1.70	1.64
5	1.31	1.42
7	1.27	1.28
8	3.00	2.24
10	1.40	1.30
11	1.55	1.79

Table 3.5: A comparison on reproductive number between the case of $\alpha = 1.00$ and $0 < \alpha < 1$

3.6 Conclusion

In this paper, we introduce a fractional derivative with order $(0 <\leq 1)$ into Latent reservoir model to embody essential features to cell rheological behavior in HIV infection of lymphocyte population. In Section 3.3, we derive our new model (3.12) and showed that it has non-negative, bounded solutions with locally asymptotically stable equilibrium points. We compare viral load measurements of HIV infected patients with the numerical solutions of nonlinear model of HIV of fractional order, obtained by using the Adams-type predictor-corrector methodimplemented in Section3.4. Employing the range of initial guess for parameters based on the reference values, we obtain the optimal fractional order better describe the data than the model of which order of derivative is restricted to integer. From the numerical results in Section3.5, we can confirm that CD4 cell counts described by fractional-order model($0 < \alpha < 1$) is lower than the one provided by the integer-order model($\alpha = 1$). This results correspond with the several clinical findings that there is an inverse correlation between CD4 T-lymphocyte counts and index of rigidity, and RBC deformability is decreased in HIV disease, in a degree mainly related to CD4 depletion, which is appeared in HIV-infected patients.

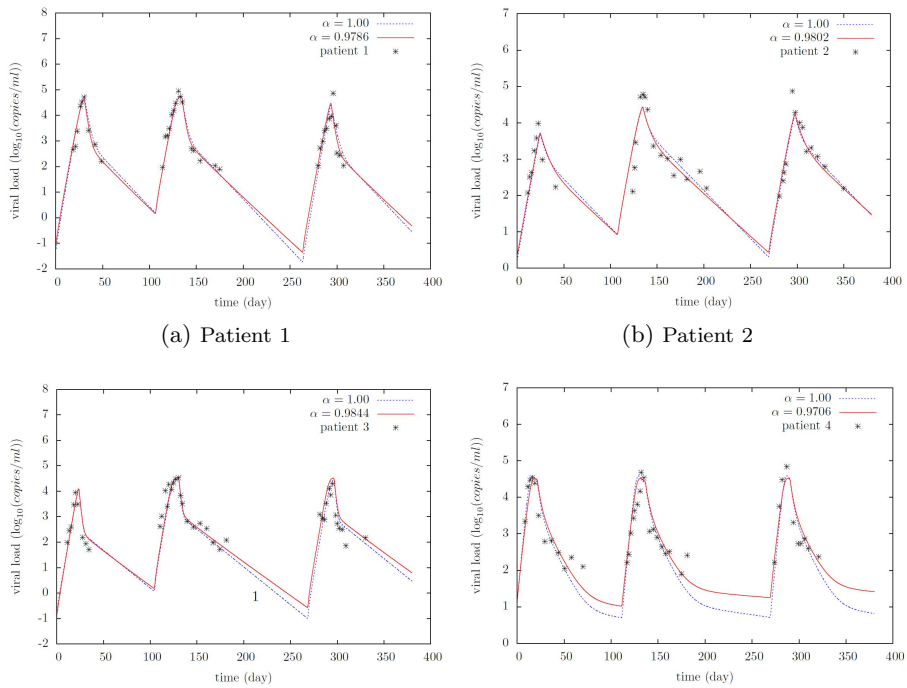

(a) Patient 1 (b) Patient 2

(c) Patient 3 (d) Patient 4

Figure 3.1: Plots with HIV-RNA measurement and estimated values(Latent reservoir model with $0 < \alpha < 1$) for patients.

In this thesis, we have tried to show how mathematical modeling has impacted our understanding of HIV pathogenesis. Before modeling was brought, AIDS was thought to be a slow disease in which treatment could be delayed until symptoms appeared, and patients were not monitored very aggressively. In conclusion, we note that our consideration in rheological property, which have been proven influential in HIV-infected patients, can provide more precise prediction for future infection and can give better design for ART in reducing the risk of AIDS overall.

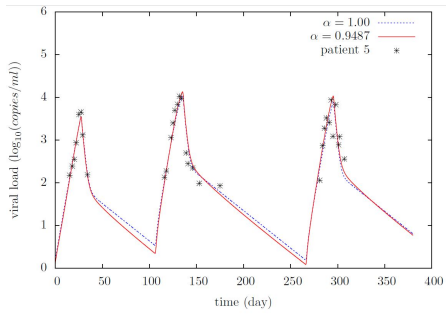

(a) Patient 5

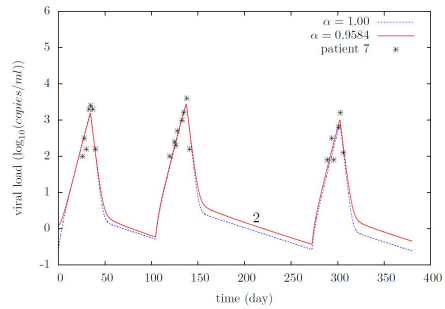

(b) Patient 7

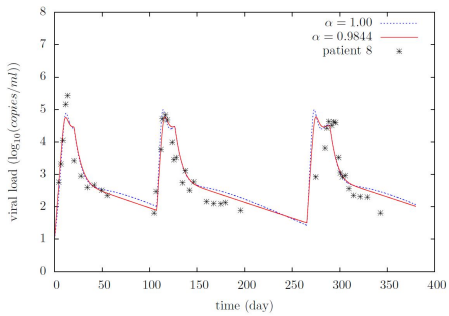

(c) Patient 8

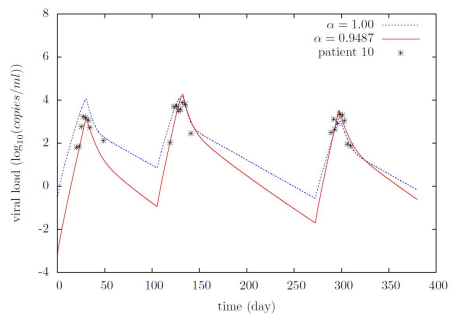

(d) Patient 10

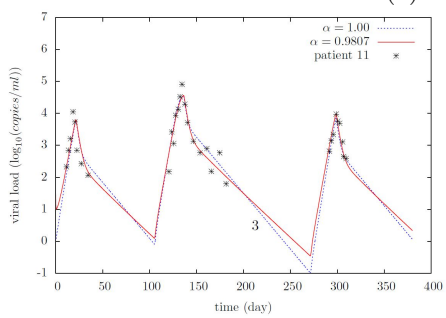

(e) Patient 11

Figure 3.2: Plots with HIV-RNA measurement and estimated values(Latent reservoir model with $0 < \alpha < 1$) for patients.

Bibliography

[1] F. Oberhettinger A. Erdelyi, W. Magnus and FG Tricomi. Higher transcendental functions, vols. i, ii, iii. mcgraw-hill, new york-toronto-london. 1955.

[2] BM Adams, HT Banks, M Davidian, and ES Rosenberg. Estimation and prediction with hiv-treatment interruption data. *Bulletin of mathematical biology*, 69(2):563–584, 2007.

[3] E Ahmed, AMA El-Sayed, and Hala AA El-Saka. Equilibrium points, stability and numerical solutions of fractional-order predator–prey and rabies models. *Journal of Mathematical Analysis and Applications*, 325(1):542–553, 2007.

[4] E Ahmed and AS Elgazzar. On fractional order differential equations model for nonlocal epidemics. *Physica A: Statistical Mechanics and its Applications*, 379(2):607–614, 2007.

[5] Htrotugu Akaike. Maximum likelihood identification of gaussian autoregressive moving average models. *Biometrika*, 60(2):255–265, 1973.

[6] Thomas J Anastasio. The fractional-order dynamics of brainstem vestibulo-oculomotor neurons. *Biological cybernetics*, 72(1):69–79, 1994.

[7] AAM Arafa, SZ Rida, and M Khalil. The effect of anti-viral drug treatment of human immunodeficiency virus type 1 (hiv-1) described by a fractional order model. *Applied Mathematical Modelling*, 37(4):2189–2196, 2013.

[8] Nancie M Archin, AL Liberty, Angela D Kashuba, Shailesh K Choudhary, JD Kuruc, AM Crooks, DC Parker, EM Anderson, MF Kearney, and MC Strain. Administration of vorinostat disrupts hiv-1 latency in patients on antiretroviral therapy. *Nature*, 487(7408):482–485, 2012.

[9] Larry Armijo. Minimization of functions having lipschitz continuous first partial derivatives. *Pacific Journal of mathematics*, 16(1):1–3, 1966.

[10] GA Athanassiou, AG Moutzouri, CA Gogos, and AT Skoutelis. Red blood cell deformability in patients with human immunodeficiency virus infection. *European journal of clinical microbiology & infectious diseases*, 29(7):845–849, 2010.

[11] F Bani-Sadr, P Palmer, C Scieux, and JM Molina. Ninety-six week efficacy of combination therapy with lamivudine and tenofovir in patients coinfected with hiv-1 and wild-type hepatitis b virus. *Clinical infectious diseases*, 39(7):1062–1064, 2004.

[12] HT Banks and DM Bortz. A parameter sensitivity methodology in the context of hiv delay equation models. *Journal of mathematical biology*, 50(6):607–625, 2005.

[13] Robert G Bartle and Donald R Sherbert. Introduction to real analysis, jon wiley and sons. *Inc., New York*, 2000.

[14] Yves Benhamou, Roland Tubiana, and Vincent Thibault. Tenofovir disoproxil fumarate in patients with hiv and lamivudine-resistant hepatitis b virus. *New England Journal of Medicine*, 348(2):177–178, 2003.

[15] Monsef Benkirane, Rene F Chun, Hua Xiao, Vasily V Ogryzko, Bruce H Howard, Yoshihiro Nakatani, and Kuan-Teh Jeang. Activation of integrated provirus requires histone acetyltransferase p300 and p/caf are coactivators for hiv-1 tat. *Journal of Biological Chemistry*, 273(38):24898–24905, 1998.

[16] David A Benson, Stephen W Wheatcraft, and Mark M Meerschaert. Application of a fractional advection-dispersion equation. *Water Resources Research*, 36(6):1403–1412, 2000.

[17] Sebastian Bonhoeffer, Michal Rembiszewski, Gabriel M Ortiz, and Douglas F Nixon. Risks and benefits of structured antiretroviral drug therapy interruptions in hiv-1 infection. *Aids*, 14(15):2313–2322, 2000.

[18] DM Bortz and PW Nelson. Model selection and mixed-effects modeling of hiv infection dynamics. *Bulletin of mathematical biology*, 68(8):2005–2025, 2006.

[19] Alberto Bosque, Marylinda Famiglietti, Andrew S Weyrich, Claudia Goulston, and Vicente Planelles. Homeostatic proliferation fails to efficiently reactivate hiv-1 latently infected central memory cd4+ t cells. *PLoS Pathog*, 7(10):e1002288, 2011.

[20] Yvonne J Bryson, Shen Pang, Lian S Wei, Ruth Dickover, Amadou Diagne, and Irvin SY Chen. Clearance of hiv infection in a perinatally infected infant. *New England Journal of Medicine*, 332(13):833–838, 1995.

[21] Valerie Calenda and Jean-Claude Chermann. The effects of hiv on hematopoiesis. *European journal of haematology*, 48(4):181–186, 1992.

[22] Duncan S Callaway and Alan S Perelson. Hiv-1 infection and low steady state viral loads. *Bulletin of mathematical biology*, 64(1):29–64, 2002.

[23] Andrew Carr, Katherine Samaras, Samantha Burton, Matthew Law, Judith Freund, Donald J Chisholm, and David A Cooper. A syndrome of peripheral lipodystrophy, hyperlipidaemia and insulin resistance in patients receiving hiv protease inhibitors. *Aids*, 12(7):F51–F58, 1998.

[24] Tae-Wook Chun, Lucy Carruth, Diana Finzi, Xuefei Shen, Joseph A DiGiuseppe, Harry Taylor, Monika Hermankova, Karen Chadwick, Joseph Margolick, and Thomas C Quinn. Quantification of latent tissue reservoirs and total body viral load in hiv-1 infection. *Nature*, 387(6629):183–188, 1997.

[25] Tae-Wook Chun, Diana Finzi, Joseph Margolick, Karen Chadwick, David Schwartz, and Robert F Siliciano. In vivo fate of hiv-1-infected t cells: quantitative analysis of the transition to stable latency. *Nature medicine*, 1(12):1284–1290, 1995.

[26] Tae-Wook Chun, J Shawn Justement, Richard A Lempicki, Jun Yang, Glynn Dennis, Claire W Hallahan, Christina Sanford, Punita Pandya, Shuying Liu, and Mary McLaughlin. Gene expression and viral prodution in latently infected, resting cd4+ t cells in viremic versus aviremic hiv-infected individuals. *Proceedings of the National Academy of Sciences*, 100(4):1908–1913, 2003.

[27] Tae-Wook Chun, Lieven Stuyver, Stephanie B Mizell, Linda A Ehler, Jo Ann M Mican, Michael Baseler, Alun L Lloyd, Martin A Nowak,

and Anthony S Fauci. Presence of an inducible hiv-1 latent reservoir during highly active antiretroviral therapy. *Proceedings of the National Academy of Sciences*, 94(24):13193–13197, 1997.

[28] Kenneth S Cole. Electric conductance of biological systems. In *Cold Spring Harbor symposia on quantitative biology*, volume 1, pages 107–116. Cold Spring Harbor Laboratory Press, 1933.

[29] Jason J Coull, Guocheng He, Christian Melander, Victor C Rucker, Peter B Dervan, and David M Margolis. Targeted derepression of the human immunodeficiency virus type 1 long terminal repeat by pyrrole-imidazole polyamides. *Journal of virology*, 76(23):12349–12354, 2002.

[30] Jason J Coull, Fabio Romerio, Jian-Min Sun, Janet L Volker, Katherine M Galvin, James R Davie, Yang Shi, Ulla Hansen, and David M Margolis. The human factors yy1 and lsf repress the human immunodeficiency virus type 1 long terminal repeat via recruitment of histone deacetylase 1. *Journal of virology*, 74(15):6790–6799, 2000.

[31] Rebecca V Culshaw and Shigui Ruan. A delay-differential equation model of hiv infection of cd4+ t-cells. *Mathematical biosciences*, 165(1):27–39, 2000.

[32] Rob J De Boer and Alan S Perelson. Target cell limited and immune control models of hiv infection: a comparison. *Journal of theoretical Biology*, 190(3):201–214, 1998.

[33] Héloïse M Delagrèverie, Constance Delaugerre, Sharon R Lewin, Steven G Deeks, and Jonathan Z Li. Ongoing clinical trials of human immunodeficiency virus latency-reversing and immunomodulatory agents.

In *Open Forum Infectious Diseases*, volume 3, page ofw189. Oxford University Press, 2016.

[34] Kai Diethelm, Neville J Ford, and Alan D Freed. A predictor-corrector approach for the numerical solution of fractional differential equations. *Nonlinear Dynamics*, 29(1):3–22, 2002.

[35] Kai Diethelm, Neville J Ford, and Alan D Freed. Detailed error analysis for a fractional adams method. *Numerical algorithms*, 36(1):31–52, 2004.

[36] Yongsheng Ding, Zidong Wang, and Haiping Ye. Optimal control of a fractional-order hiv-immune system with memory. *IEEE Transactions on Control Systems Technology*, 20(3):763–769, 2012.

[37] Yongsheng Ding and Haiping Ye. A fractional-order differential equation model of hiv infection of cd4+ t-cells. *Mathematical and Computer Modelling*, 50(3):386–392, 2009.

[38] Vladan D Djordjević, Jovo Jarić, Ben Fabry, Jeffrey J Fredberg, and Dimitrije Stamenović. Fractional derivatives embody essential features of cell rheological behavior. *Annals of biomedical engineering*, 31(6):692–699, 2003.

[39] Jaão Caramalho Domingues. Sf lacroix, traité du calcul différentiel et du calcul intégral, (1797–1800)-chapter 20.

[40] Gregory J Dore, David A Cooper, Anton L Pozniak, Edwin DeJesus, Lijie Zhong, Michael D Miller, Biao Lu, and Andrew K Cheng. Efficacy of tenofovir disoproxil fumarate in antiretroviral therapy-naive and-experienced patients coinfected with hiv-1 and hepatitis b virus. *Journal of Infectious Diseases*, 189(7):1185–1192, 2004.

[41] Geethanjali Dornadula, Hui Zhang, Bonnie VanUitert, John Stern, Lawrence Livornese Jr, Mark J Ingerman, James Witek, Richard J Kedanis, Jaan Natkin, and Joseph DeSimone. Residual hiv-1 rna in blood plasma of patients taking suppressive highly active antiretroviral therapy. *Jama*, 282(17):1627–1632, 1999.

[42] M Egerstedt, Y Wardi, and F Delmotte. Optimal control of switching times in switched dynamical systems. In *Decision and Control, 2003. Proceedings. 42nd IEEE Conference on*, volume 3, pages 2138–2143. IEEE, 2003.

[43] AMA El-Sayed, AEM El-Mesiry, and HAA El-Saka. Numerical solution for multi-term fractional (arbitrary) orders differential equations. *Computational & Applied Mathematics*, 23(1):33–54, 2004.

[44] AMA El-Sayed, AEM El-Mesiry, and HAA El-Saka. On the fractional-order logistic equation. *Applied Mathematics Letters*, 20(7):817–823, 2007.

[45] AMA El-Sayed, SZ Rida, and AAM Arafa. On the solutions of time-fractional bacterial chemotaxis in a diffusion gradient chamber. *International Journal of Nonlinear Science*, 7(4):485–492, 2009.

[46] Robert E Engstrom, Gary N Holland, Hardy David, and Herbert J Meiselman. Hemorheologic abnormalities in patients with human immunodeficiency virus infection and ophthalmic microvasculopathy. *American journal of ophthalmology*, 109(2):153–161, 1990.

[47] Neil M Ferguson, Azra C Ghani, Christophe Fraser, Christl A Donnelly, Peter Reiss, Joep MA Lange, Sven A Danner, Geoff P Garnett, Jaap

Goudsmit, and Roy M Anderson. Antigen-driven cd4+ t cell and hiv-1 dynamics: residual viral replication under highly active antiretroviral therapy. *Proceedings of the National Academy of Sciences*, 96(26):15167–15172, 1999.

[48] Diana Finzi, Joel Blankson, Janet D Siliciano, Joseph B Margolick, Karen Chadwick, Theodore Pierson, Kendall Smith, Julianna Lisziewicz, Franco Lori, and Charles Flexner. Latent infection of cd4+ t cells provides a mechanism for lifelong persistence of hiv-1, even in patients on effective combination therapy. *Nature medicine*, 5(5):512–517, 1999.

[49] Diana Finzi, Monika Hermankova, Theodore Pierson, Lucy M Carruth, Christopher Buck, Richard E Chaisson, Thomas C Quinn, Karen Chadwick, Joseph Margolick, and Ronald Brookmeyer. Identification of a reservoir for hiv-1 in patients on highly active antiretroviral therapy. *Science*, 278(5341):1295–1300, 1997.

[50] Wendell H Fleming and Raymond W Rishel. *Deterministic and stochastic optimal control*, volume 1. Springer Science & Business Media, 2012.

[51] Roger Fletcher. A modified marquardt subroutine for non-linear least squares. 1971.

[52] Joseph Fourier. *Theorie analytique de la chaleur, par M. Fourier*. Chez Firmin Didot, père et fils, 1822.

[53] Paul M Frank. *Introduction to system sensitivity theory*, volume 1. Academic press New York, 1978.

[54] Manohar R Furtado, Duncan S Callaway, John P Phair, Kevin J Kunstman, Jennifer L Stanton, Catherine A Macken, Alan S Perelson, and

Steven M Wolinsky. Persistence of hiv-1 transcription in peripheral-blood mononuclear cells in patients receiving potent antiretroviral therapy. *New England Journal of Medicine*, 340(21):1614–1622, 1999.

[55] C. Gallegos. *Rheology - Volume II:*. 2010.

[56] Ahmet Gökdoğan, Ahmet Yildirim, and Mehmet Merdan. Solving a fractional order model of hiv infection of cd4+ t cells. *Mathematical and Computer Modelling*, 54(9):2132–2138, 2011.

[57] Rudolf Gorenflo and Francesco Mainardi. Fractional calculus. In *Fractals and fractional calculus in continuum mechanics*, pages 223–276. Springer, 1997.

[58] Huldrych F Günthard, Judith A Aberg, Joseph J Eron, Jennifer F Hoy, Amalio Telenti, Constance A Benson, David M Burger, Pedro Cahn, Joel E Gallant, and Marshall J Glesby. Antiretroviral treatment of adult hiv infection: 2014 recommendations of the international antiviral society–usa panel. *Jama*, 312(4):410–425, 2014.

[59] Monika Hermankova, Janet D Siliciano, Yan Zhou, Daphne Monie, Karen Chadwick, Joseph B Margolick, Thomas C Quinn, and Robert F Siliciano. Analysis of human immunodeficiency virus type 1 gene expression in latently infected resting cd4+ t lymphocytes in vivo. *Journal of virology*, 77(13):7383–7392, 2003.

[60] Rudolf Hilfer. *Applications of fractional calculus in physics*. World Scientific, 2000.

[61] David D Ho, Avidan U Neumann, Alan S Perelson, Wen Chen, John M Leonard, and Martin Markowitz. Rapid turnover of plasma virions and cd4 lymphocytes in hiv-1 infection. *Nature*, 373(6510):123–126, 1995.

[62] Richard D Hockett, J Michael Kilby, Cynthia A Derdeyn, Michael S Saag, Michael Sillers, Kathleen Squires, Scott Chiz, Martin A Nowak, George M Shaw, and R Pat Bucy. Constant mean viral copy number per infected cell in tissues regardless of high, low, or undetectable plasma hiv rna. *Journal of Experimental Medicine*, 189(10):1545–1554, 1999.

[63] Robert S Hogg, Benita Yip, Keith J Chan, Evan Wood, Kevin JP Craib, Michael V O'Shaughnessy, and Julio SG Montaner. Rates of disease progression by baseline cd4 cell count and viral load after initiating triple-drug therapy. *Jama*, 286(20):2568–2577, 2001.

[64] Adolf Hurwitz. Ueber die bedingungen, unter welchen eine gleichung nur wurzeln mit negativen reellen theilen besitzt. *Mathematische Annalen*, 46(2):273–284, 1895.

[65] Shingo Iwami, Tomoyuki Miura, Shinji Nakaoka, and Yasuhiro Takeuchi. Immune impairment in hiv infection: Existence of risky and immunodeficiency thresholds. *Journal of theoretical biology*, 260(4):490–501, 2009.

[66] Isabel S Jesus, JA Machado, J Boaventura Cunha, and Manuel F Silva. Fractional order electrical impedance of fruits and vegetables. In *Proceedings of the 25th IASTED international conference on Modeling, indentification, and control*, pages 489–494. ACTA Press, 2006.

[67] Isabel S Jesus, JA Tenreiro Machado, and J Boaventure Cunha. Fractional electrical impedances in botanical elements. *Journal of Vibration and Control*, 14(9-10):1389–1402, 2008.

[68] Eric Jones, Peter Roemer, Mrinal Raghupathi, and Stephen Pankavich. Analysis and simulation of the three-component model of hiv dynamics. *arXiv preprint arXiv:1312.3671*, 2013.

[69] G Stephen Jones. Fundamental inequalities for discrete and discontinuous functional equations. *Journal of the Society for Industrial and Applied Mathematics*, 12(1):43–57, 1964.

[70] Richard Brad Jones, Rachel O'Connor, Stefanie Mueller, Maria Foley, Gregory L Szeto, Dan Karel, Mathias Lichterfeld, Colin Kovacs, Mario A Ostrowski, and Alicja Trocha. Histone deacetylase inhibitors impair the elimination of hiv-infected cells by cytotoxic t-lymphocytes. *PLoS Pathog*, 10(8):e1004287, 2014.

[71] Beda Joos, Marek Fischer, Herbert Kuster, Satish K Pillai, Joseph K Wong, Jürg Böni, Bernard Hirschel, Rainer Weber, Alexandra Trkola, and Huldrych F Günthard. Hiv rebounds from latently infected cells, rather than from continuing low-level replication. *Proceedings of the National Academy of Sciences*, 105(43):16725–16730, 2008.

[72] Guy Jumarie. New stochastic fractional models for malthusian growth, the poissonian birth process and optimal management of populations. *Mathematical and Computer Modelling*, 44(3):231–254, 2006.

[73] Jonathan E Kaplan, Debra L Hanson, David L Cohn, John Karon, Susan Buskin, Melanie Thompson, Patricia Fleming, and Mark S Dworkin. When to begin highly active antiretroviral therapy evidence supporting initiation of therapy at cd4+ lymphocyte counts¡ 350 cells/μl. *Clinical infectious diseases*, 37(7):951–958, 2003.

[74] Hassan K Khalil. Noninear systems. *Prentice-Hall, New Jersey*, 2(5):5–1, 1996.

[75] Alisa Kim, Hajir Dadgostar, Gary N Holland, Rosalinda Wenby, Fei Yu, Brian G Terry, and Herbert J Meiselman. Hemorheologic abnormali-

ties associated with hiv infection: altered erythrocyte aggregation and deformability. *Investigative ophthalmology & visual science*, 47(9):3927–3932, 2006.

[76] Denise Kirschner. Using mathematics to understand hiv immune dynamics. *AMS notices*, 43(2), 1996.

[77] Denise Kirschner, Suzanne Lenhart, and Steve Serbin. Optimal control of the chemotherapy of hiv. *Journal of mathematical biology*, 35(7):775–792, 1997.

[78] Denise Kirschner and Glenn F Webb. A model for treatment strategy in the chemotherapy of aids. *Bulletin of mathematical biology*, 58(2):367–390, 1996.

[79] RA Koup, Jeffrey T Safrit, Yunzhen Cao, Charla A Andrews, Gavin McLeod, William Borkowsky, Charles Farthing, and David D Ho. Temporal association of cellular immune responses with the initial control of viremia in primary human immunodeficiency virus type 1 syndrome. *Journal of virology*, 68(7):4650–4655, 1994.

[80] Hee-Dae Kwon. Optimal treatment strategies derived from a hiv model with drug-resistant mutants. *Applied Mathematics and Computation*, 188(2):1193–1204, 2007.

[81] Karine Lacombe, Joël Gozlan, Pierre-Yves Boelle, Lawrence Serfaty, Fabien Zoulim, Alain-Jacques Valleron, and Pierre-Marie Girard. Long-term hepatitis b virus dynamics in hiv–hepatitis b virus-co-infected patients treated with tenofovir disoproxil fumarate. *Aids*, 19(9):907–915, 2005.

[82] LS Lasdon, SK Mitter, and AD Waren. The conjugate gradient method for optimal control problems. *Automatic Control, IEEE Transactions on*, 12(2):132–138, 1967.

[83] Mihailo P Lazarević. Finite time stability analysis of pd α fractional control of robotic time-delay systems. *Mechanics Research Communications*, 33(2):269–279, 2006.

[84] Yan Li, YangQuan Chen, and Igor Podlubny. Mittag–leffler stability of fractional order nonlinear dynamic systems. *Automatica*, 45(8):1965–1969, 2009.

[85] Wei Lin. Global existence theory and chaos control of fractional differential equations. *Journal of Mathematical Analysis and Applications*, 332(1):709–726, 2007.

[86] Julianna Lisziewicz, Eric Rosenberg, Judy Lieberman, Heiko Jessen, Lucia Lopalco, Robert Siliciano, Bruce Walker, and Franco Lori. Control of hiv despite the discontinuation of antiretroviral therapy. *New England Journal of Medicine*, 340(21):1683–1683, 1999.

[87] Chongyang Liu and Zhaohua Gong. Optimal control of switched autonomous systems. In *Optimal Control of Switched Systems Arising in Fermentation Processes*, pages 77–87. Springer, 2014.

[88] Stephen Locarnini, Angelos Hatzakis, Jenny Heathcote, Emmet B Keeffe, T Jake Liang, David Mutimer, Jean-Michel Pawlotsky, and Fabien Zoulim. Management of antiviral resistance in patients with chronic hepatitis b. *Antiviral therapy*, 9(5):679–693, 2004.

[89] Sophie Low-Beer, Benita Yip, Michael V O'Shaughnessy, Robert S Hogg, and Julio SG Montaner. Adherence to triple therapy and viral load

response. *JAIDS Journal of Acquired Immune Deficiency Syndromes*, 23(4):360–361, 2000.

[90] D.L. Lukes. *Differential Equations: Classical to Controlled*. Mathematics in science and engineering. Academic Press, 1982.

[91] Rutao Luo, Michael J Piovoso, Javier Martinez-Picado, and Ryan Zurakowski. Hiv model parameter estimates from interruption trial data including drug efficacy and reservoir dynamics. *PLoS One*, 7(7):e40198, 2012.

[92] Katherine Luzuriaga, Hulin Wu, Margaret McManus, Paula Britto, William Borkowsky, Sandra Burchett, Betsy Smith, Lynne Mofenson, and John L Sullivan. Dynamics of human immunodeficiency virus type 1 replication in vertically infected infants. *Journal of virology*, 73(1):362–367, 1999.

[93] Richard L Magin. *Fractional calculus in bioengineering*. Begell House Redding, 2006.

[94] Francesco Mainardi. *Fractional calculus and waves in linear viscoelasticity: an introduction to mathematical models*. World Scientific, 2010.

[95] Denis Matignon. Stability results for fractional differential equations with applications to control processing. In *Computational engineering in systems applications*, volume 2, pages 963–968. IMACS, IEEE-SMC Lille, France, 1996.

[96] HJ Meiselman, B Neu, MW Rampling, and OK Baskurt. Rbc aggregation: laboratory data and models. 2007.

[97] Ann J Melvin, Allen G Rodrigo, Kathleen M Mohan, Paul A Lewis, Laura Manns-Arcuino, Robert W Coombs, James I Mullins, and Lisa M Frenkel. Hiv-1 dynamics in children. *JAIDS Journal of Acquired Immune Deficiency Syndromes*, 20(5):468–473, 1999.

[98] Ralf Metzler. Generalized chapman-kolmogorov equation: A unifying approach to the description of anomalous transport in external fields. *Physical Review E*, 62(5):6233, 2000.

[99] Hongyu Miao, Carrie Dykes, Lisa M Demeter, and Hulin Wu. Differential equation modeling of hiv viral fitness experiments: model identification, model selection, and multimodel inference. *Biometrics*, 65(1):292–300, 2009.

[100] Kenneth S Miller and Bertram Ross. An introduction to the fractional calculus and fractional differential equations. 1993.

[101] Veronica Miller. Structured treatment interruptions in antiretroviral management of hiv-1. *Current opinion in infectious diseases*, 14(1):29–37, 2001.

[102] John E Mittler, Martin Markowitz, David D Ho, and Alan S Perelson. Improved estimates for h1v-1 clearance rate and intracellular delay. *Aids*, 13(11):1415, 1999.

[103] John E Mittler, Bernhard Sulzer, Avidan U Neumann, and Alan S Perelson. Influence of delayed viral production on viral dynamics in hiv-1 infected patients. *Mathematical biosciences*, 152(2):143–163, 1998.

[104] Christiane Moog, Gaelle Kuntz-Simon, Catherine Caussin-Schwemling, and Georges Obert. Sodium valproate, an anticonvulsant drug, stimu-

lates human immunodeficiency virus type 1 replication independently of glutathione levels. *Journal of general virology*, 77(9):1993–1999, 1996.

[105] Ven Natarajan, Marjorie Bosche, Julia A Metcalf, Douglas J Ward, H Clifford Lane, and Joseph A Kovacs. Hiv-1 replication in patients with undetectable plasma virus receiving haart. *The Lancet*, 353(9147):119–120, 1999.

[106] George W Nelson and Alan S Perelson. Modeling defective interfering virus therapy for aids: conditions for div survival. *Mathematical biosciences*, 125(2):127–153, 1995.

[107] Patrick W Nelson and Alan S Perelson. Mathematical analysis of delay differential equation models of hiv-1 infection. *Mathematical biosciences*, 179(1):73–94, 2002.

[108] Daan W Notermans, Jaap Goudsmit, Sven A Danner, Frank De Wolf, Alan S Perelson, and John Mittler. Rate of hiv-1 decline following antiretroviral therapy is related to viral load at baseline and drug regimen. *Aids*, 12(12):1483–1490, 1998.

[109] Martin A Nowak and Charles RM Bangham. Population dynamics of immune responses to persistent viruses. *Science*, 272(5258):74, 1996.

[110] Martin A Nowak, Sebastian Bonhoeffer, George M Shaw, and Robert M May. Anti-viral drug treatment: dynamics of resistance in free virus and infected cell populations. *Journal of theoretical biology*, 184(2):203–217, 1997.

[111] Zaid M Odibat and Nabil T Shawagfeh. Generalized taylor's formula. *Applied Mathematics and Computation*, 186(1):286–293, 2007.

[112] Alan S Perelson, Paulina Essunger, Yunzhen Cao, Mika Vesanen, Arlene Hurley, Kalle Saksela, Martin Markowitz, and David D Ho. Decay characteristics of hiv-1-infected compartments during combination therapy. 1997.

[113] Alan S Perelson, Denise E Kirschner, and Rob De Boer. Dynamics of hiv infection of cd4+ t cells. *Mathematical biosciences*, 114(1):81–125, 1993.

[114] Alan S Perelson, Denise E Kirschner, and Rob De Boer. Dynamics of hiv infection of cd4+ t cells. *Mathematical biosciences*, 114(1):81–125, 1993.

[115] Alan S Perelson and Patrick W Nelson. Mathematical analysis of hiv-1 dynamics in vivo. *SIAM review*, 41(1):3–44, 1999.

[116] Alan S Perelson, Avidan U Neumann, Martin Markowitz, Johm M Leonard, and David D Ho. Hiv-1 dynamics in vivo: virion clearance rate, infected cell life-span, and viral generation time. *Science*, 271(5255):1582, 1996.

[117] Ljubomir M Petrovic, Dragan T Spasic, and Teodor M Atanackovic. On a mathematical model of a human root dentin. *Dental Materials*, 21(2):125–128, 2005.

[118] Christopher J Phiel, Fang Zhang, Eric Y Huang, Matthew G Guenther, Mitchell A Lazar, and Peter S Klein. Histone deacetylase is a direct target of valproic acid, a potent anticonvulsant, mood stabilizer, and teratogen. *Journal of Biological Chemistry*, 276(39):36734–36741, 2001.

[119] Andrew N Phillips. Reduction of hiv concentration during acute infection: independence from a specific immune response. *Science*, 271(5248):497, 1996.

[120] Benedetto Piccoli. Necessary conditions for hybrid optimization. In *Decision and Control, 1999. Proceedings of the 38th IEEE Conference on*, volume 1, pages 410–415. IEEE, 1999.

[121] Theodore Pierson, Justin McArthur, and Robert F Siliciano. Reservoirs for hiv-1: mechanisms for viral persistence in the presence of antiviral immune responses and antiretroviral therapy. *Annual review of immunology*, 18(1):665–708, 2000.

[122] Stephen C Piscitelli and Keith D Gallicano. Interactions among drugs for hiv and opportunistic infections. *New England Journal of Medicine*, 344(13):984–996, 2001.

[123] Igor Podlubny. *Fractional differential equations: an introduction to fractional derivatives, fractional differential equations, to methods of their solution and some of their applications*, volume 198. Academic press, 1998.

[124] Lev Semenovich Pontryagin. *Mathematical theory of optimal processes*. CRC Press, 1987.

[125] Deliang Qian, Changpin Li, Ravi P Agarwal, and Patricia JY Wong. Stability analysis of fractional differential system with riemann–liouville derivative. *Mathematical and Computer Modelling*, 52(5):862–874, 2010.

[126] Vincent Quivy, Emmanuelle Adam, Yves Collette, Dominique Demonte, Alain Chariot, Caroline Vanhulle, Ben Berkhout, Rémy Castellano, Yvan

De Launoit, and Arsène Burny. Synergistic activation of human immunodeficiency virus type 1 promoter activity by nf-κb and inhibitors of deacetylases: potential perspectives for the development of therapeutic strategies. *Journal of virology*, 76(21):11091–11103, 2002.

[127] MW Rampling, HJ Meiselman, B Neu, and OK Baskurt. Influence of cell-specific factors on red blood cell aggregation. *Biorheology*, 41(2):91–112, 2004.

[128] Ramratnam. The decay of the latent reservoir of replication-competent hiv-1 is inversely correlated with the extent of residual viral replication during prolonged anti-retroviral therapy. *Nature medicine*, 6(1):82–85, 2000.

[129] Bharat Ramratnam, Sebastian Bonhoeffer, James Binley, Arlene Hurley, Linqi Zhang, John E Mittler, Martin Markowitz, John P Moore, Alan S Perelson, and David D Ho. Rapid production and clearance of hiv-1 and hepatitis c virus assessed by large volume plasma apheresis. *The Lancet*, 354(9192):1782–1785, 1999.

[130] Ruy M Ribeiro, Narendra M Dixit, and Alan S Perelson. Modelling the in vivo growth rate of hiv: implications for vaccination. *Studies in Multidisciplinarity*, 3:231–246, 2005.

[131] Ruy M Ribeiro, Li Qin, Leslie L Chavez, Dongfeng Li, Steven G Self, and Alan S Perelson. Estimation of the initial viral growth rate and basic reproductive number during acute hiv-1 infection. *Journal of virology*, 84(12):6096–6102, 2010.

[132] SZ Rida, HM El-Sherbiny, and AAM Arafa. On the solution of the fractional nonlinear schrödinger equation. *Physics Letters A*, 372(5):553–558, 2008.

[133] P Riedinger, FR Kratz, C Iung, and C Zanne. Linear quadratic optimization for hybrid systems. In *IEEE Conference on Decision and Control*, volume 3, pages 3059–3064. IEEE; 1998, 1999.

[134] Libin Rong and Alan S Perelson. Asymmetric division of activated latently infected cells may explain the decay kinetics of the hiv-1 latent reservoir and intermittent viral blips. *Mathematical biosciences*, 217(1):77–87, 2009.

[135] Libin Rong and Alan S Perelson. Modeling hiv persistence, the latent reservoir, and viral blips. *Journal of theoretical biology*, 260(2):308–331, 2009.

[136] Libin Rong and Alan S Perelson. Modeling latently infected cell activation: viral and latent reservoir persistence, and viral blips in hiv-infected patients on potent therapy. *PLoS Comput Biol*, 5(10):e1000533, 2009.

[137] Eric S Rosenberg, Marcus Altfeld, Samuel H Poon, Mary N Phillips, Barbara M Wilkes, Robert L Eldridge, Gregory K Robbins, TD Richard, Philip JR Goulder, and Bruce D Walker. Immune control of hiv-1 after early treatment of acute infection. *Nature*, 407(6803):523–526, 2000.

[138] Edward John Routh. Stability of a dynamical system with two independent motions. *Proceedings of the London Mathematical Society*, 1(1):97–99, 1873.

[139] Lidia Ruiz, Guislaine Carcelain, Javier Martínez-Picado, Simon Frost, Silvia Marfil, Roger Paredes, Joan Romeu, Esther Ferrer, Kristina

Morales-Lopetegi, and Brigitte Autran. Hiv dynamics and t-cell immunity after three structured treatment interruptions in chronic hiv-1 infection. *Aids*, 15(9):F19–F27, 2001.

[140] M Shahid Shaikh and Peter E Caines. On the optimal control of hybrid systems: Optimization of trajectories, switching times, and location schedules. In *Hybrid systems: Computation and control*, pages 466–481. Springer, 2003.

[141] Liang Shan, Kai Deng, Neeta S Shroff, Christine M Durand, S Alireza Rabi, Hung-Chih Yang, Hao Zhang, Joseph B Margolick, Joel N Blankson, and Robert F Siliciano. Stimulation of hiv-1-specific cytolytic t lymphocytes facilitates elimination of latent viral reservoir after virus reactivation. *Immunity*, 36(3):491–501, 2012.

[142] Mark E Sharkey, Ian Teo, Thomas Greenough, Natalia Sharova, Katherine Luzuriaga, John L Sullivan, R Pat Bucy, Leondios G Kostrikis, Ashley Haase, and Claire Veryard. Persistence of episomal hiv-1 infection intermediates in patients on highly active anti-retroviral therapy. *Nature medicine*, 6(1):76–81, 2000.

[143] Philip L Sheridan, Timothy P Mayall, Eric Verdin, and Katherine A Jones. Histone acetyltransferases regulate hiv-1 enhancer activity in vitro. *Genes & development*, 11(24):3327–3340, 1997.

[144] Siliciano. Long-term follow-up studies confirm the stability of the latent reservoir for hiv-1 in resting cd4+ t cells. *Nature medicine*, 9.6:727–728, 2003.

[145] Janet D Siliciano, Joleen Kajdas, Diana Finzi, Thomas C Quinn, Karen Chadwick, Joseph B Margolick, Colin Kovacs, Stephen J Gange, and

Robert F Siliciano. Long-term follow-up studies confirm the stability of the latent reservoir for hiv-1 in resting cd4+ t cells. *Nature medicine*, 9(6):727–728, 2003.

[146] Janet M Siliciano and Robert F Siliciano. The remarkable stability of the latent reservoir for hiv-1 in resting memory cd4+ t cells. *Journal of Infectious Diseases*, page jiv219, 2015.

[147] Robert F Siliciano and Warner C Greene. Hiv latency. *Cold Spring Harbor perspectives in medicine*, 1(1):a007096, 2011.

[148] Eric D Smith, Ferenc Szidarovszky, William J Karnavas, and ATerry Bahill. Sensitivity analysis, a powerful system validation technique. *Open Cybernetics & Systemics Journal*, 2:39–56, 2008.

[149] Max A Stafford, Lawrence Corey, Yunzhen Cao, Eric S Daar, David D Ho, and Alan S Perelson. Modeling plasma virus concentration during primary hiv infection. *Journal of theoretical biology*, 203(3):285–301, 2000.

[150] Timothy R Sterling, Richard E Chaisson, Jeanne Keruly, and Richard D Moore. Improved outcomes with earlier initiation of highly active antiretroviral therapy among human immunodeficiency virus–infected patients who achieve durable virologic suppression: longer follow-up of an observational cohort study. *Journal of Infectious Diseases*, 188(11):1659–1665, 2003.

[151] Matthew C Strain, Susan J Little, Eric S Daar, Diane V Havlir, Huldrych F Günthard, Ruby Y Lam, Otto A Daly, Juin Nguyen, Caroline C Ignacio, and Celsa A Spina. Effect of treatment, during primary

infection, on establishment and clearance of cellular reservoirs of hiv-1. *Journal of Infectious Diseases*, 191(9):1410–1418, 2005.

[152] MC Strain, HF Günthard, DV Havlir, CC Ignacio, DM Smith, AJ Leigh-Brown, TR Macaranas, RY Lam, OA Daly, and M Fischer. Heterogeneous clearance rates of long-lived lymphocytes infected with hiv: intrinsic stability predicts lifelong persistence. *Proceedings of the National Academy of Sciences*, 100(8):4819–4824, 2003.

[153] N Sugimoto. Propagation of nonlinear acoustic waves in a tunnel with an array of helmholtz resonators. *Journal of Fluid Mechanics*, 244:55–78, 1992.

[154] Hector J Sussmann. A maximum principle for hybrid optimal control problems. In *Decision and Control, 1999. Proceedings of the 38th IEEE Conference on*, volume 1, pages 425–430. IEEE, 1999.

[155] Xiping Wei, Sajal K Ghosh, Maria E Taylor, Victoria A Johnson, Emilio A Emini, Paul Deutsch, Jeffrey D Lifson, Sebastian Bonhoeffer, Martin A Nowak, and Beatrice H Hahn. Viral dynamics in human immunodeficiency virus type 1 infection. *Nature*, 373(6510):117–122, 1995.

[156] Lawrence M Wein, Rebecca M D'Amato, and Alan S Perelson. Mathematical analysis of antiretroviral therapy aimed at hiv-1 eradication or maintenance of low viral loads. *Journal of theoretical biology*, 192(1):81–98, 1998.

[157] Xiang-Jun Wen, Zheng-Mao Wu, and Jun-Guo Lu. Stability analysis of a class of nonlinear fractional-order systems. *IEEE Transactions on circuits and systems II: Express Briefs*, 55(11):1178–1182, 2008.

[158] Fiona Wightman, Paula Ellenberg, Melissa Churchill, and Sharon R Lewin. Hdac inhibitors in hiv. *Immunology and cell biology*, 90(1):47–54, 2012.

[159] Myriam Witvrouw, JEAN-CLAUDE SCHMIT, BARBARA VAN REMOORTEL, Dirk Daelemans, JOSÉ A ESTÉ, A-M Vandamme, Jan Desmyter, and Erik De Clercq. Cell type-dependent effect of sodium valproate on human immunodeficiency virus type 1 replication in vitro. *AIDS research and human retroviruses*, 13(2):187–192, 1997.

[160] Philip Wolfe. Convergence conditions for ascent methods. *SIAM review*, 11(2):226–235, 1969.

[161] Philip Wolfe. Convergence conditions for ascent methods. ii: Some corrections. *SIAM review*, 13(2):185–188, 1971.

[162] Joseph K Wong, Marjan Hezareh, Huldrych F Günthard, Diane V Havlir, Caroline C Ignacio, Celsa A Spina, and Douglas D Richman. Recovery of replication-competent hiv despite prolonged suppression of plasma viremia. *Science*, 278(5341):1291–1295, 1997.

[163] Hulin Wu, Daniel R Kuritzkes, Daniel R McClernon, Harold Kessler, Elizabeth Connick, Alan Landay, Greg Spear, Margo Heath-Chiozzi, Franck Rousseau, and Lawrence Fox. Characterization of viral dynamics in human immunodeficiency virus type 1-infected patients treated with combination antiretroviral therapy: relationships to host factors, cellular restoration, and virologic end points. *The Journal of infectious diseases*, 179(4):799–807, 1999.

[164] Xuping Xu and Panos J Antsaklis. Results and perspectives on computational methods for optimal control of switched systems. In *Hybrid Systems: Computation and Control*, pages 540–555. Springer, 2003.

[165] Xuping Xu and Panos J Antsaklis. Optimal control of switched systems based on parameterization of the switching instants. *Automatic Control, IEEE Transactions on*, 49(1):2–16, 2004.

[166] Linqi Zhang, Chris Chung, Bor-Shen Hu, Tian He, Yong Guo, Alexandria J Kim, Eva Skulsky, Xia Jin, Arlene Hurley, and Bharat Ramratnam. Genetic characterization of rebounding hiv-1 after cessation of highly active antiretroviral therapy. *The Journal of clinical investigation*, 106(7):839–845, 2000.

[167] Linqi Zhang, Bharat Ramratnam, Klara Tenner-Racz, Yuxian He, Mika Vesanen, Sharon Lewin, Andrew Talal, Paul Racz, Alan S Perelson, and Bette T Korber. Quantifying residual hiv-1 replication in patients receiving combination antiretroviral therapy. *New England Journal of Medicine*, 340(21):1605–1613, 1999.

[168] Z-Q Zhang, T Schuler, M Zupancic, S Wietgrefe, KA Staskus, KA Reimann, TA Reinhart, M Rogan, W Cavert, and Chris J Miller. Sexual transmission and propagation of siv and hiv in resting and activated cd4+ t cells. *Science*, 286(5443):1353–1357, 1999.

[169] Fabien Zoulim. Mechanism of viral persistence and resistance to nucleoside and nucleotide analogs in chronic hepatitis b virus infection. *Antiviral research*, 64(1):1–15, 2004.